Norwegian University of Life Sciences
Faculty of Environmental Science and Technology
Department of Ecology and Natural Resource Management

Master Thesis 2015
60 credits

Space use and harvest selection of sea trout (*Salmo trutta*) living in a marine protected area

An acoustic telemetry study

Thomas Ruud

Space use and harvest selection of sea trout (*Salmo trutta*) living in a marine protected area – An acoustic telemetry study

Photo credit: Tommy Egra

Preface

This study has been part of the BiodivERsA program, an agency funded by the EU to coordinate research programs on European biodiversity. My study was subject of the BUFFER project, which aims to “identify drivers of resilience in partially protected areas” within coastal zones.

Firstly, I must give my deepest gratitude and regards to my main supervisor Thrond Oddvar Haugen (NMBU). Without his support with the thesis and especially the statistics, I would have been completely lost in the world of Rstudio. He is truly a master of teaching and a good friend. Thank you!

Many thanks to all my helpers from the Institute of Marine Research at Flødevigen. My co-supervisors and scientists Even Moland Olsen and Esben Moland, post.doc Carla Freitas and oceanograph Jon Albretsen, you all provided me with quick responses, enthusiasm and a lot of data. This thesis could not have happened without you!

I would like to thank my good friend and classmate Torkil Dokk for all the help and time he has given. Everything from ArcGIS to Rstudio, there have always been a helping hand in the neighboring booth. He also dragged me out on long-term training sessions, which might have saved my mental stability and body from overweight.

My old friend Martin Jullum helped me understand the statistics and evaluate the results. I would never have understood the results without you!

Thanks to Reidar Borgstrøm, Ingemar Näslund, Erik Rasmussen and Roar Økseter for their perusal and constructive feedback on the thesis.

A special thanks to my mom for a continuous supply of cakes in the thesis-battle. Needed that sugar! And thanks to my father for helping me with the rusted Ruud-wagon.

Finally yet importantly, I would like to thank my dear Marie for her patience, support and inspiration during my work with the thesis. We can truly manage anything together!

May 2015

Thomas Ruud

Abstract

The sea trout (*Salmo trutta*) is popular anadromous fish that has long traditions as game for recreational and sports fishing. However, the habitat utilization of the sea trout in fjord systems is poorly studied. It may be influenced by internal factors like size, sex and early life-history in freshwater, as well as external factors like season and weather conditions. As valuable target species for anglers, the sea trout is subject to unknown harvest pressure in the marine environment. Individuals may experience different harvest pressure according to their different behavior types and habitat use. Marine protected areas (MPA) has become a leading measure to reduce selective harvest pressure on exposed species. However, the degree of protection against anglers is dependent on species behavior types.

The objectives of this study were to quantify full-year space use of the sea trout in Tvedestrandsfjorden, and how space use is affected by early life-history in freshwater and environmental agents. The results were later used to assess the efficacy of the MPA, and how utilization of the MPA influenced the final fates of the sea trout.

I used acoustic telemetry to monitor 56 tagged sea trout from April 2013 to September 2014 in Tvedestrandsfjorden. By triangulating the receiver data, habitat use metrics like utilization distribution and volume, total daily distance, turboness and mean depth utilization could be estimated. The spatiotemporal data was coupled with the use of the MPA along with the final fates of the tagged specimens, to see the efficacy of the reserve.

The results revealed that length at tagging, probability of using the no-take zone and smolt length influenced the behavior and final fates of the tagged individuals. Large individuals with large smolt length, and small individuals with small smolt length, were highly exposed to fishing mortality. Intermediate individuals with middle smolt length had high survivability. The sea trout in Tvedestrandsfjorden is thus vulnerable to size-selective harvest, whereas the MPA has a limited size-selective protection efficacy and the survivability in the fjord is merely 14 %.

In order to provide better protection of large sea trout individuals a maximum landing size limit is proposed as a more efficient measure compared to the current MPA, as the current MPA dimensions seems too small. The strong influence of smolt size on fjord space use should be brought into consideration whenever habitat alterations takes place in the nursery streams.

Contents

1. Introduction 1
2. Materials and methods 5
2.01 Study area 5
2.02 Study species 7
2.03 Fish handling procedure 9
2.04 Scales readings 10
2.05 Weather data 12
2.06 Tracking procedure 12
2.07 Monitoring 13
2.08 Fate assignment 14
2.09 Range testing 14
2.10 Position averaging 16
2.11 Utilization distributions and movement metrics 16
2.12 Statistical analyses 17
3. Results 20
3.01 Studied individuals 20
3.02 Smolt lengths 20
3.03 Home range 50 21
3.04 Home range 95 24
3.05 Turboness 26
3.06 Total daily distance 30
3.07 Depth use 34
3.08 Utilization volume 50 36
3.09 Utilization volume 95 38
3.10 Probability of using the no-take zone 41
3.11 Fate and use of no-take zone 43
4. Discussion 48
4.01 Fates and no-take zone utilization 48
4.02 Harvest selection 50
4.03 Fjord residency 51
4.05 Acoustic telemetry 52
4.06 Reproducibility 53

4.07 Management implications 53
5. Conclusion 55
6. References 56
7. Appendix 63

1. Introduction

The brown trout (*Samlo trutta* L. 1758) has a wide natural distribution and is therefore subject to a great variety of ecological, physiological and morphological variation within the species (Elliott 1989). A variety of local adaptations are thus abundant and this results in different colors and size (Frost & Brown 1967), life-history traits and habitat use (Jonsson 1985). The habitat use is vital to the brown trout, and may highly influence individual survival, reproduction and their ability to exploit available resources (Kramer et al. 1997). In the freshwater nursery areas, young parr of brown trout utilize the slow-flowing shallow banks in the riverbed, while older individuals tend to dwell in the faster and deeper stream habitats (Keeley & Grant 1995). As the individuals grow, their requirements for food will change and their preference of habitat change to larger rivers, lakes, estuaries and even the marine environment if it is available (Jonsson & Jonsson 2011).

Brown trout with an anadromous life style that includes migration to the marine environment, are known as sea trout. This seaward migration pattern is probably influenced by a complex interplay between genetics and environmental agents like temperature, river discharge, interspecific competition, metabolism and juvenile growth rate (L'Abèe-Lund et al. 1989; Jonsson et al. 2001; Cucherousset et al. 2005; Pulido 2011). The seaward migration of sea trout occur every spring and is an adaption in order to increase nutrient intake and maximize individual growth (Pemberton 1976a; Klemetsen et al. 2003; Jonsson & Jonsson 2011; Boel et al. 2014). Increased individual growth will reduce mortality and increase reproductive success and thus fitness (Jonsson 1985; Klemetsen et al. 2003; Jonsson & Jonsson 2011). Before migrating to sea, the juvenile sea trout grow up in freshwater habitats and experience a smoltification prior to the migration. This is a physiological change where the individuals are adapted to a life in the marine environment with higher salinity and osmotic stress (Gordon 1959; Prunet et al. 1989). However, little is known about the fjord residency and behavior of the sea trout beyond the so-called post-smolt period. Since timing of smoltification is influenced by early-life growth and possibly behavior (Boel et al. 2014), both survival and habitat use in the fjord may be affected by earlier stages in freshwater and the size at which the individual smoltify.

The sea trout is a desirable fish for recreational and sports fishing in Norway, where it is subjected to harvest from predominantly recreational anglers, but also from artisan fisheries. The fish is caught in rivers and lakes which are located and linked to nearby marine

environment, and along the entire Norwegian coast during the sea dwelling period. However, the catch figures of sea trout are difficult to estimate, and are probably under estimated compared to Atlantic salmon (*Salmo salar*). Catches of sea trout in the marine environment are seldom reported, whereas Atlantic salmon are caught in large rivers where most captured individuals are reported (Fiske & Aas 2001). Studies of cod (*Gadus morhua*) have shown that mortality caused by recreational and artisan fisheries were perceptibly higher than the natural mortality (Olsen & Moland 2011). Individual differences in behaviors such as exploration and aggressiveness are receiving increasingly attention as explanation of individual traits like growth and reproduction (Biro & Stamps 2008). Fisheries may however lead to harvest selection that influence behavior and life-history traits of the species (Conover & Munch 2002; Allendorf & Hard 2009). The coastal cod in Tvedestrandsfjorden showed altered population dynamics probably due to human harvest selection, in which the largest and most active individuals where caught (Olsen et al. 2012). There may thus be a significant harvest pressure from recreational fishing on sea trout that is not part of the species management. This harvest can alter the population dynamics and reduce population viability (Olsen & Moland 2011).

In 2012, a temporary marine protected area (MPA) was established in Tvedestrandsfjorden, in Aust-Agder county in Norway that will be maintained until 2017 (Lovdata 2012). Marine protected areas are worldwide growing as a leading conservation action to preserve biodiversity and ecosystem structure, or as measure to restore fish populations from overexploitation (Seytre & Francour 2008) and counter harvest induced selection (Conover & Munch 2002). The preservation of marine areas have shown positive results with greatly increased abundance and species richness (Seytre & Francour 2008; Lester et al. 2009; Stobart et al. 2009), where the individual growth also increases with higher total biomass and more trophic levels (Lester et al. 2009; Stobart et al. 2009). These effects apply to partly protected areas as well as strict prohibition zones (Alos & Arlinghaus 2013). However, the same positive effect may not influence all species pooled together (March et al. 2014) as it may on specific species, because of different life history patterns (Alos & Arlinghaus 2013).

The size of reserves is often a clash of interests, though any reserve is often better than none. Studies have shown that small reserves may contribute locally with a positive biological response (Lester et al. 2009), but size does matter, and a larger reserve will probably give a higher positive response. Increasing the no-take zone of a MPA may therefore increase the density of fish species and biomass, though increasing the size of the buffer zone has the

opposite outcome (Claudet et al. 2008). Species have different characteristics and behavior, and a reserve will thus have different impact on species with various mobility (Lester et al. 2009). A mobile species need a much larger reserve then a more stationary species. Larger pelagic reserves may therefore be as important as small costal reserves (Hyrenbach et al. 2000). When planning MPAs, it is thus vital to recognize the broad range of species and habitats. Connecting reserves together in an ecosystem-based network may accordingly give a decent representation of the complete biodiversity that utilize the area (Johnson et al. 2014) .

Another demonstration that MPAs may contribute to increased abundance and biomass of fish species, is the increased fishing effort and catches along the reserve borders (Stobart et al. 2009; Olsen et al. 2012). This is called "fishing-the-line" when the main tactic is to place the effort directly along the reserve borders to catch spillover effects (Kellner et al. 2007). The spillover effects are a surplus of fishes that disperse out of the area, and is often marked in local catches and benefit the local fishermen. Around an MPA at Apo Island in the Philippines, the hook-and-line catches increased with 50 % after almost 20 years with protection, while the fishing effort had decreased with 46 % in the same period (Russ et al. 2004; Alos & Arlinghaus 2013). Marine protection is a long-term precaution and need enough space and time to give a high biological yield (Russ et al. 2004; Claudet et al. 2008).

Acoustic telemetry has become a useful tool to study home range and spatiotemporal habitat utilization (Heupel & Webber 2012). The method can present high resolution results in the monitoring of long-term utilization pattern (Lucas & Baras 2000) and may give a better understanding of individuals behavior and their mortality sources (Hightower et al. 2001). Home range studies of painted comber (*Serranus scriba*) (March et al. 2010), shark-like batoids (families *Rhynchobatidae* and *Rhinobatidae*) (White et al. 2014) and several shark species in different habitats (Voegeli et al. 2001; Heupel et al. 2004; Andrews et al. 2010) shows the variety and usage of the method. The latter years, acoustic telemetry have been used to find species usage of marine protected areas and the efficiency of the reserves (Friedlander & Monaco 2007; Marshell et al. 2011; Knip et al. 2012; March et al. 2014).

In the present study, I used acoustic telemetry to investigate how sea trout utilize the marine habitat throughout the year in Tvedestrandsfjorden. In particular, I aimed at quantifying the influence of environmental and individual factors, including early-life growth in freshwater, on various aspects of the fjord habitat use, as well as quantifying how the use of an MPA may influence the individual's fate. Finally I discuss possible alterations of the MPA regulations.

This study may be the most detailed long-term positions and utilization distribution of sea trout in their coastal marine habitat.

2. Materials and methods

2.01 Study area

The current study used of acoustic telemetry data from Tvedestrandsfjorden (Figure 1), in Southern Norway, at the 58° 36' 23"N and 08° 56' 56"E. The study area is about 4.5 km long (from Tvedestrand to Saltneset in a straight line) and 3.9 km^2, with a maximum depth of 85 m (Ciannelli et al. 2010), and a catchment area of 38 km^2 (Helland et al. 2003). The complete fjord system is about 8 km from Tvedestrand to the Skagerak sea (Knutsen et al. 2010).

Tvedestrandsfjorden is narrow and sheltered in the inner coastal areas of the Skagerrak Sea. Two islands, Furøya and Hestøya situated in the center of the fjord, divide the fjord and create areas with shallow water. The shallow areas hold dense meadows of eel grass (*Zostera marina*) (Miljødirektoratet 2015), considered as a locally important nature type and suitable habitat for smolts of sea trout (Pemberton 1976b). These shallows also create a 15 m deep threshold in the fjord inlet, which creates the inner and outer basins in Tvedestrandsfjorden (Helland et al. 2003). Several small freshwater streams have their outlets into the fjord, giving freshwater discharge to the top layers nearby the outlets. The stream Østeråbekken is the largest and main spawning stream of the sea trout in the fjord (pers. comm Even Moland). The inner part of the fjord has severe low oxygen saturation due to the inlet threshold. Oxygen values drops to <1.5 ml/L at 30-40 meters subsurface (Helland et al. 2003).

The MPA in Tvedestrandsfjorden covers the main part of the fjord (Figure 1), from Saltneset and northward towards Tvedestrand and Østeråbekken. The reserve is divided into four zones with two types of restriction levels in permitted fishing gear (Lovdata 2012). Furøya prohibition zone (1.4 km^2) is a non-fishing area and covers the central part of the fjord (marked as red in Figure 1). Any type of fishing inside this area is strictly forbidden. Indre Oksfjord (0.8 km^2), Sagesund (1.1 km^2) and Kvastadkilen (0.5 km^2) are conservation zones with the permission only to use hook-and-line fishing. Kvastadkilen conservation zone is not part of my study area, as the study area is confined at Hantosundet where the last receiver is placed.

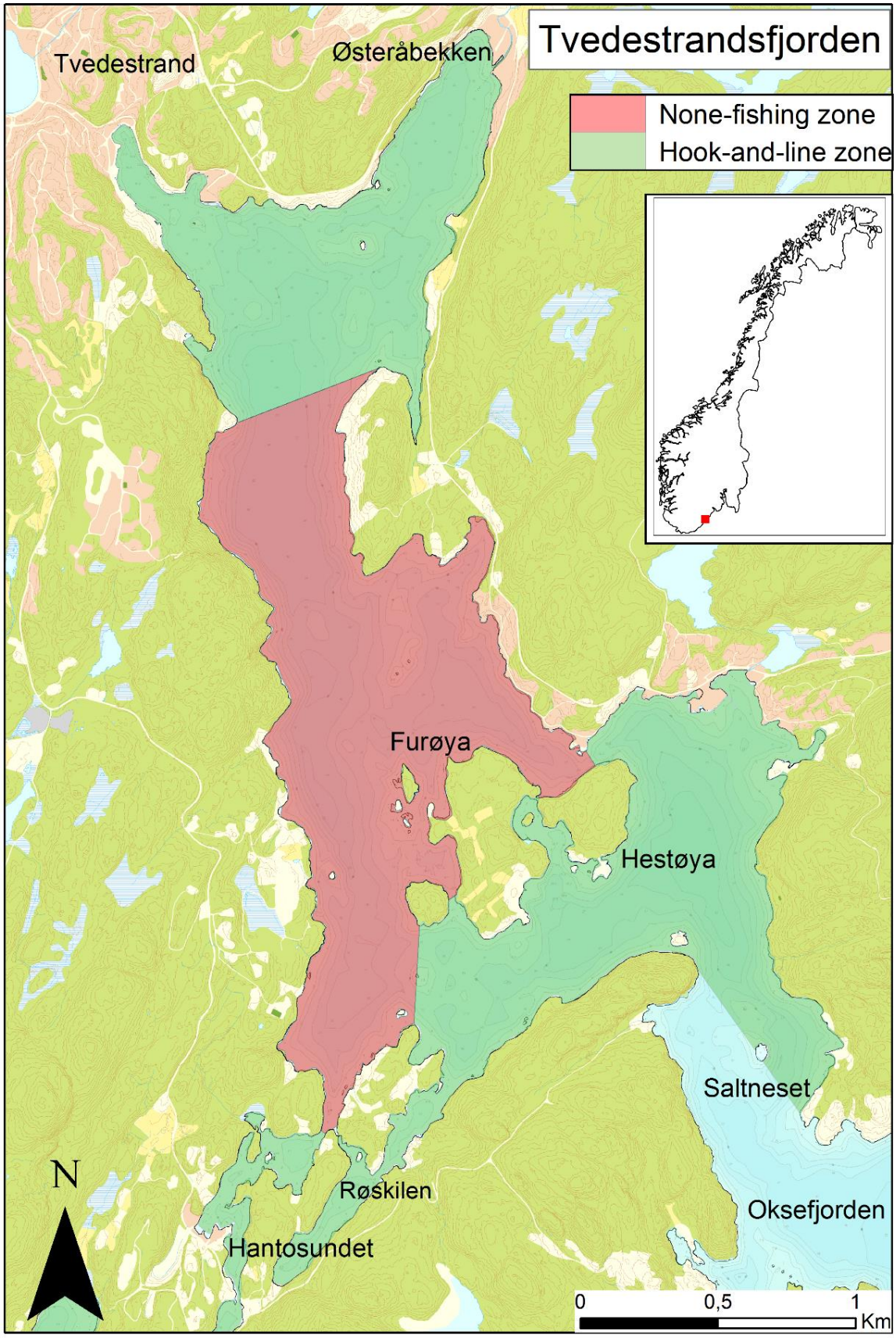

Figure 1: Tvedestrandsfjorden with the three fishing zones. Red zone indicate no fishing, turquoise indicate hook-and-line permit.

2.02 Study species

The brown trout is a predatory fish that originates from Europe and North Africa (Frost & Brown 1967). The fish flourish in oxygen rich streams, rivers and lakes (Elliott 1994) from the Bay of Biscay (41^{o}N) in the south, to the north of Scandinavia (71^{o}N), and from Iceland in the west to the Ural Mountains and the Caspian Sea in the east (Frost & Brown 1967; Elliott 1994). The silvery sea trout (Figure 2) and the brown trout is the same species. In the same population, residential and migratory individuals can coexist, and they may spawn together (Frost & Brown 1967; Jonsson 1985). Harris and Milner (2006) defines a sea trout as "a brown trout that spend periods of time feeding in the sea, before returning to freshwater to reproduce". They indicate that the brown trout always has some kind of migration, independent of location. It could be in a river stretch or a lake, or from a stream down to the marine environment. A "sea trout" has the most extreme migration that takes the individuals all the way to the sea (Harris & Milner 2006).

In Scandinavia smolt and overwintering anadromous brown trout migrate from their spawning stream to seawater from February (Jonsson & Jonsson 2002), but mainly from April to June (Pemberton 1976a; Klemetsen et al. 2003; Jonsson & Jonsson 2011; Boel et al. 2014). The onset of this migration is likely influenced by both genetics and environmental agents such as water and air temperature, river discharge, interspecific competition and juvenile growth rate (Jonsson et al. 2001; Cucherousset et al. 2005; Pulido 2011). The migration is likely an adaption to increase nutrient uptake, whereas increased growth may increase reproductive success and reduce mortality (Jonsson 1985; Jonsson & Jonsson 2011). The disadvantages of migration are increased mortality while migrating in the marine environment and increased energy cost of the journey (Bohlin et al. 2001).

Sea trout are individuals that mature sexually at sea, while residents mature in the river or stream of origin without migrating (Jonsson 1985). Mature and older individuals migrate earlier than first time migrants to the sea (Jonsson & Gravem 1985; Jonsson & Jonsson 2002), where they can migrate great distances into coastal areas. Studies have shown migration up to 100 km from the outlet of their spawning river (Jensen 1968; Nordeng 1977; Jonsson 1985). This pattern suggests a continuum of migration patterns from freshwater areas to the outer coastal areas and the sea (Boel et al. 2014; del Villar-Guerra et al. 2014). However, some sea trout rarely dwell more than 10-15 km from the spawning river outlet (Frost & Brown 1967; Jensen 1968; Jonsson 1985). These individuals have a partial migration within the fjord with brackish water, and thus a fjord residency than rather a migration continuum to the sea (Boel

et al. 2014; Davidsen et al. 2014c; del Villar-Guerra et al. 2014). The migratory tendency is often negatively correlated with distance and cost of migration (Kristoffersen et al. 1994; Jonsson & Jonsson 2006). The migratory distance may thus be subject of the physical conditions of the brown trout before leaving the stream, whereas individuals with the lowest energy levels migrate a shorter distance than individuals with higher levels of lipid deposition (Sheridan et al. 1983; Sheridan 1989; Boel et al. 2014). Studies also show that the migration distance is shortened when encountering suitable habitats that satisfy the metabolic needs (Cucherousset et al. 2005).

After the sea dwelling period, the sea trout inhabit strong homing behavior (Jonsson & Jonsson 2011), and return from August towards the winter months to spawn in their natal rivers and streams (Nordeng 1977; Jonsson 1985; Jonsson & Jonsson 2002; Jonsson & Jonsson 2011). Of the migrating brown trout, the sexually mature returns first before the immature and younger specimens (Jonsson 1985). The majority of the sea migrants are female. Up to 60% of the females migrate to the sea, while only 40 % of the males migrate (Jonsson 1985; Knutsen et al. 2001b; Knutsen et al. 2004; Cucherousset et al. 2005). The reason for the female dominance is probably connected to reproduction (Jonsson 1985). The female fitness increases with body size as large females hold more eggs with higher quality, while males can fertilize eggs independent of size (Jonsson & Jonsson 1999; Jonsson et al. 2001). Small “sneakers” and large “fighters” may both have high reproductive success (Jonsson 2000).

Figure 2: A freshly caught sea trout (Photo credit: http://www.orkneytroutfishing.co.uk)

2.03 Fish handling procedure

The fish handling and tagging procedure (Figure 3) in the present study where conducted by my co-supervisors from the Institute of Marine Research (IMR) in Flødevigen: the scientists Even Moland and Esben Moland Olsen.

During four periods (April, May, September and November) in 2013, 59 wild sea trout where caught and selected for tagging. In order to sample a study population without selecting for active or more "catchable" individuals (Allendorf & Hard 2009), active gear were used and targeted naïve fish near habitat likely used for feeding or resting (between Furøya og Hestøya). The sea trout were caught using a beach seine (60 x 3 m), with 30 m hauling ropes at each end, deployed from a rowing boat. Deployment was carried out by positioning a person on shore holding one of the ropes. The seine was deployed in a U-shape with the rower bringing the second hauling rope to shore. As the seine was hauled, the two ends where brought together at a suitable landing site. Great care was taken when beaching the seine and hauling the outermost seine wall in to form a pocket in shallow water. Any trout caught in the pocket were lifted over in 40 – 80 l basins on shore with a hand net/ scoop net. Clove oil was used as anesthetic (Munday & Wilson 1997; Bridger & Booth 2003) *in situ*, and was administered in a bath. Surgery was conducted in a U-shaped half-tube when fish showed signs of complete anesthesia (belly up, gentle ventilation). Following the implantation protocol of Mulcahy (2003), each candidate got surgically implanted an acoustic tag (Vemco V9P-2L). The tag was inserted into the abdominal cavity (Bridger & Booth 2003; Bøe 2013) through a small wound that was closed using two absorbable sutures (Olsen et al. 2012). After surgery, width and height (in mm) of the caudal peduncle using vernier calipers, and body weight (g) of each individual were measured as fork length to nearest millimeter (Olsen et al. 2012). Length varied from 230 mm to 635 mm with a mean length of 338 $\pm$ 161 mm ($\pm$ SD). Scales were sampled from the peduncle for aging, and a tissue sample were removed from the anal fin for latter genetic analysis. The whole procedure lasted less than five minutes. Trout were then transferred to a container with well oxygenated sea water for recovery. After full recovery, the individuals were observed for 10-20 minutes before being released at the location of capture.

Figure 3: Fish handling and tagging by Even Moland and Esben Moland Olsen. The middle picture on the upper row shows a V9P-2L transmitter that was used for tagging (Photo credit: Even Moland and Carla Freitas).

2.04 Scales readings

I used the scales samples to determine the age of the fish, back-calculate the smolt length and register life-history events (e.g., spawning events). From the scales the age is estimated by reading the among-circuli density pattern in each scale (Jonsson 1976). During winter the circuli are formed tighter as the growth is reduced (Jonsson & Jonsson 2011), and when spring and summer comes, the distance between two circuli is much broader. Often, clear winter and summer zones can be read. In anadromous individuals, the fish experience increased growth as post smolt, up to 20-25 cm during the first year at sea (de Leeuw et al. 2007), illustrated in Figure 4. Scales comprise handy tools for estimating age when dealing with fast-growing individuals (Jonsson & Jonsson 2011), like the individuals in my study. I also estimated the smolt length of each individual (Figure 5), by back-calculating the fish length from the scales (Francis 1990), assuming a proportional growth of scales and body.

Figure 4: The scale from fish ID 1158183. The crossing red lines indicate end of winter zones. This individual spent two years in freshwater and then migrated to the sea, as indicated by a substantial increase in growth during the third yea.

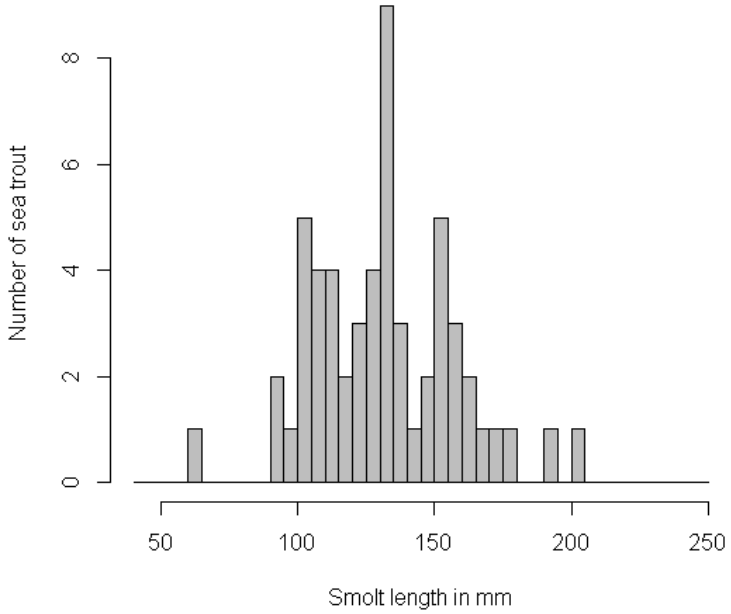

Figure 5: The back calculated smolt lengths (mm) of the 56 individuals studied in Tvedestrandsfjorden.

2.05 Weather data

Air pressure, air temperature, precipitation, wind direction and wind speed data were retrieved from eklima.no, based on weather stations located close to Tvedestrandsfjorden. The main dataset consists of measurements from the Torungen lighthouse, located at 58° 39' 88"N and 08° 78' 93"E in more open seawaters. The lighthouse is still located approximately 24 km southwest from Tvedestrandsfjorden and was assumed to have roughly the same weather conditions. In the time series of precipitation and wind speed and direction, there were some data gaps though. The final wind data consists of regression values between Torungen and the Lyngør lighthouse, with a 74% overlap in wind direction and 81% overlap in wind speed data. The Lyngør lighthouse is located at 58° 63' 61"N and 09° 14' 79"E, 12 km northeast of Tvedestrandsfjorden. Precipitation data consisted of regression values between the Torungen lighthouse and the fire station in Arendal, and showed a 75% overlap. The fire station is located at 58° 46' 13"N and 08° 72' 28"E, west of the Torungen lighthouse. In the periods 1-5.4.2014 and 29-30.06.2014 though, there were lack of data. The Torungen lighthouse had no measurements these days and no weather station nearby could provide data in the same slot. To compensate, I used direct precipitation values from the Porsgrunn fire station these days. The fire station is located too far away and gave rather poor regression ratio, thus no regression values were estimated by this station. The direct values indicated minor precipitation with no significant importance.

2.06 Tracking procedure

The 59 sea trout individuals were equipped with V9P-2L transmitter tags (Figure 3) (Vemco Division, Amirix System Inc., Halifax, Canada) implanted for acoustic monitoring. These cylindrical transmitters were 29 mm in length, with diameter 9 mm, weighing 4.7g in air. Hence, tag weight-to-fish ratio was < 3.8%. Each transmitter had a unique identity code that was transmitted as ultrasonic signals or "pings" every 100-250 second. The random interval of the signals reduced the chance of code collisions (Olsen & Moland 2011). In addition, the tags have a pressure sensor that provides vertical positions as well (accuracy ± 2.5 m when deployed at max. 50 m depth). The acoustic transmitter's battery life lasted for approximately 660 days. When the battery is empty, it simply stops sending signals (Olsen et al. 2012), but the tags remains within the fish until death.

2.07 Monitoring

A network constituting 51 passive stationary VR2Ws receivers (Figure 6; Table A13) (Vemco Dicision, Amirix Systems Inc.) were constantly logging transducer signals received via omnidirectional hydrophones. These receivers where moored to the sea floor and deployed at around three meters depth (Olsen et al. 2012). The receivers were placed to give maximum coverage of the fjord (Figure 10), and secure a large enough minimum convex polygon (MCP) for the mean-position estimates (Simpfendorfer et al. 2002). Sentinel receivers where placed at Hantosundet, Saltneset and the outlet of Østerråbekken (Figure 1) to ensure recordings of roaming sea trout (Olsen & Moland 2011). The receiver at Østerråbekken and Hantosundet were used to register movement to the spawning streams, and the receiver at Saltneset to register movement in and out of the study area. The narrow little strait called Røskilen, was not covered with hydrophones. The receivers collected data from 30.04.2013 to 12.09.2014 and the data were downloaded during several periods: 17-27. June and 3-17. December 2013, and 7-14, April and 9-12. September 2014. Downloaded data where stored in a VUE database (Vemco Division, Amirix System Inc.) (Olsen et al. 2012; Simpfendorfer et al. 2012) and later exported to R (R- Core Team 2012).

Figure 6: A VR2w receiver for passive monitoring of tagged sea trout (Photo credit: www.Vemco.com)

2.08 Fate assignment

To determine if the fish was dead by anthropogenic or natural causes, a careful inspection of all individual depth- and position time trajectories were undertaken by Ruud, Haugen and Moland. If the tag suddenly disappeared from the study area, we decided that the fish where caught by a fisherman. If the tag, after long periods of normal behavior, abruptly was fixed at a position and depth for a long period, we concluded that the fish was caught and gutted on the same place at typical fishing sites. The tag was assumed thrown into the water after gutting or just followed unobserved with the gutting into the water. If the dataset showed a tag at nearly the same position during a long period, but with some differences in depth, we concluded that the fish was dead by natural or elusive causes. The depth variance where probably caused by the tidal water or currents. Lee and Bergersen (1996) did some of the same assumptions in their study. When a tagged fish was still at the same location for more than 48 hours, it was assigned dead. A candidate was assumed emigrated when the movement steered straight out to sea, and the last detection was at the furthest receiver in the system with no further detections during the study period (Olsen et al. 2012). Concluding the fate assessment, a total of three sea trout individuals were removed from the dataset due death following shortly after release. These candidates gave insufficient data to the study. The total number of sea trout retained for further analyses were 56 specimens. Following the fate assessment, the study specimens where categorized as “Dead”, “Alive”, “Caught” or “Emigrated”.

2.09 Range testing

A range testing was done in 2011 in Tvedestrandsfjorden with 33 receivers deployed, to test the range of the tags with the same transmitting strength that were used in the later study. However, now with a fixed signal transmitting interval of 5 seconds. The range test revealed a high detection rate with very few none-detected positions (Figure 7). The positions that were not detected where in narrow bays and along the shoreline. The detection ratio was high within 200 meters of the hydrophones (Figure 8), but decreased with increasing distance from the receiver. However, even at 1000 m distance there was an average detection probability larger than 20%.

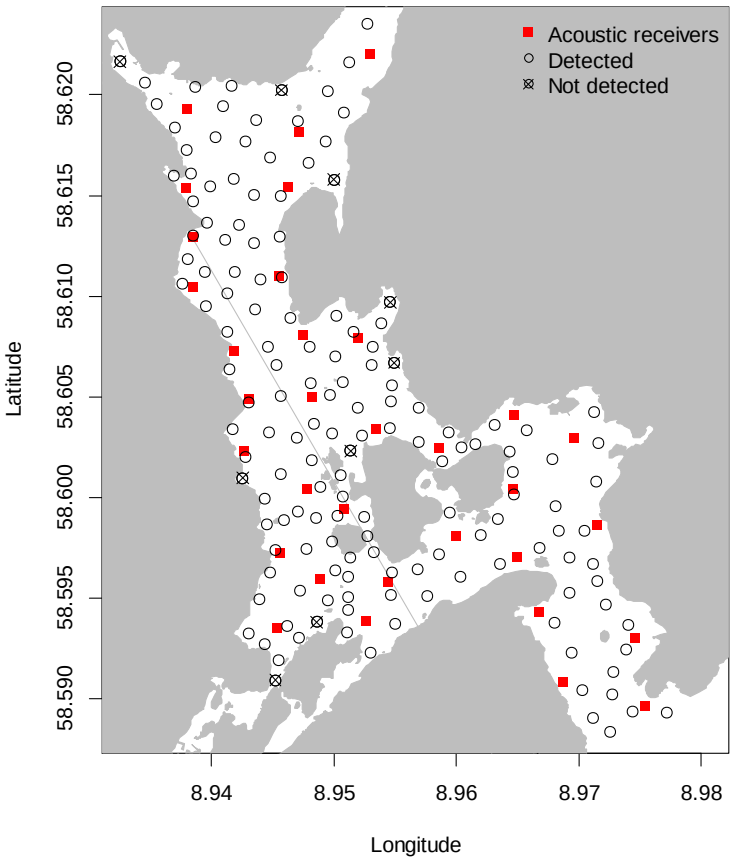

Figure 7: Sites where a test tag was deployed and the signals either where picked up (open circles) or not picked up (crossed open circles) by one or more of the acoustic receivers (red squares).

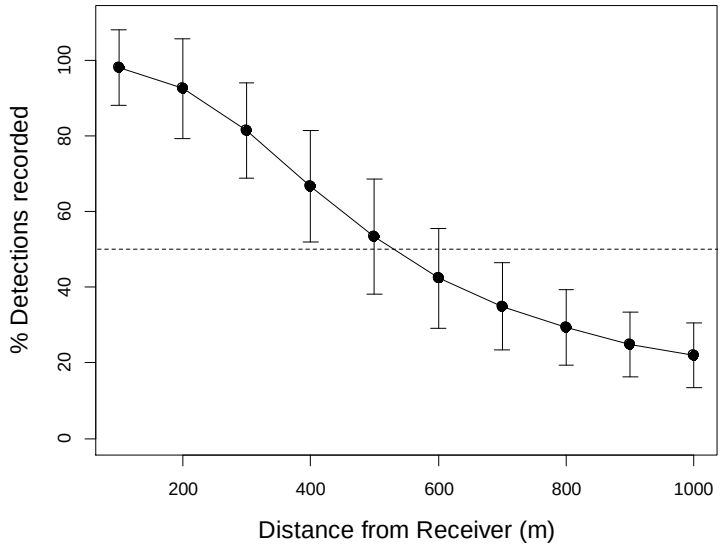

Figure 8: Mean (± standard deviation) percentage of test locations recorded as a function of distance to the receiver.

2.10 Position averaging

To estimate the sea trout positions, I used the mean-position-algorithm, available from Simpfendorfer et al. (2002) This was done at 15 minutes intervals per individual. The method uses the presence or absence of signals from the transmitters to the hydrophones at a given time, and estimates mean positions weighted by the number of signals received at each hydrophone. These signals are omni-directional pressure waves that travel through water and are received at omni-directional submerged hydrophones (VR2W) (Thorstad et al. 2013). The receivers partly overlap, so one unique signal can be detected by multiple hydrophones and subsequently estimate a mean position between the hydrophones for each fish over a given period. In my study, 15 min time slots were used. These signals are then summed and weighted by the number of detections at each receiver to give a mean position (Olsen et al. 2012). The accuracy of the positioning increases with the number of received signals within the time slot. This method is also called "the weighted-mean method" (Hedger et al. 2008). In a triangulation situation, if a receiver has more signals than other neighboring and overlapping receivers, this indicate that a fish has been proximal to this receiver (Simpfendorfer et al. 2002). The method will not give an exact position of the fish, but an approximate position between all hydrophones that received a signal during the chosen time slot (Olsen et al. 2012), also called position averaging (PAV).

2.11 Utilization distributions and movement metrics

The volumetric UD (XYZ-dimension) where given with horizontal UD (XY) added approximate mean depth (Z-dimension) during the same time slot (15 min). Overlapping horizontal position estimates are corrected with volumetric data, which can give individuals different depth distribution (Simpfendorfer et al. 2012). Figure 9 illustrates the mean volumetric utilization distribution of the individual with ID 1158183 during week 16. The depth data where given from depth sensors within the V9P-2L transmitters that each fish where tagged with. The estimates of the volumetric UD, were fitted and smoothed using the kde-function within in the ks-package in Rstudio (R- Core Team 2012).

The estimated PAVs were used for estimating individual utilization distributions (UDs), for the area within one removes outliers and only includes the area mostly used by the individual (Rogers & White 2007). I estimated UDs using the same smoothing parameter, h=28.7, across all individuals. This h-value constitutes the median value when running individual-wise least

squared cross validation kernel fittings across all individuals. By forcing the same *h*-parameter on all individuals, direct comparison of home range sizes among individuals becomes relevant, without having to consider eventual effects from differential smoothing parameter on the UDs. Daily UDs were estimated using the kernelUD function embedded in the R package adehabitatHR (R- Core Team 2012).

The PAVs were also used for estimating daily linear distances at individual level, i.e., the total distance an individual swims per day. These linear distances were estimated using the R-package adehabitatLS (R- Core Team 2012). Volumetric UDs were estimated using the 3D PAVs. Technically, this was done using the kde-function available from the ks-package in R. In order to explore the activity level with the home ranges, I estimated a metric framed "turboness" which was simply the daily linear distance divided by UD 95.

In the triangulation of the horizontal home range estimates, a minimum of three VR2Ws had to be involved with every triangulation. That gave a potential of 96 unique relocations every twenty-four-hours. Days with less than 20 observations and 20 unique relocations from each ID where removed from further analysis. In the volumetric estimates, we used the average positioning of every 15 min, and days with more than 30 observations and each ID needed at least 10 unique relocations to be included. In the volumetric and depth estimates, the dataset showed 34907 positions above sea surface, and 11686 positions 50 meters below the surface. These positions where removed as well to simplify and avoid corrupted data.

The definition of activity within the 95 % favoring utilization area (delta displacement), has in this study been called "turboness". The turboness unity is meters/hectare/day, and has the importance to show how much the sea trout utilize their favoring areas. The 50 % home range where not covered with turboness analysis since the areas were considered too limited.

2.12 Statistical analyses

Space-use variables (depth, horizontal UDs and volumetric UDs) were included in univariate linear mixed effect models (LME) fitted to estimate effects from a range of external (e.g., air temperature, wind speed and precipitation) and internal (smolt length and length at capture) variables on the within Tvedestrandsfjorden habitat use. For UDs, the 50% and 95% distribution levels (i.e., the core distribution area/volume) were used as responses in the LMEs. Individual IDs were used as random intercepts to account for within-individual

dependency of observations (Nakagawa & Schielzeth 2010). Model selection followed the procedures described in Zuur et al. (2009) utilizing Akaikes information criteria (Akaike 1974) for model selection. Model selection tables along with parameter estimate using tables of the selected models are shown in the appendix, and corresponding prediction plots of the selected models are displayed in the results chapter.

In order to quantify eventual effects of using the no-take zone on individual fate, a multinomial modelling approach was undertaken by the fate data as response and fraction of time spent inside no-take area as predictor. The fraction spent inside the no-take zone was based on PAV assignments to either “inside” or “outside” using the over-procedure in sp-package in R. This procedure overlays the PAVs with the no-take GIS-polygone. I also fitted generalized linear mixed effect models to explore which environmental and individual characteristics that most efficiently predicted the probability of using the no-take zone. This was done by using the glmer-function in the lme4-package. I followed same model selection procedures as described for the UD modelling.

In the analysis of examining the probability of using the no-take zone, I simplified the data to make the process easier, and used the triangulation positions inside the no-catch area compared with positions outside for fate of the individuals. Outside positions were called Buffer zone and inside positions called No-take zone (
Table 1). In the selection of parameters for this test, I wanted to see what individual characteristics would determine the probability of using the no-take zone. Therefore, no climatic parameters were included in the model selection.

Table 1: A summary of the numbers of positions inside and outside the No-take zone according to their preliminary fate

Fates	Buffer zone	No-take zone
Alive	41280	17665
Caught	87322	80470
Dead	59449	84693
Emigrated	100795	50582
Total	288846	233410

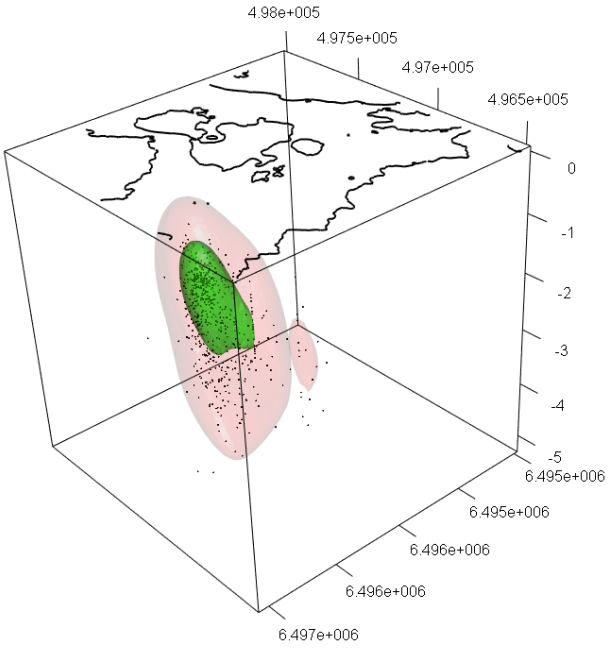

Figure 9: The mean volumetric distribution of the sea trout with ID1158183 during week 16. Green area indicate UV 50 and pink area UV 95. XY-axis are coordinates in UTM 32, datum WGS 84, and Z-axis depth in meters.

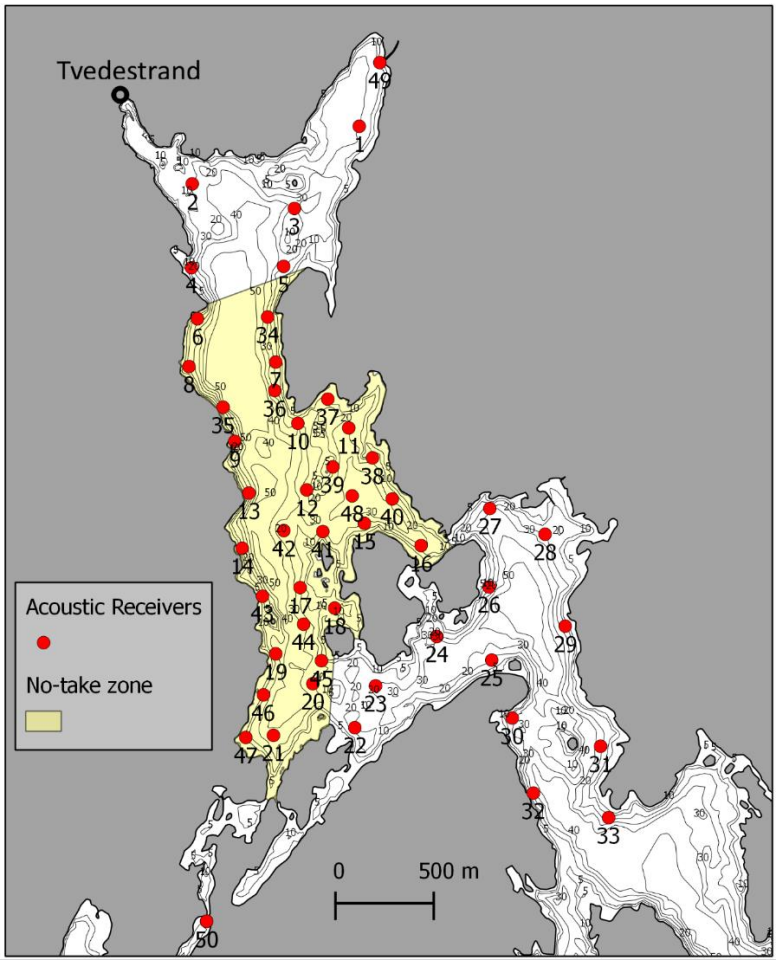

Figure 10: The location of the first 50 stationary receivers in the study area. (Figure credits: Carla Freitas, IMR)

3. Results

3.01 Studied individuals

Of the 56 sea trout that remained, I got 498 days of continuous passive monitoring of their horizontal and vertical movements, resulting in estimations of their favoring utilization distribution. Position plots of every specimen are available in Table A14. Of the 56 studied specimens (Table A1), 38 sea trout remained in the fjord system during the whole study period, while 18 fishes emigrated from the system, never to return. Of the resident sea trout in the fjord, only 8 individuals were alive at the end of the study. In total, 30 fishes were either captured by fishermen or dead due to other elusive causes. A simplified overview of their fates is presented in Table 2.

Table 2: The final fates of the 56 individuals equipped with transmitters in Tvedestrandsfjorden.

Total	Alive	Caught	Dead	Emigrated
56	8	16	14	18
100%	14%	29%	25%	32%

3.02 Smolt lengths

The mean back-calculated smolt length was estimated to 131.9 ± 27.7 mm, with a minimum length of 60.3 mm and maximum length of 203.0 mm (Figure 11). The growth in length during the first season in the marine environment is was expressive, as illustrated in Figure 4. The individuals have a continuous growth the forthcoming years after their first season at sea, however with a reduced growth rate as they age. The estimated mean growths was 125 mm from smoltification to first year at sea, 65.9 mm from first to second year at sea, and 57.4 mm mean growth from second to third year at sea.

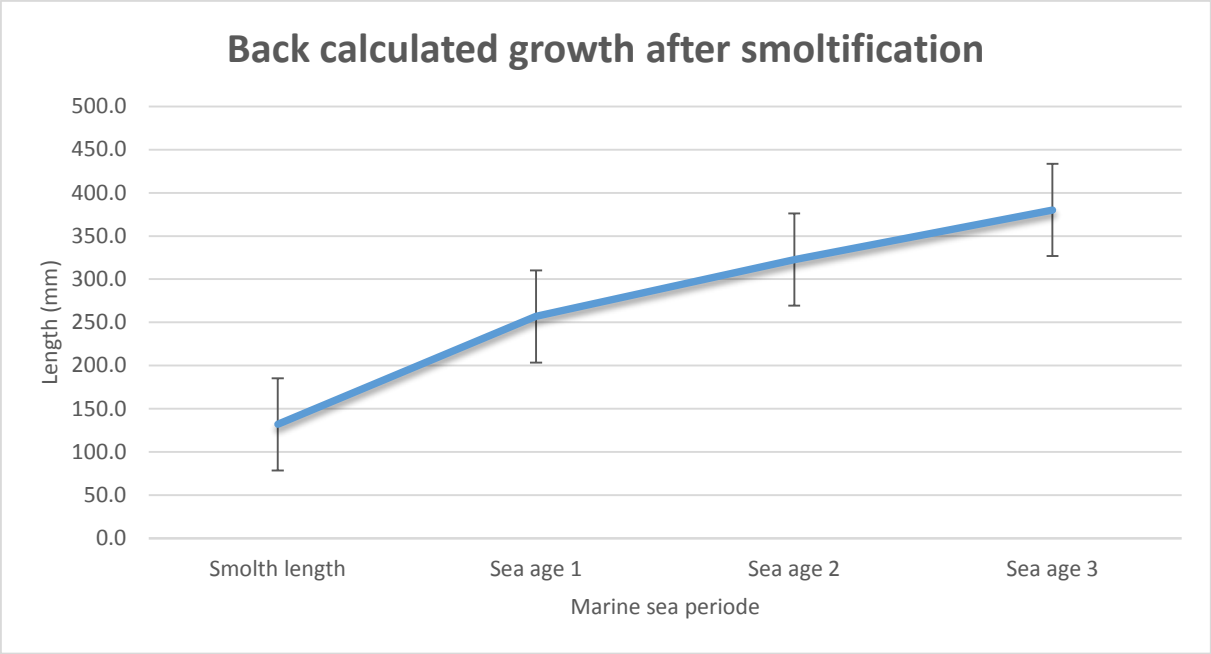

Figure 11: Back calculated growth in the sea from smolt lengths, estimated from scales.

3.03 Home range 50

When analyzing the UD kernels that contained 50% of the probability distribution of the triangulated positions in the horizontal plane, the most supported linear mixed effect model (Table 3) showed an additive effect between month and smolt length to explain the log-transformed home range 50. The results indicated a trend towards reduced home range with increasing smolt length (Figure 12). The home range 50 had highest effect in April, May and September (Table 4). These effects were also significant.

Table 3: AIC values for the five most supported LME-model structures fitted to predict ln(HR50). The models were fitted using ID as a random factor. A complete AIC table is provided in the Appendix (Table A2).

Model	df		AIC	ΔAIC
Month + Smolt length	15		3937.92	
Month + Smolt length + Air pressure	16		3946.11	8.19
Month + Smolt length + Air pressure^2	17		3951.56	13.64
Month + Smolt length + Air temperature^2	17		3951.70	13.79
Month + Smolt length * Air temperature^2	19		3954.45	16.53

Table 4: Fixed effects parameter estimates for the most supported LME-model fitted to predict HR50. The random structure, ID, yielded variance = 0.06±0.25 (SD).

Terms	Estimate	SE	t	p
Intercept	1.349025	0.050162	26.893	0.00044
Month [2]	-0.17463	0.048791	-3.579	0.02305
Month [3]	0.006125	0.043572	0.141	0.31210
Month [4]	0.118687	0.043653	2.719	0.03793
Month [5]	0.287354	0.039867	7.208	0.00601
Month [6]	0.007838	0.044784	0.175	0.30885
Month [7]	-0.09778	0.044812	-2.182	0.05525
Month [8]	0.006693	0.042465	0.158	0.31056
Month [9]	0.108658	0.041339	2.628	0.04026
Month [10]	0.018659	0.043455	0.429	0.26883
Month [11]	0.070571	0.044361	1.591	0.09014
Month [12]	-0.01212	0.040397	-0.3	0.29203
Smolt length	-0.05323	0.032413	-1.642	0.08612

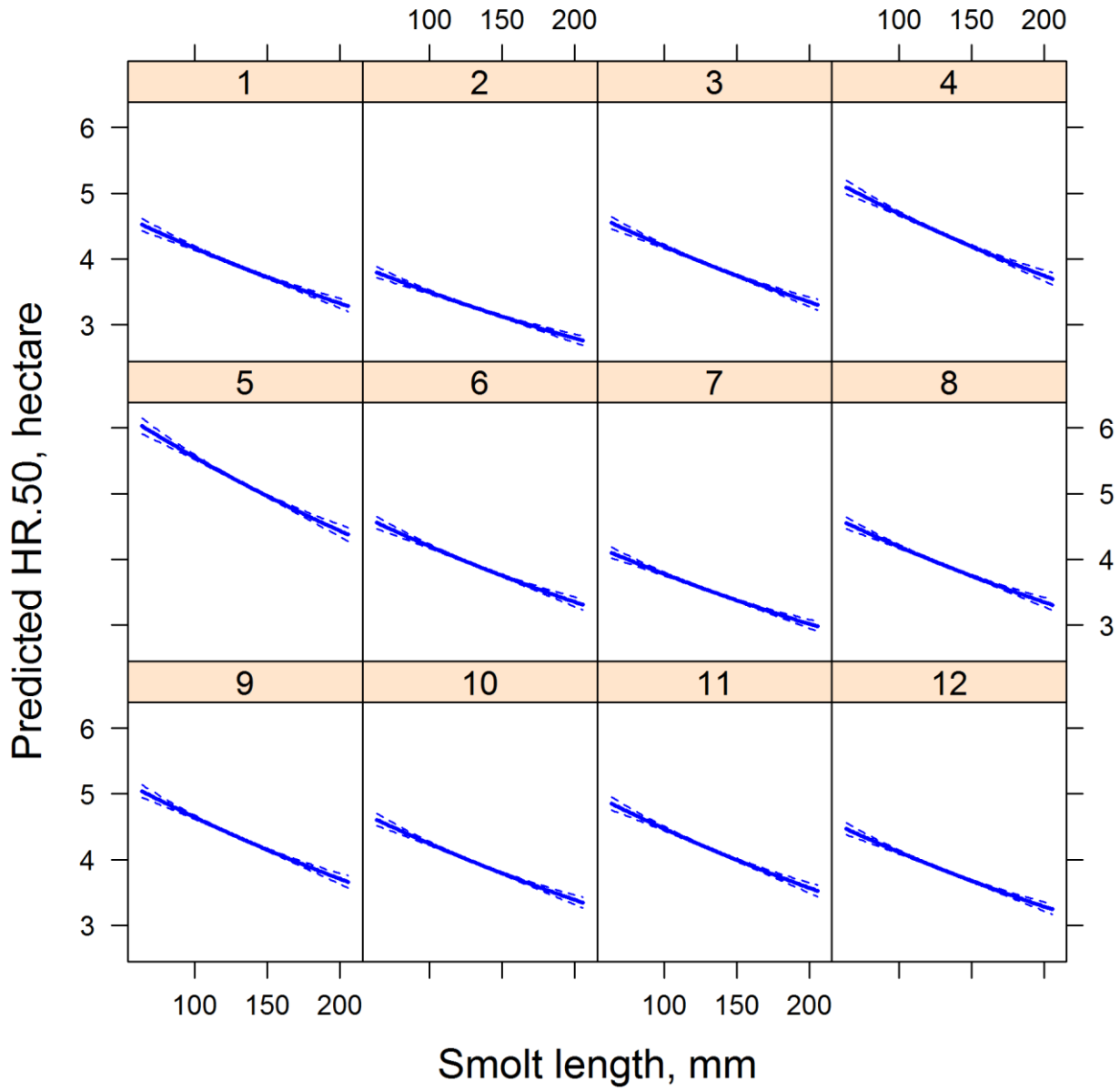

Figure 12: Prediction plot showing predicted 50 % home range (hectare) dependent on smolt length (mm) for each month of the year. The predictions where gathered from the most supported LME-model reported in Table 3.

3.04 Home range 95

The results from the model selection of the 95% horizontal utilization distribution area also revealed an additive effect between month and smolt length (Table 5). The prediction plot (Table 11) of the most supported model to predict the log-transformed home range 95 also showed a trend that indicated reducing home range with increasing smolt length. This effect where strongest in April, May and June, as they were also significant. In February, the effects where highly negative, indicating a significant reduced home range compared to January.

Table 5: AIC values for the five most supported LME-model structures fitted to predict ln(HR95). The models were fitted using ID as a random factor. A complete AIC table is provided in the Appendix (Table A3).

Models	df	AIC	ΔAIC
Month + Smolt length	15	4628.26	
Month + Smolt length + Air pressure	16	4636.88	8.62
Month + Smolt length + Air temperature^2	17	4642.54	14.28
Month + Smolt length + Wind direction^2	17	4644.76	16.49
Month + Smolt length + Air pressure^2	17	4645.73	17.47

Table 6: Fixed effects parameter estimates for the most supported LME-model fitted to predict HR95. The random structure, ID, yielded variance = 0.13±0.37 (SD).

Terms	Estimate	SE	t	p
Intercept	3.07946	0.06532	47.14	0.00014
month2	-0.15493	0.05454	-2.84	0.03511
month3	0.01434	0.04865	0.29	0.29362
month4	0.19387	0.04878	3.97	0.01899
month5	0.37403	0.04453	8.4	0.00445
month6	0.11227	0.05011	2.24	0.05290
month7	-0.07883	0.0502	-1.57	0.09187
month8	0.02772	0.04747	0.58	0.23818
month9	0.04942	0.04629	1.07	0.14840
month10	-0.01084	0.04864	-0.22	0.30361
month11	0.07816	0.04945	1.58	0.09104
month12	-0.01487	0.04514	-0.33	0.28705
Smolt length	-0.08186	0.04613	-1.77	0.07702

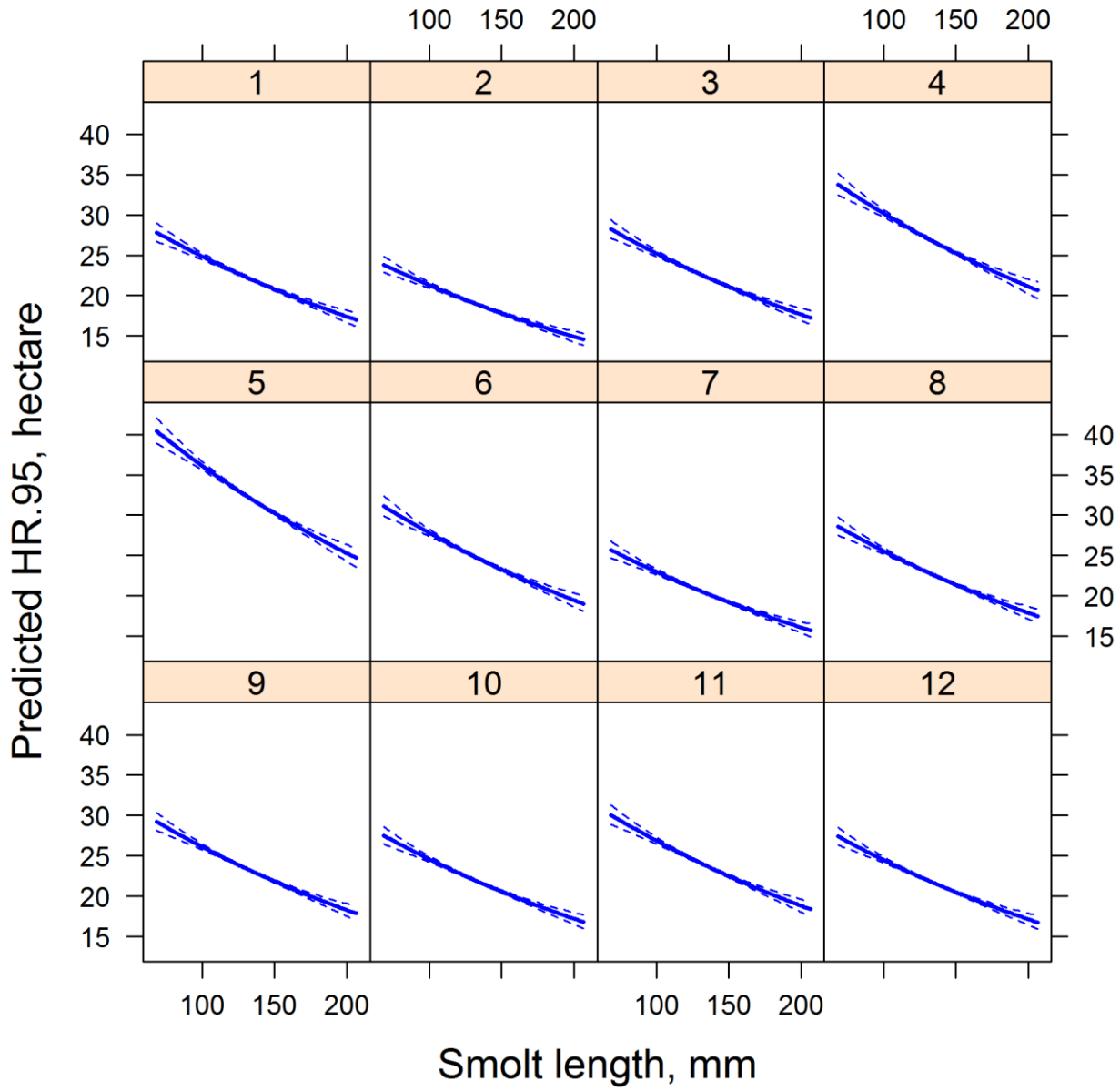

Figure 13: Prediction plot showing predicted 95 % home range (hectare) dependent on smolt length (mm) for each month of the year. The predictions where gathered from the most supported LME-model reported in Table 5.

3.05 Turboness

The model selection results showed two supporting models fitted to predict log-transformed turboness (Table 7). The most supported model revealed purely additive effects of month, smolt length and air temperature^2, and an additive effect of month and smolt length for the second-most supported LME-model.

The turboness-effect in the most supported model was almost entirely dependent on the smolt length, as illustrated in Figure 14. The turboness increased with increasing smolt length, however decreased with increasing temperature. The temperature effect were low though (Table 8). The effect of turboness were high in the summer, and increase from June to September, where the significance also was highest.

The prediction plot for the second most supported model (Figure 15) showed a trend that increasing smolt length increased the turboness. The turbo-effect also grew stronger from June towards September (Table 9), where the significance also is strongest.

Table 7: AIC values for the five most supported LME-model structures fitted to predict ln(turboness) in HR95. The models were fitted using ID as a random factor. A complete AIC table is provided in the Appendix (Table A4).

Models	df	AIC	ΔAIC
Month + Smolt length + Air temperature^2	17	3534.89	
Month + Smolt length	15	3536.02	1.13
Month + Smolt length + Air pressure	16	3537.72	2.83
Month + Smolt length * Air pressure	17	3540.87	5.97
Month + Smolt length + Air pressure^2	17	3545.06	10.17

Table 8: Fixed effects parameter estimates for the most supported LME-model fitted to predict turboness in HR.95. The random structure, ID, yielded variance = 0.11±0.33 (SD).

Term	Estimate	SE	t	p
Intercept	5.62365	0.06325	88.91000	0.00004
month2	0.08395	0.04615	1.82000	0.07381
month3	0.08534	0.04247	2.01000	0.06316
month4	0.05708	0.04516	1.26000	0.12301
month5	0.07853	0.04419	1.78000	0.07636
month6	0.16880	0.05363	3.15000	0.02914
month7	0.25591	0.06053	4.23000	0.01685
month8	0.31690	0.05558	5.70000	0.00950
month9	0.41491	0.04975	8.34000	0.00451
month10	0.21328	0.04738	4.50000	0.01498
month11	-0.00660	0.04282	-0.15000	0.31131
month12	0.10958	0.03963	2.77000	0.03670
Smolt length	0.09392	0.04179	2.25000	0.05250
Air temperature	-0.06694	0.01529	-4.38000	0.01577
Air temperature^2	-0.00326	0.00953	-0.34000	0.28533

Table 9: Fixed effects parameter estimates for the second most supported LME-model fitted to predict turboness in HR.95. The random structure, ID, yielded variance = 0.11±0.33 (SD).

Term	Estimate	SE	t	p
Intercept	5.70416	0.05794	98.46000	0.00003
month2	0.08880	0.04626	1.92000	0.06792
month3	0.06490	0.04126	1.57000	0.09187
month4	0.00475	0.04138	0.11000	0.31450
month5	-0.00109	0.03779	-0.03000	0.31802
month6	0.03161	0.04251	0.74000	0.20568
month7	0.06879	0.04259	1.62000	0.08782
month8	0.14873	0.04027	3.69000	0.02178
month9	0.28842	0.03928	7.34000	0.00580
month10	0.13617	0.04128	3.30000	0.02677
month11	-0.02955	0.04195	-0.70000	0.21363
month12	0.08422	0.03829	2.20000	0.05451
Smolt length	0.09505	0.04169	2.28000	0.05135

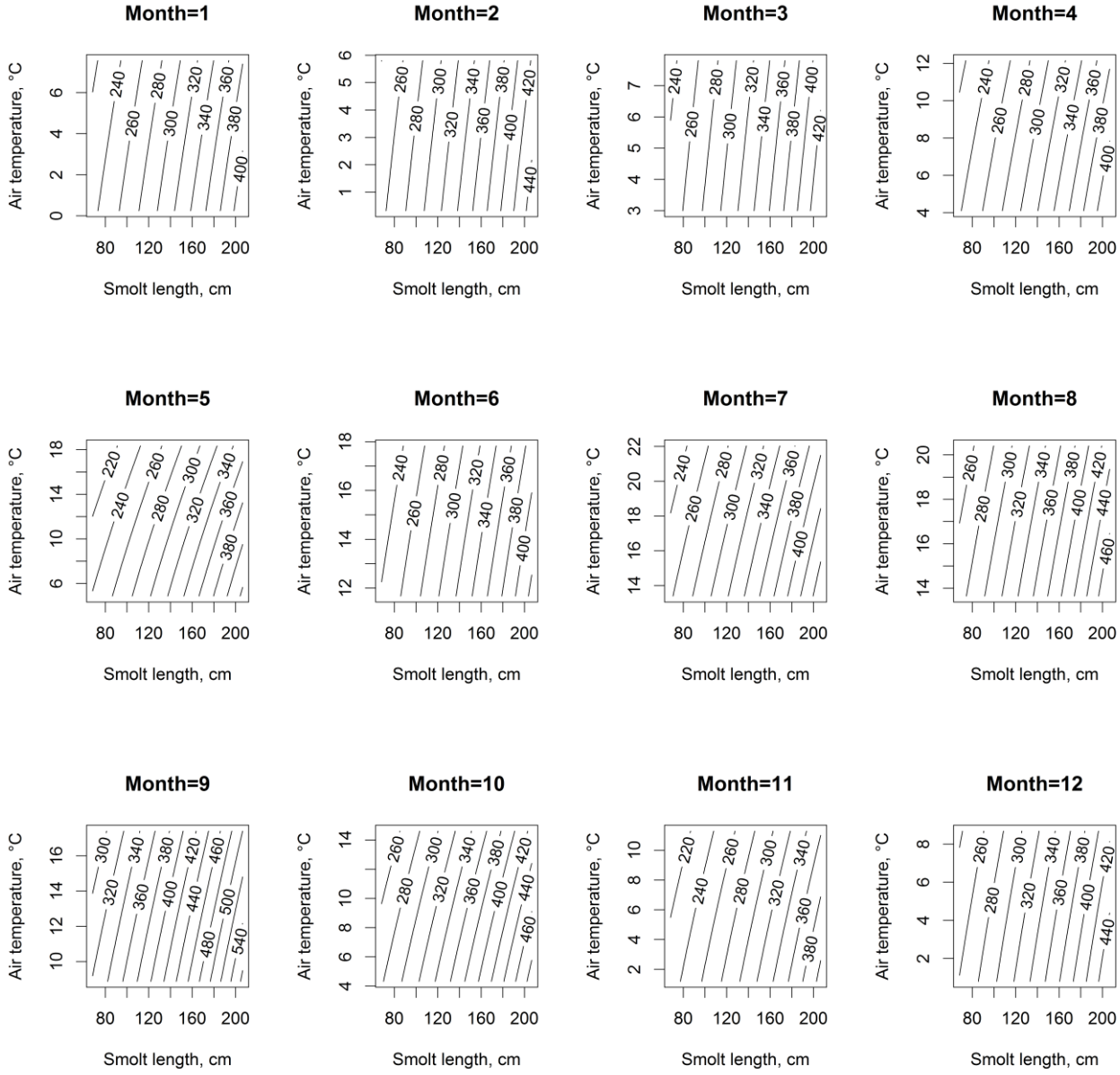

Figure 14: Prediction plot showing predicted turboness (m/hectare/day) within home range 95 dependent on smolt length (mm) and air temperature (°C) for each month of the year. The predictions where gathered from the most supported LME-model reported in Table 7.

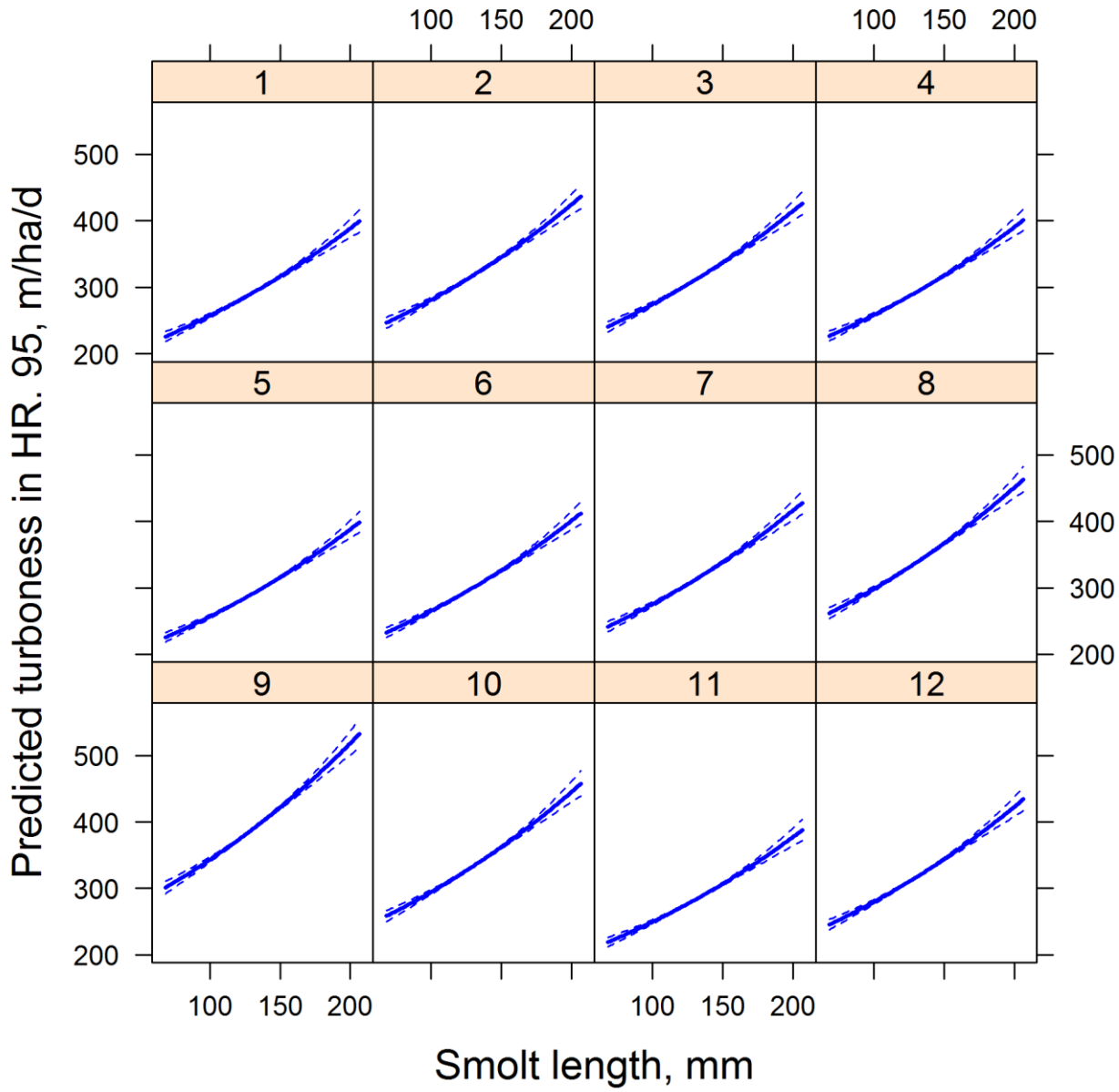

Figure 15: Prediction plot showing predicted turboness (m/hectare/day) within home range 95 dependent on smolt length (mm) for each month of the year. Head numbers indicating months. The predictions where gathered from the most supported LME-model reported in Table 8.

3.06 Total daily distance

Two models where fitted to predict the log-transformed results for the total distance per day (in meters) (Table 10). The most supported LME-model revealed additive effects of month, smolt length and air pressure^2, and the second most supported model showed factorial effects of month, smolt length and air pressure.

The prediction plot for the most supported LME-model (Figure 16) illustrate additive effects that describe the mean total distance per day, where the air pressure weights the prediction of mean total distance per day compared with the smolt length. At a given air pressure of approximately 1000 hPa, the mean total distance were at its lowest, with increasing distance with increasing and decreasing air pressure interconnected with increasing smolt length. The effects of smolt length and air pressure on the mean total distance where however low. The effect of total distance per day where high from April to June, and from August to October (Table 11). The total distance was at its peak in May, and at its lowest in July.

Figure 17 shows the far more complex interactions that describes the second most supported model. The plot reveals saddle points, which mean that the mean total distance per day increases with increasing air pressure and increasing smolt length, but also increases with decreasing air pressure and decreasing smolt length. These effects where however low (Table 12). The monthly effects were also in this model strongest from April to June, and August to October, where the effect was strongest and most significant in May and lowest in July.

Table 10: AIC values for the five most supported LME-model structures fitted to predict ln(total distance). The models were fitted using ID as a random factor. A complete AIC table is provided in the Appendix (Table A5).

Models	**df**	**AIC**	**ΔAIC**
Month + Smolt length + Air pressure^2	17	2665.62	
Month + Smolt length * Air pressure	17	2666.14	0.52
Month + Smolt length * Air pressure^2	19	2670.05	4.43
Month + Smolt length + Air pressure	16	2671.20	5.58
Month + Smolt length + Air pressure^2 + Air temperature^2	19	2676.14	10.52

Table 11: Fixed effects parameter estimates for the most supported LME-model fitted to predict total distance. The random structure, ID, yielded variance = 0.03±0.17 (SD).

Terms	Estimate	SE	t	p
Intercept	8.78467	0.03874	226.73000	0.00001
month2	-0.05991	0.04075	-1.47000	0.10070
month3	0.04451	0.03645	1.22000	0.12792
month4	0.17259	0.03647	4.73000	0.01362
month5	0.36724	0.03301	11.12000	0.00255
month6	0.12243	0.03733	3.28000	0.02707
month7	-0.05153	0.03752	-1.37000	0.11064
month8	0.14803	0.03538	4.18000	0.01723
month9	0.31265	0.03433	9.11000	0.00379
month10	0.11012	0.03614	3.05000	0.03090
month11	0.03497	0.03686	0.95000	0.16731
month12	0.05221	0.03357	1.56000	0.09270
Smolt length	0.00983	0.02334	0.42000	0.27058
Air pressure	0.04190	0.00714	5.87000	0.00898
Air pressure^2	0.01818	0.00446	4.08000	0.01804

Table 12: Fixed effects parameter estimates for the second most supported LME-model fitted to predict total distance. The random structure, ID, yielded variance = 0.03±0.17 (SD).

Terms	Estimate	SE	t	p
Intercept	8.79759	0.03859	227.98000	0.00001
month2	-0.05184	0.04067	-1.27000	0.12182
month3	0.06378	0.03624	1.76000	0.07768
month4	0.17721	0.03647	4.86000	0.01293
month5	0.35955	0.03298	10.90000	0.00266
month6	0.12026	0.03733	3.22000	0.02800
month7	-0.04959	0.03753	-1.32000	0.11607
month8	0.14820	0.03539	4.19000	0.01715
month9	0.31475	0.03434	9.17000	0.00374
month10	0.12284	0.03603	3.41000	0.02521
month11	0.05587	0.03676	1.52000	0.09615
month12	0.06426	0.03343	1.92000	0.06792
Smolt length	0.01341	0.02335	0.57000	0.24025
Air pressure	0.02980	0.00646	4.61000	0.01430
Smolt length: Air pressure	-0.02495	0.00636	-3.92000	0.01945

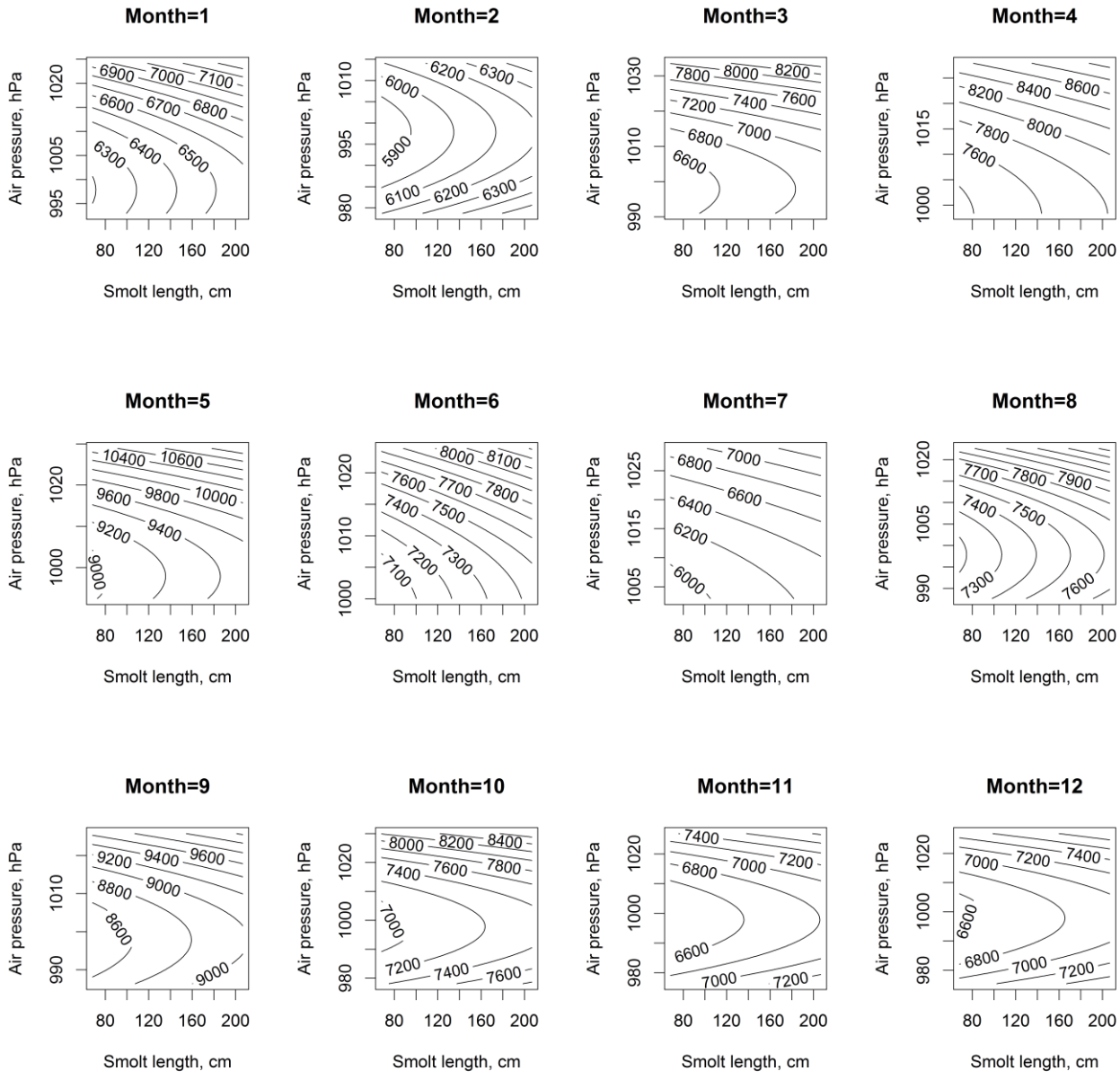

Figure 16: Prediction plot showing total distance (meters) dependent on smolt length (mm) and air pressure (hPa) for each month of the year. Head numbers indicating months. The predictions where gathered from the most supported LME-model reported in Table 10.

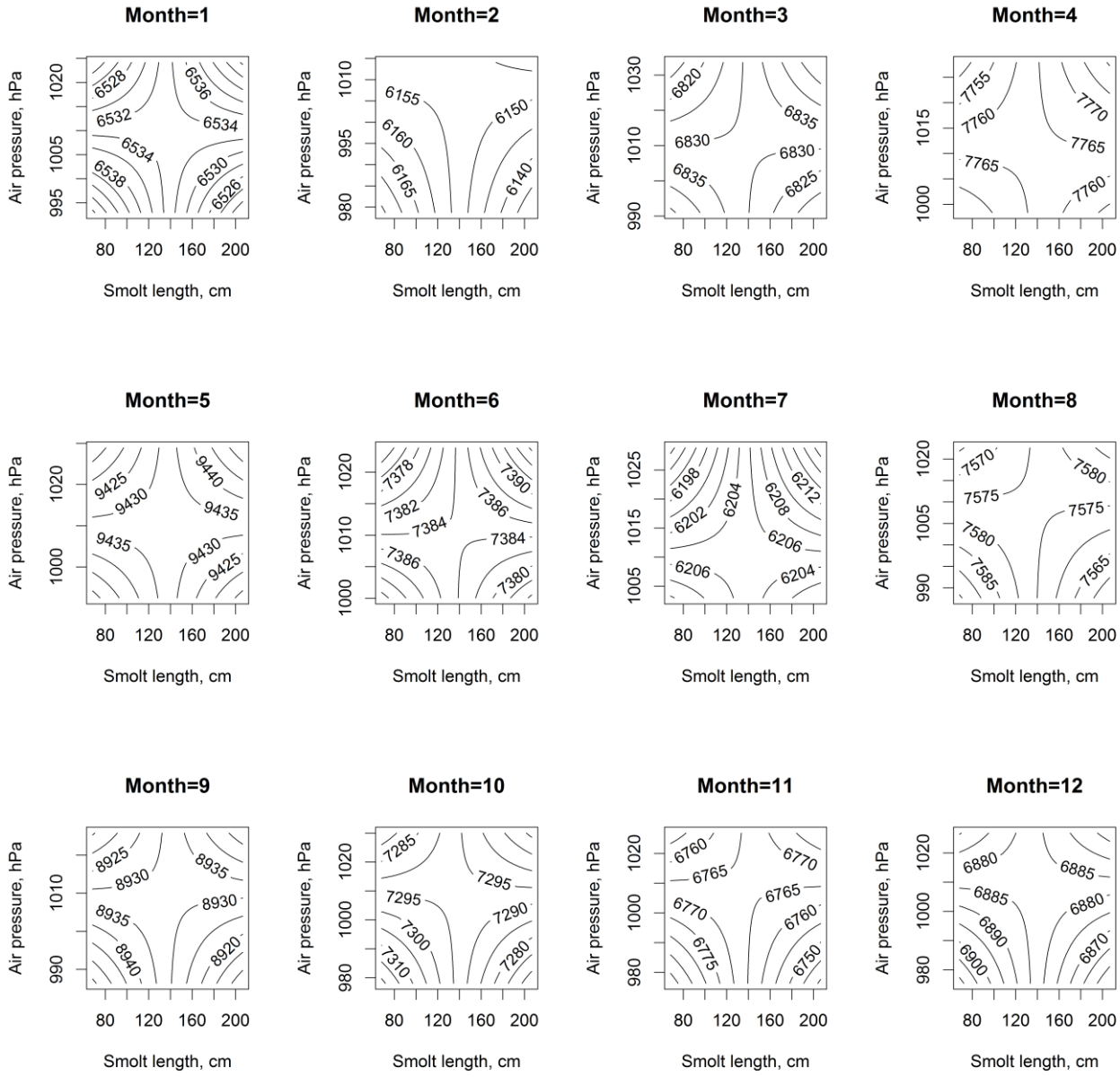

Figure 17: Prediction plot showing total distance (meters) dependent on smolt length (mm) and air pressure (hPa) for each month of the year. Head numbers indicating months. The predictions where gathered from the second most supported LME-model reported in Table 10.

3.07 Depth use

The model selection for the log-transformed mean depth use (Table 13), showed complex and exclusively factorial effects of month, smolt length and air pressure^2. The corresponding ANOVA-test revealed highly significant interaction effects (Table 14). The fixed effect parameters estimates for the most supported LME-model fitted to predict mean depth use, are available from Table A7.

The depth use is, throughout the year, almost entirely dependent on smolt length. However, in the months May, August and September, the air pressure may explain the depth use also (Figure 18). In August, there is an optimum depth use at around 1010 hPa. At the same optimum, the depth use increases even further with increasing smolt length. The maximum mean depth utilization from January to April is heavily dependent on smolt length, whereas fish with longer smolt length had a deeper mean depth. The depth use trend from Figure 18 indicate a shallow use in the water layers, with depths ranging from around 0.7 to 7 meters, independent of the max depth at the location.

Table 13: AIC values for the five most supported LME-model structures fitted to predict ln(mean depth use). The models were fitted using ID as a random factor. A complete AIC table is provided in the Appendix (Table A6).

Models	**df**	**AIC**	**ΔAIC**
Month * Smolt length * Air pressure^2	74	837902.304	
Month * Smolt length * Air pressure	50	841782.151	3879.84735
Month + Smolt length * Air pressure^2 + Air temperature^2 + Wind speed^2 + Wind direction^2 + Precipitation^2	27	841899.627	3997.32313
Month + Smolt length + Air pressure^2 + Air temperature^2 + Wind speed^2 + Wind direction^2	23	842260.503	4358.1994
Month + Smolt length + Air pressure^2 + Air temperature^2 + Wind speed^2 + Wind direction^2 + Precipitation^2	25	842267.162	4364.85881

Table 14: The ANOVA test of the most supported LME-model that explain the log-transformed mean depth use per day.

Analysis of Deviance Table (Type II Wald chisquare tests)			
	Chisq	Df	Pr (>Chisq)
month	40455.75	11	<2e-16
Smolt.length	2.1093	1	0.1464
poly(PO, 2, raw = T)	1736.057	2	<2e-16
month:Smolt.length	2382.414	11	<2e-16
month:poly(PO, 2, raw = T)	7765.791	22	<2e-16
Smolt.length:poly(PO, 2, raw = T)	215.5371	2	<2e-16
month:Smolt.length:poly(PO, 2, raw = T)	929.4314	22	<2e-16

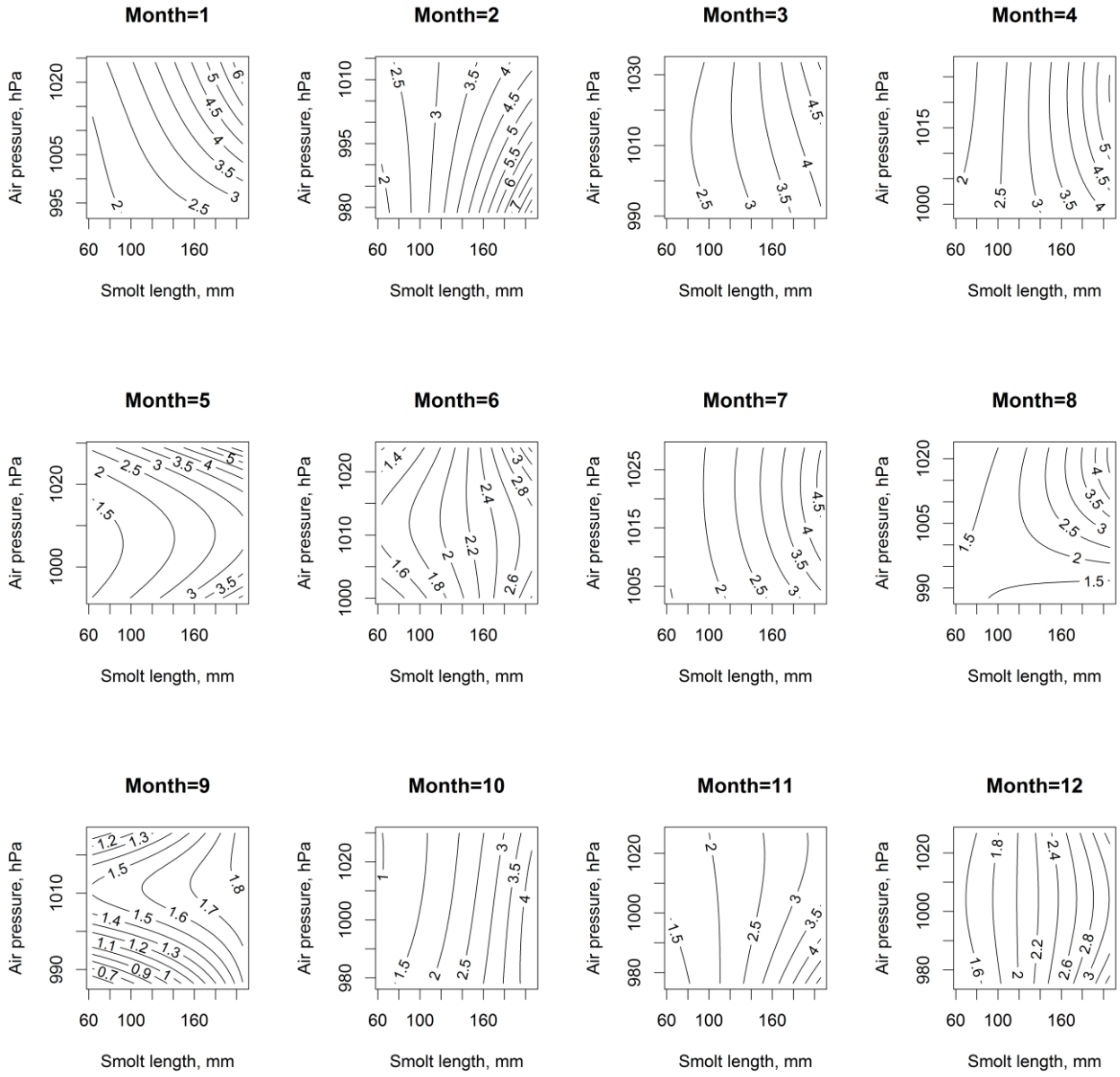

Figure 18: Prediction plot showing the mean depth utilization dependent on smolt length (mm) and air pressure (hPa). The predictions where gathered from the most supported LME-model reported in Table 13.

3.08 Utilization volume 50

The results of the utilization volume 50 (UV 50) were backward-selected because of complex interactions. The complete list of fixed effects parameter estimates for the most supported LME-model fitted to predict log-transformed UV 50, is presented in Table A9. The most supported LME-model showed complex interactions effects of month, smolt length and air temperature^2 (Table 15). The corresponding ANOVA-test revealed significant interaction effects (Table 16).

From February to May, UV 50 increased with air temperature and smolt length, however best explained by the individual's smolt lengths (Figure 19). During the warm summer moths of June and July, the UV 50 became reduced. In June, the UV 50 was optimal at approximately 14 ^{o}C. In August, the UV 50 is again increased, but was reduced in September and the following autumn months. However, with an optimum temperature each month to explain the spatiotemporal usage. In November the usage is union with the smolt length, and only dependent on the air temperature.

Table 15: AIC values for the five most supported LME-model structures fitted to predict ln(UV 50). The models were fitted using ID as a random factor. A complete AIC table is provided in the Appendix (Table A8).

Models	**df**	**AIC**	**ΔAIC**
Models	df	AIC	ΔAIC
Month + Smolt length + Air temperature^2 + Month:Smolt.length + Month:Air temperature^2	50	16973.7269	
Month + Smolt length + Air temperature^2 + Month:Smolt.length + Month:Air temperature^2 + Smolt.length:Air temperature^2	52	16984.5119	10.7849669
Month * Smolt length * Air temperature^2	74	16993.7988	20.0718808
Month * Smolt length	26	17000.6108	26.8839072
Month * Smolt length + Air pressure	27	17004.9495	31.2225236

Table 16: The ANOVA test of the most supported LME-model that explain the log-transformed UV 50.

Analysis of Deviance Table (Type II Wald chisquare tests)			
	Chisq	Df	Pr(>Chisq)
month	303.3157	11	< 2.2e-16
Smolt.length	0.0409	1	0.83965
poly(TA.all, 2, raw = T)	5.2802	2	0.07135
month:Smolt.length	61.7722	11	4.34E-09
month:poly(TA.all, 2,raw = T)	67.3572	22	1.71E-06

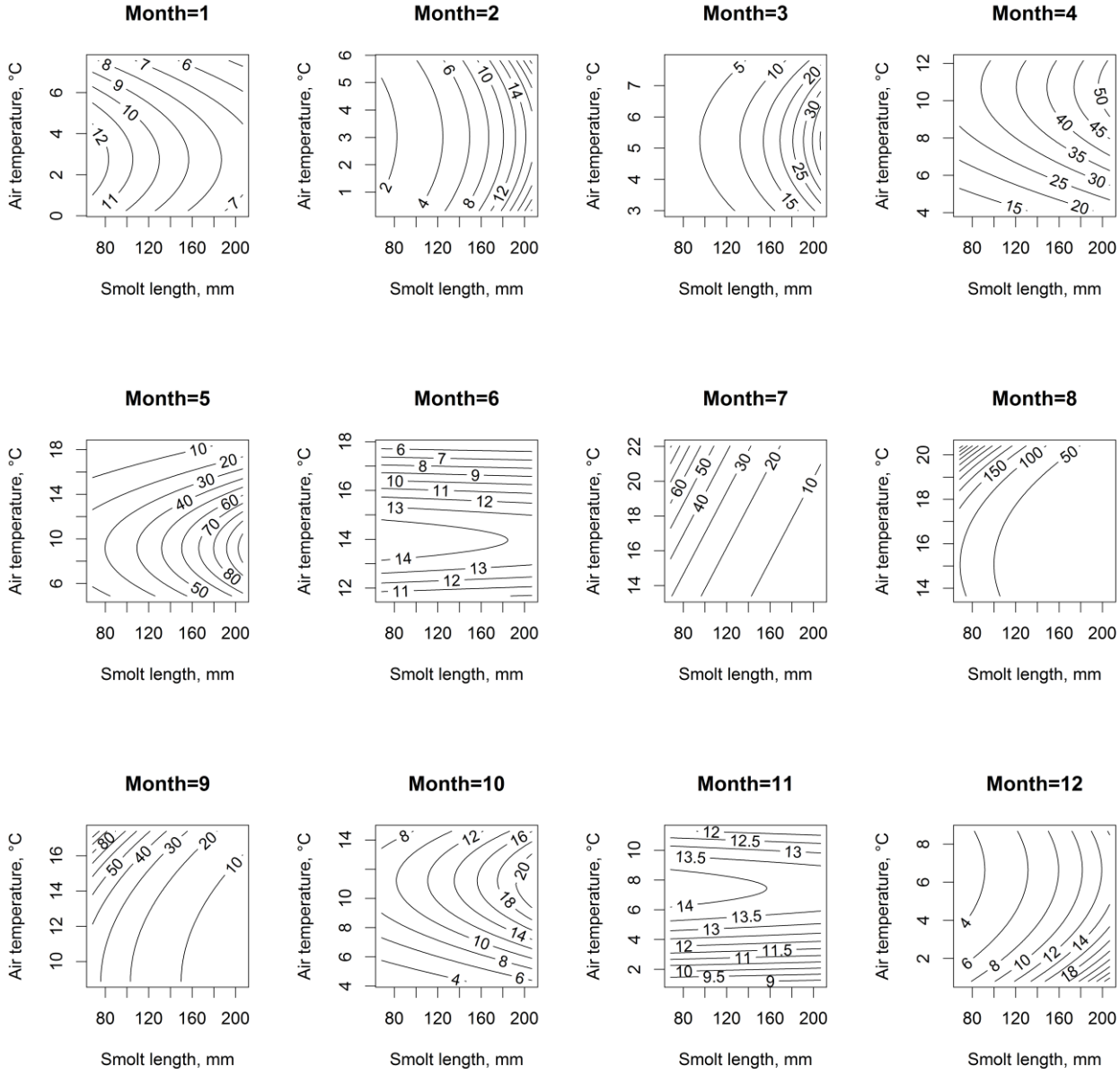

Figure 19: Prediction plot showing UV 50 (gigaliters, 10^9 L) dependent on smolt length (mm) and air temperature (°C). The predictions where gathered from the most supported LME-model reported in Table 15, and are divided by 1000 to simplify the numbers.

3.09 Utilization volume 95

The most supported LME-model to explain utilization volume 95 (UV 95) showed fully factorial effects between month and smolt length (Table 17). In the prediction plot (Figure 20), there were trends towards increased UV 95 from February to May with increased smolt length. In June, UV 95 was compressed and reduced. From July to October, the trend where opposite. The UV 95 decreased with increasing smolt length. From October to January, the UV 95 was again compressed and reduced, however with a weak increase with increasing smolt length. However, the effect of the smolt length on the UV 95 was low, with low significance (Table 18). The effect of the UV 95 where highest in April and May, whereas significance also where high (Table 18).

Table 17: AIC values for the five most supported LME-model structures fitted to predict ln(UV 95). The models were fitted using ID as a random factor. A complete AIC table is provided in the Appendix (Table A10).

Models	df	AIC	ΔAIC
Month * Smolt length	26	16633	
Month * Smolt length + Air temperature^2	28	16635.79	2.79
Month * Smolt length * Air temperature^2	74	16638.04	5.03
Month * Smolt length + Air pressure	27	16638.31	5.31
Month + Smolt length	15	16639.11	6.1

Table 18: Fixed effects parameter estimates for the most supported LME-model fitted to predict UV 95. The random structure, ID, yielded variance = 1.68±1.30 (SD).

Terms	Estimate	SE	t	p
(Intercept)	10.15674	0.22724	44.7	0.00016
month2	-0.40238	0.18173	-2.21	0.05410
month3	0.08531	0.16624	0.51	0.25261
month4	1.06631	0.16563	6.44	0.00749
month5	1.45395	0.15371	9.46	0.00352
month6	0.33177	0.16279	2.04	0.06167
month7	0.55038	0.16979	3.24	0.02768
month8	0.8853	0.164	5.4	0.01055
month9	0.48189	0.16521	2.92	0.03341
month10	0.22097	0.17333	1.27	0.12182
month11	0.33236	0.1725	1.93	0.06737
month12	-0.08305	0.15714	-0.53	0.24850
Smolt.length	0.02239	0.22722	0.1	0.31516
month2:Smolt.length	0.52084	0.23791	2.19	0.05492
month3:Smolt.length	0.38278	0.17668	2.17	0.05576
month4:Smolt.length	0.03103	0.17847	0.17	0.30937
month5:Smolt.length	0.15779	0.16847	0.94	0.16899
month6:Smolt.length	-0.0202	0.18905	-0.11	0.31450
month7:Smolt.length	-0.27043	0.19203	-1.41	0.10653
month8:Smolt.length	-0.44176	0.18389	-2.4	0.04709
month9:Smolt.length	-0.31128	0.18609	-1.67	0.08401
month10:Smolt.length	0.16191	0.2085	0.78	0.19790
month11:Smolt.length	0.16171	0.19412	0.83	0.18847
month12:Smolt.length	0.17127	0.17082	1	0.15915

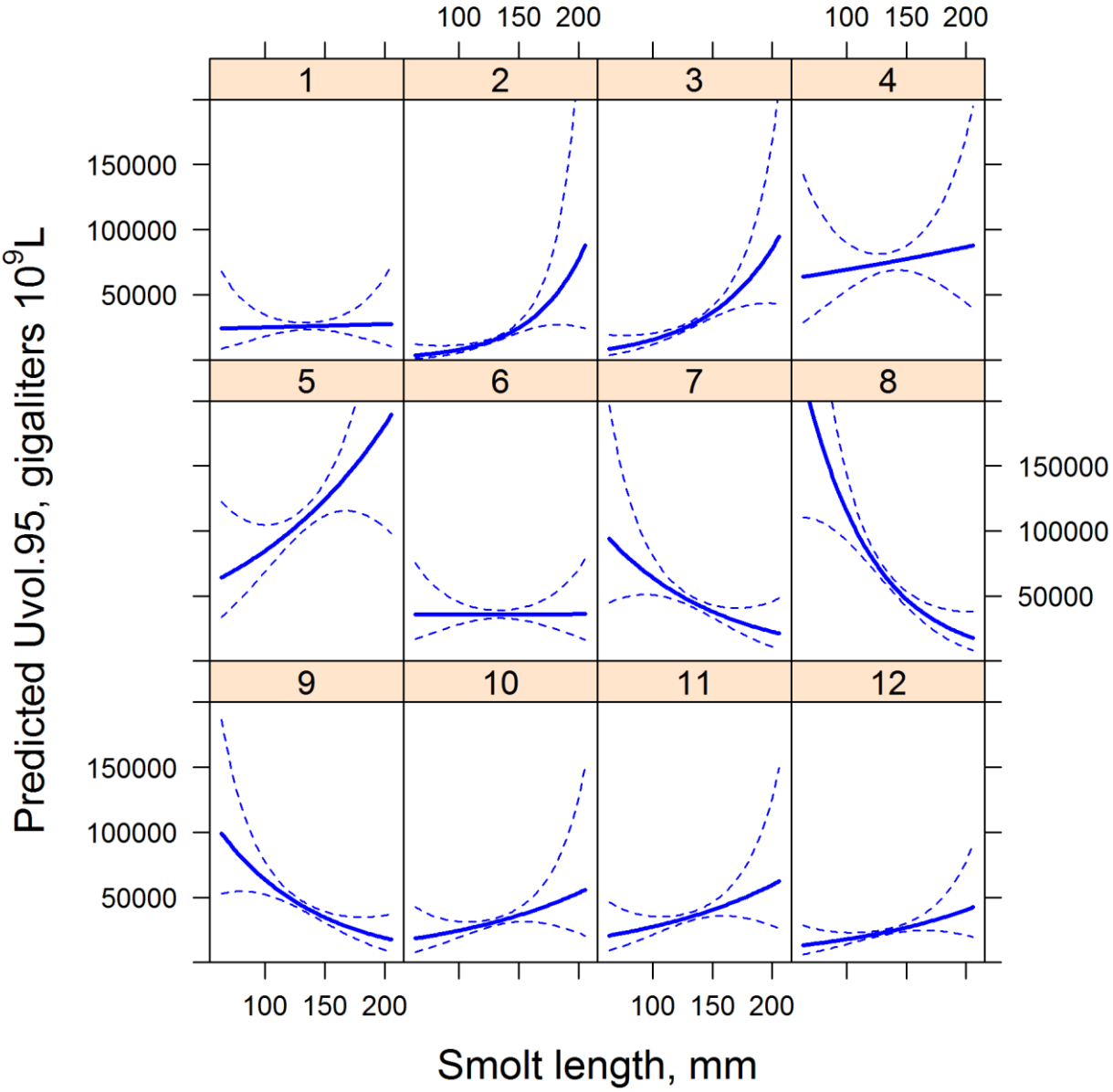

Figure 20: Prediction plot showing UV 95 (gigaliters, 10^9 L) dependent on smolt length (mm). The predictions where gathered from the most supported LME-model reported in Table 17.

3.10 Probability of using the no-take zone

The most supported no-take zone model revealed fully factorial effects among month, length at capture and the smolt length (Table 19). The complete list of logit parameter estimates for the most supported LME-model, is presented in Table A12. The corresponding ANOVA test indicate highly significant interaction effect among month, length at capture and smolt length (Table 20).

The prediction plot (Figure 21Table 11) for the most supported model showed complex and fluctuating effects between smolt length and length at capture during the year. In the winter months from December to March, there was a uniform trend where length at capture determined the use of the no-take zone, whereas longer individuals had a higher utilization of the zone. In the months May and June, there was a clear smolt length effect, whereas individuals with shorter smolt lengths had a higher probability of utilizing the no-take zone. In the transitions between spring and summer, and summer to autumn, there were strong interaction effects between smolt length and length at capture.

Table 19: AIC values for the five most supported LME-model structures fitted to predict probability of using the no-take zone. The models were fitted using ID as a random factor. A complete AIC table is provided in the Appendix in Table A11.

Model	df	AIC	ΔAIC
Month * Length * Smolt length	49	220817.7	
Month * Smolt length * Air pressure^2	73	225122.4	4304.722289
Month * Smolt length * Air temperature^2	73	226311.6	5493.973514
Month * Smolt length * Air pressure	49	226508.6	5690.982044
Month * Smolt length * Precipitation^2	73	228223.6	7405.955556

Table 20: The ANOVA test of the most supported LME-model that explain the probability of using the no-take zone.

Analysis of Deviance Table (Type II Wald chisquare tests)			
	Chisq	Df	Pr(>Chisq)
month	5953.812	11	< 2.2e-16
Length	26.427	1	2.74E-07
Smolt.length	124.455	1	< 2.2e-16
month:Length	2534.019	11	< 2.2e-16
month:Smolt.length	10845.95	11	< 2.2e-16
Length:Smolt.length	2.409	1	0.1206
month:Length:Smolt.length	6352.501	11	< 2.2e-16

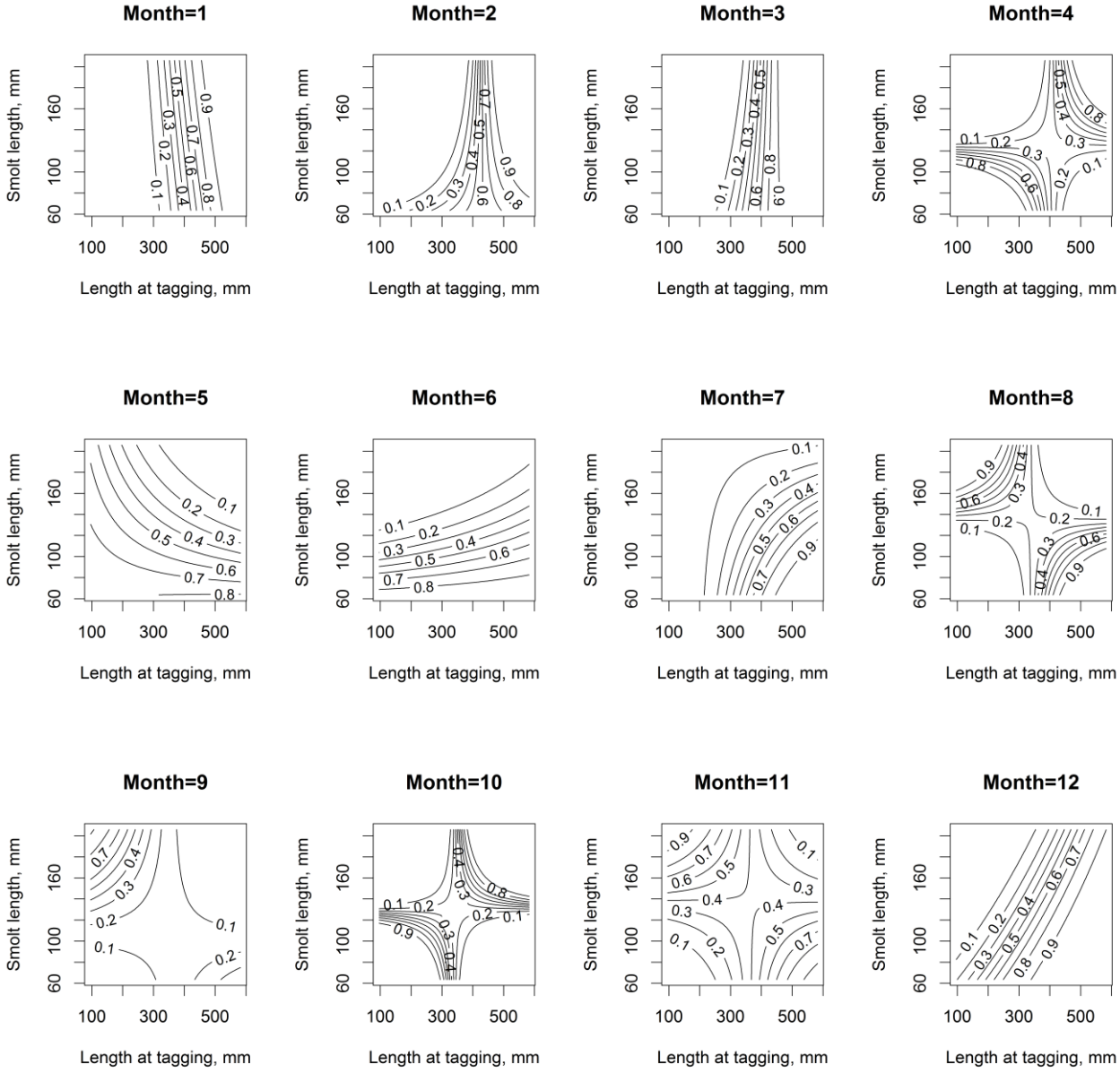

Figure 21: Prediction plot showing the probability of using the no-take zone in Tvedestrandsfjorden dependent on smolt length (mm) and length at capture (mm). The predictions where gathered from the most supported LME-model reported in Table 19

3.11 Fate and use of no-take zone

The model selection among candidate models fitted to predict fates of the monitored individuals favored fully factorial effects among the probability of using the no-take zone, smolt length and length at capture (Table 21). The utilization of the no-take zone from individuals with the final fate as “alive” and “caught” are illustrated in Figure 22 and Figure 23. The two plots show that the individuals that are caught utilize the fjord more frequently during the entire year, compared to the individuals that are alive at the end of the study.

The prediction plot (Figure 24) for the most supported fate model showed complex effects of probability of using the no-take zone, length at capture and smolt length. The individuals that finally emigrated from the study area had all the same trend at an optimum smolt length at approximately 130-140 mm; with decreasing length at tagging, the chance of emigration increased. This effect increased even further with increasing use of the no-take zone.

The non-harvest mortality were highest with small individuals, and the effect increased the larger these small individuals were as smolt. The non-harvest mortality among these individuals, increased with increasing use of the no-take zone. Small individuals that also were small as smolt, experienced the same high non-harvest mortality, and the effect increased with increasing use of the no-take zone.

The catchability were highest with large individuals, and this effect was stronger the larger these large individuals were as smolt. Interestingly, the larger individuals had higher catchability the more they utilized the no-take zone. Small individuals, that also were small as smolt, also experienced high probability of being caught with increasing utilization of the no-take zone.

The probability of staying alive, favored only individuals with short length at tagging. This effect increased with increasing probability of using the no-take zone.

Table 21: All AIC values for the supported LME-model structures fitted to predict the fate dependent on the use of the no-take zone and individual characteristics.

Model	df	AIC	AIC
Probability of no-take * Smolt length * Length	24	1043400	
Probability of no-take + Smolt length * Length	15	1107378	63978
Probability of no-take * Smolt length + Length	15	1203410	160010
Probability of no-take + Smolt length + Length	12	1223143	179743
Probability of no-take * Length	12	1229228	185828
Probability of no-take + Length	9	1247204	203804
Probability of no-take * Smolt length	12	1306050	262650
Probability of no-take + Smolt length	9	1322441	279041
Probability of no-take	6	1348328	304928

Table 22: Logit parameter estimates for the fate of the individuals that utilize the no-take zone, compared with

	Caught			Dead			Emigrated	
Term	Estimate	SE		Estimate	SE		Estimate	SE
Intercept	-33.9755	1.23E-06		-54.2776	1.56E-06		-54.2767	1.4E-06
prob.notake	96.14128	1.03E-06		-20.4002	1.03E-06		38.79681	1.23E-06
Smolt.length	0.307073	0.000169		0.507036	0.0002		0.524299	0.000158
Length	0.119382	0.000115		0.179051	0.000109		0.171985	0.00012
prob.notake:Smolt.length	-0.84732	0.000121		0.036847	0.000128		-0.36978	0.000152
prob.notake:Length	-0.34034	0.000141		0.018902	0.000125		-0.14276	0.00013
Smolt.length:Length	-0.001	8.4E-07		-0.00159	9.7E-07		-0.00161	9.7E-07
prob.notake:Smolt.length:Length	0.002885	1.11E-06		0.000151	1.03E-06		0.001293	1.01E-06

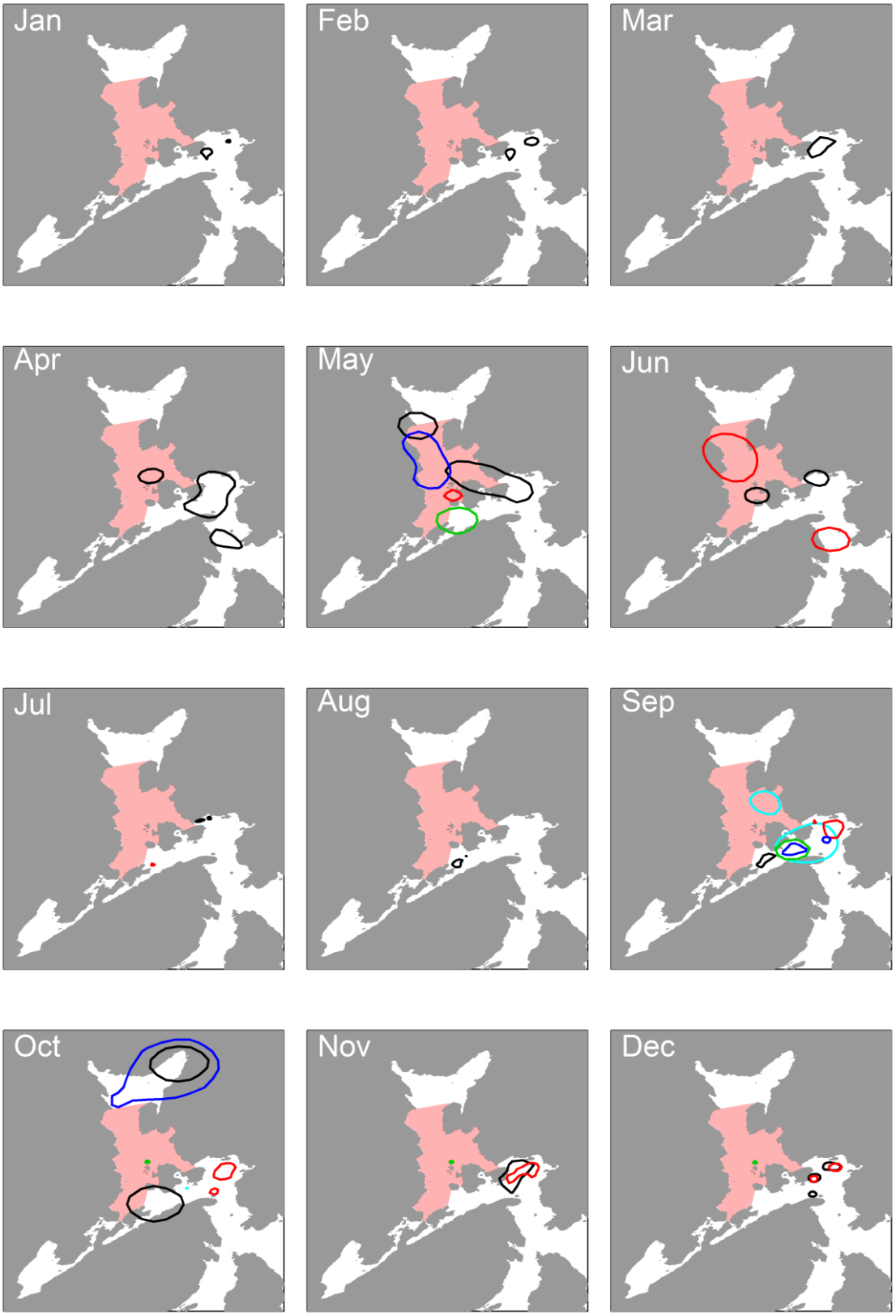

Figure 22: Prediction plot showing the HR.50 compared with the no-take zone (pink area) of individuals that are alive in the end of the study period. . The colored circles are not linked to one unique individual, but may be several different individuals from each month. Logit parameters reported in Table 22.

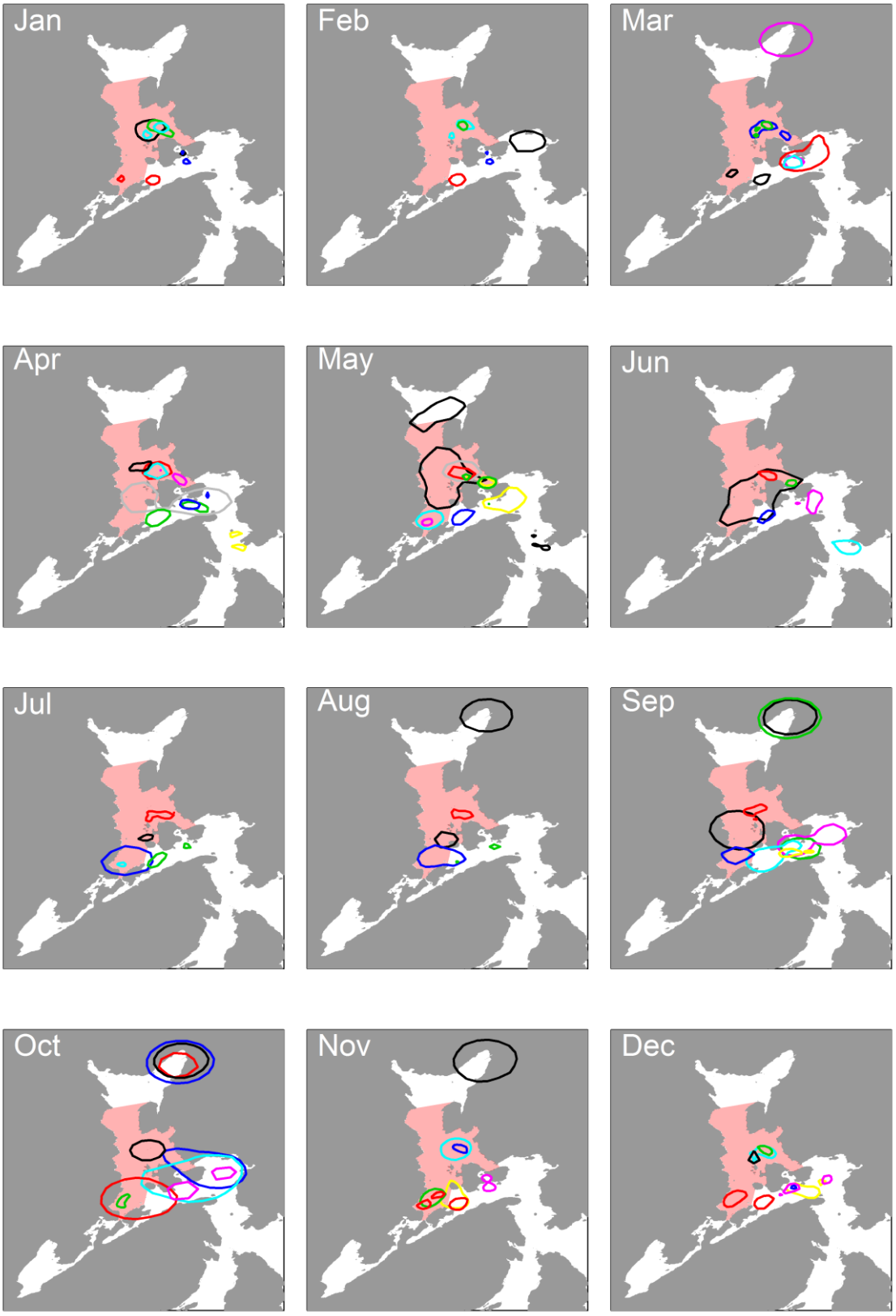

Figure 23: Prediction plot showing the HR.50 compared with the no-take zone (pink area) of individuals that are caught in the end of the study period. The colour circles are not linked to one unique individual, but may be several different individuals from each month. Logit parameters reported in Table 22.

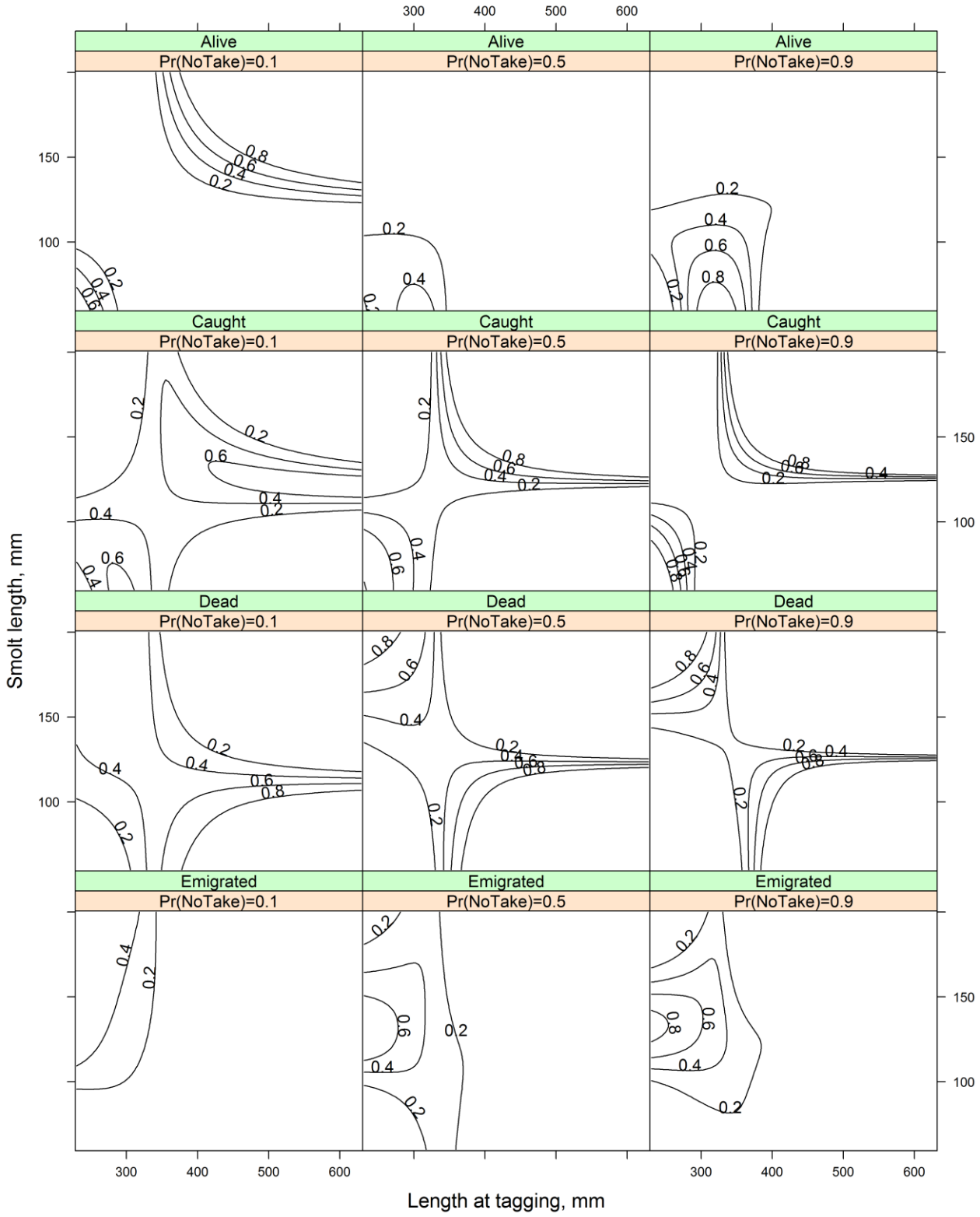

Figure 24: Prediction plot showing the fates dependent on smolt length (mm) and length at tagging (mm) as isoclines of three probability chances (0.1, 0.5 and 0.9) of using the no-take zone. The predictions where gathered from the most supported fate-test provided in Table 21.

4. Discussion

4.01 Fates and no-take zone utilization

In the present study, smolt length, air temperature and air pressure had strong effects on the space use in Tvedestrandsfjorden. In addition did smolt length, length at capture and probability of using the no-take zone highly influence the fates and behavior of the sea trout in the fjord. Of these variables, smolt length was the one variable that showed significance and decisive effects on all behavior traits.

Horizontal and vertical activity of the sea trout varied throughout the year. The results indicated increased activity from April towards June, and in early autumn from August towards October, while activity was reduced in July and the winter months. This may be interconnected with seasonal feeding intensity. Earlier examinations of feeding activity of sea trout indicated that the fish fed most heavily during spring (April-May)(Pemberton 1976b) and autumn (August-September) (Borgstrøm & Heggenes 1988; Knutsen et al. 2001b; Olsen et al. 2006), with a minimum during July (Knutsen et al. 2001b) and the winter months (Rikardsen et al. 2006). However, the activity peaks also coincide and may be explained with smolt migration from freshwater to the sea in the spring (Jonsson 1985; Jonsson & Gravem 1985), spawning activity in the autumn (Jonsson 1985; Elliott 1994; Klemetsen et al. 2003), and possibly optimal growth temperatures (Elliott 1975; L'Abèe-Lund et al. 1989; Forseth et al. 2009; Jensen et al. 2014).

The smolt length and length at capture affected the probability of using the no-take zone, and these three variables highly influenced the fates of the sea trout in Tvedestrandsfjorden. With increasing smolt length, individuals had characteristics towards increased turboness, mean depth, mean total daily distance and increased utilization volume in autumn. However, increased smolt length gave reduced utilization distribution. Moreover, individuals with smaller smolt length had increased utilization volume in spring, however not in autumn. The utilization distribution increased during both spring and autumn with decreasing smolt length. The depth use was also at a minimum in September with decreasing smolt length. The present findings correlates with observations recorded by Dzadey (2014), who also found that smolt length highly influenced the distribution and activity of sea trout in the marine environment.

Individuals with large smolt length may have been more exposed to fishing as they had high activity and increased utilization volume in the spring. However, individuals with smaller smolt length were also exposed. These individuals had the largest utilization distribution during the entire year, and high utilization volume in the autumn. If individuals with smolt length resulting in high activity did not have their distribution pattern inside the no-take zone, probability of mortality to harvest would increase even further.

The mean back-calculated smolt length (Figure 11) at 131.9 ± 27.7 mm, with a minimum and a maximum length of 60.3 mm and 203.0 mm, respectively, are within the smolt lengths recorded in several other sea trout studies in the Aust-Agder. Ingebrigtsen (1998) recorded the mean smolt length to be 120 ± 38 mm in Østeråbekken. In the nearby river Langangselva, the smolt length was somewhat larger and had a mean length of 143 ± 0.90 mm (L'Abèe-Lund et al. 1989). L'Abèe-Lund et al. (1989) explained varying smolt lengths to be influenced by abiotic factors, in which increasing river length, water discharge and latitude seemed to give increased smolt length, while smolt length decreased highly with decreasing temperature at sea.

The no-take zone in Tvedestrandsfjorden had a varying impact on the sea trout fate, as illustrated in Figure 24. Large individuals, which also had large smolt length, showed high probability of being caught. However, individuals with small sizes, which also had small smolt lengths, were also exposed to high catchability as well. Surprisingly, these trends were applied with increasing utilization of the no-take zone. However, non-harvest mortality also played a significant part of the final fates and survival in the fjord. Small individuals, which had small smolt length, and large individuals with small smolt length, had high probability of non-harvest mortality. These trends increased even further with high utilization of the no-take zone. The fate results indicated that the harvest selection favored sea trout with "middle size" (i.e. 300 mm), which also had intermediate smolt length. These individuals had the highest probability of survival. This suggest that the mortality in Tvedestrandsfjorden is size-selective from the recreational fisheries, whereas the no-take zone only has a limited size-dependent protection efficacy where reproducing and future reproducing individuals are less safeguarded. Such size selective harvest can alter the population dynamics towards reduced growth rate, smaller average size and smaller age and size at spawning, resulting in reduced fitness of the sea trout population (Olsen & Moland 2011).

4.02 Harvest selection

Fish harvesting will never be random, and is thus selective. Some individuals with predictable behavior or size may be more vulnerable to harvesting, influencing the population and adaptive behavior (Allendorf et al. 2008). Individuals having bold and active behavior are especially exposed to fishing, as their behavior might actually increase the selective mortality, and they may locally be removed from populations during long-term harvest (Biro & Stamps 2008). Studies of cod and largemouth bass (*Micropterus salmoides*) with hook-and-line, showed a correlation between the possibility of catch and the behavior of the fish, whereas individuals caught with hook-and-line had a very different behavior and moving pattern compared to those that were caught with nets (Philipp et al. 2009; Bøe 2013). The cod in Tvedestrandsfjorden also suffered from intense harvest pressure, with significant selection towards older and larger individuals (Olsen et al. 2012). The present study has shown that sea trout in Tvedestrandsfjorden are exposed to size-selective harvest. Recreational and commercial fishing could therefore contribute to a change of the gene pool of the afflicted population, and alter the adaptive behavior and preference of habitat utilization, which influence the growth and survival of the individuals (Conover & Munch 2002; Biro & Stamps 2008; Allendorf & Hard 2009; Olsen & Moland 2011).

After analyzing the scales of the specimens in my study, I got strong indications that the sea trout in Tvedestrandsfjorden remained in the marine environment the entire year. Compared with scales from resident freshwater brown trout, these scales showed lesser indications to growth stagnation during the winter (pers. comm Reidar Borgstrøm). After entering the marine environment, the sea trout is inclined to remain there, with exceptions of mature individuals who leave the marine environment in the autumn to spawn in freshwater for a short time, only to return swiftly to brackish fjord areas as post-spawners (Borgstrøm & Heggenes 1988). Similar lasting marine behavior have been observed earlier in coastal Aust-Agder (Knutsen et al. 2004; Olsen et al. 2006) and even by Pemberton (1976a) in Scotland, where they documented feeding by sea trout during the entire winter season. However, the winter-feeding was probably not with the sole purpose of growth. Olsen et al. (2006) believed the feeding was to utilize maintenance and lipid deposition, especially after spawning. Spent fish have low energy reserves and need to increase the feeding (Knutsen et al. 2004). Olsen et al. (2006) also believed that continued marine stay is due to higher survival and reduced migratory cost of immature sea trout. However, such marine winter residency indicate that

the sea trout unfortunately is exposed to fishing harvest also during the winter, and thus the entire year in Tvedestrandsfjorden.

4.03 Fjord residency

In later years has the concept of partial migration in the marine environment received much attention and recognition. Several studies have documented that the sea trout actually may remain in high numbers in a fjords inner coastal systems during their entire marine stay (Knutsen et al. 2001b; Knutsen et al. 2004; Olsen et al. 2006), without a continuum migration to the sea (Urke et al. 2010; Aldvén et al. 2014; Davidsen et al. 2014c; del Villar-Guerra et al. 2014). The sea trout in Tvedestrandsfjorden had a tendency towards fjord residency, whereas 32% of the tagged sea trout emigrated and 68% remained in the system. This differ somewhat, but not greatly from the observations published by del Villar-Guerra et al. (2014), who found that 53% of the tagged sea trout emigrated and 47% remained. They found no evidence that size (length or weight) nor body condition (Fulton's K) affected the fate.

However, Bendall et al. (2005) saw that migration in coastal waters were size dependent, whereas larger fish migrated faster and further than smaller fish. Davidsen et al. (2014c) also found migration to be size dependent, but at smolt level. Larger and older smolts had a longer continuum migration, though these individuals also had poorer body conditions than the fjord residents. These findings differ somehow from the present study. I found that the smolt length highly influenced the marine behavior, and that short lengths at tagging in the marine environment induced emigration from the fjord. The seaward migration alternatives may also be affected by nutritional status (Boel et al. 2014; Davidsen et al. 2014b) and lipid depletion (Boel et al. 2014) in addition to smolt length prior to the downward journey from the spawning stream to the marine environment. Individuals with high growth rate as 0+ and poor growth as 1+, but still had high metabolic needs, sought better conditions at sea and migrated (Jonsson & Jonsson 1993; Forseth et al. 1999; Cucherousset et al. 2005). The energy storage and condition of the fish may thus decide the distance of migration when entering the marine environment, whereas individuals with low energetic levels and low lipid depositions as smolts are inclined to a shortened partial migration within the fjord (Sheridan 1989; Jonsson & Jonsson 1998; Forseth et al. 1999; Boel et al. 2014; Davidsen et al. 2014b). If these individuals also have a high metabolic demand, the chance of fjord residency increase even further, if these needs are fulfilled with early encounters of suitable habitats (Cucherousset et al. 2005). This can also explain the negative tendency of migration if the distance and cost of

wandering exceeds the internal energetic status of the smolts (Kristoffersen et al. 1994; Jonsson & Jonsson 2006), and force the individuals to an early partial migration and fjord residency.

Other studies (Davidsen et al. 2014a; del Villar-Guerra et al. 2014) including the current results, indicate a relative high ratio of lacking returns of the local sea trout to their natal spawning areas. After an emigration and migration continuum to the outer coastal areas and the sea, these individuals have an uncertain fate, but may have dispersed to other coastal areas. Earlier examination from coastal Aust-Agder shows colonization and dispersal of sea trout to new fjords and river systems (Knutsen et al. 2001a). This may help explain the high emigration ratio, and might as well be a genetic dispersal mechanism within the sea trout species (Bekkevold et al. 2004).

4.05 Acoustic telemetry

Acoustic telemetry is now one of the most cost and labor-effective methods to monitor marine habitat utilization (Kessel et al. 2014), however climatic and biological factors may alter the detection rate and results of the ultrasonic hydrophones. Wind and waves may highly affect the detection rate of hydrophones, together with rain and the depth of the hydrophones (Gjelland & Hedger 2013). Stratification and thermocline creation following different seasons, with tidal and flood currents may also create variability and reduced detection rates. (Mathies et al. 2014). Sound travels faster in increasing water temperature, fish at depths of 4-5 meters have therefor the highest probability of detection. However, probability of detection may decrease if the receiver is located deep and the transmitter is above the thermocline (Gjelland & Hedger 2013). In the present study, the depth utilization showed favoring depths between 1-5 meters. The data may therefore have some errors caused by wind and waves, however the depth utilization where at levels of high detection rate. Optimal days of detections of sea trout may thus be clear warm days with little wind disturbance.

To minimize errors, detection ranges should be tested before, during and after a study. A sentinel receiver may also be placed and act as a reference to detection tests (Kessel et al. 2014). The kernel method which smooth's the utilization distribution will easily uncover areas with high activity (Worton 1987), though optimized interpolation of the spatiotemporal utilization will highly depend on the kernel size. A box kernel will give higher errors than a

"normal" kernel, and additionally a high density of hydrophones will give significantly reduced errors (Hedger et al. 2008).

Biological errors caused by predation could however be difficult to counteract. Cod, sea birds and seals are present in Tvedestrandsfjorden and could predate especially young sea trout (Lyse et al. 1998; Dieperink et al. 2001). Data may have been corrupted if a tagged individual was consumed by a cod or caught by larger predatory animals. There may actually be a chance that some of the data were recordings from within a cod, however such inconceivable errors may not last longer than a few days before the tag has passed through the cod (Zeller 1999).

4.06 Reproducibility

This study is unique as there have been few studies on the spatiotemporal use of sea trout in their marine habitat, and in a short fjord system with a mosaic of depths, habitats and no estuaries. The reproducibility to other studies may therefore be limited. However, studies conducted in similar fjord systems or in Southern-Norway east of Lindesnes may officiate. Studies conducted in quite different systems, such as long shallow fjords, almost as lake systems towards the sea in Denmark (Boel et al. 2014; del Villar-Guerra et al. 2014), or long and very deep fjords at the west coast and in northern parts of Norway (Jensen & Rikardsen 2008; Urke et al. 2010; Davidsen et al. 2014c) may be less comparable. The arrangement of the receivers are also highly important. The current study has used a long-term triangulation setting of receivers to maximize coverage of Tvedestrandsfjorden, whereas other studies used "curtains" of receivers as transects crossing the fjords at certain sections (Aldvén et al. 2014; Davidsen et al. 2014c; Jensen et al. 2014). Curtain arrangement of the receivers will not give the same detailed XY positioning opportunity, and will therefore not have the same basis of comparison. The latitudinal difference between Europe and Norway also has consequences for the life-history of the sea trout as well (Jonsson & L'Abèe-Lund 1993).

4.07 Management implications

The MPA in Tvedestrandsfjorden probably has a positive impact on species biomass, distribution and abundance, however the results may be improved with adjusted management implications. The present study has demonstrated that large and small sea trout are barely

protected, even with high utilization of the no-take zone. These individuals are thus highly exposed to harvest and non-harvest mortality. This is unfortunately the reproducing and future recruiting part of the population (Jonsson 1985; Klemetsen et al. 2003; Jonsson & Jonsson 2006). These individuals have the highest importance for the population, and without actions, the sea trout population in Tvedestrandsfjorden can suffer severe harvest selection deformities (Conover & Munch 2002; Hansen et al. 2002; Olsen et al. 2012). Today, there exist a lower catch size limit of 35 cm when fishing sea trout in southern Norway (Lovdata 2003), and fishing in Tvedestrandsfjorden is restricted to hook-and-line use outside the no-take zone. Possible new regulations are ponderations between usage and preservation, and have to be feasible and easy to maintain. I suggest that the hook-and-line restriction continues along with the ban of fishing nets. Unintended catches of sea trout in nets will then be avoided, and other species such as the limited fjord cod may thrive from such regulations. However, I also suggest that a slot limit is introduced, as the objective is to conserve the population and perhaps increase future available fishing stock. This will result in a lower and upper catch size limit when fishing sea trout. In that way, both reproducing and future reproducing individuals are protected, and recreational and sport fishing activity of sea trout can be sustained.

Another management implication is the possibility to expand the no-take zone southwards, and include the Sagesund conservation zone. The incorporation of the Sagesund conservation zone will secure the highly trafficable sea trout areas around the south of Furøya and Hestøya. A larger no-take zone may also have positive biologic effects not only for the sea trout, but also obviously for the other species in the fjord. The cod utilize the deeper areas of the Fruøya and Sagesund zones as spawning territory (Ciannelli et al. 2010), and will benefit a larger no-take zone. This species is of highly commercial and recreational interest and can influence the decision towards preservation, if the increased no-take-zone gives an increased harvest to the neighboring areas.

Future measures to improve the spawning and nursery areas in freshwater, must be done with great care and consideration. Results from the present study indicate that measures that can alter the smolt length, will influence the life history and behavior of the sea trout in the marine environment. Ultimately, measures that change the smolt length, may influence the efficacy of the no-take zone.

5. Conclusion

The marine protected area in Tvedestrandsfjorden has a limited size-biased protection efficiency towards sea trout. The harvest of sea trout is highly size-biased as well, resulting in a limited survival of 14% within in the fjord. The current protection protocol would probably benefit from a revision. I suggest that today's restrictions are continued, with an extension of a maximum landing size. A size-slot limited harvest will secure reproduction and future reproducing individuals of sea trout in the fjord system. Currently, the no-take zone seem to be too small for a relevant protection of all size groups of se trout, but what a relevant protection area would be remains enigmatic.

The marine behavior of the sea trout seems to be highly influenced by smolt length, and hence the life and development in early stages in freshwater. More studies on individual traits like growth, metabolism and lipid deposition of sea trout compared to their utilization of the marine environment, will give a better understanding of the behavior and life history of the sea trout in coastal waters.

6. References

Akaike, H. (1974). A new look at the statistical model identification. *Automatic Control, IEEE Transactions on*, 19 (6): 716-723.

Aldvén, D., Hedger, R., Økland, F., Rivinoja, P. & Höjesjö, J. (2014). *Migration of sea trout (Salmo trutta) smolts and kelts through a complex costal habitat*. PhD. Unpublished: University of Gothenburg, Institution of Biology and Environmental Sciences.

Allendorf, F. W., England, P. R., Luikart, G., Ritchie, P. A. & Ryman, N. (2008). Genetic effects of harvest on wild animal populations. *Trends in Ecology & Evolution*, 23 (6): 327-337.

Allendorf, F. W. & Hard, J. J. (2009). Human-induced evolution caused by unnatural selection through harvest of wild animals. *Proceedings of the National Academy of Sciences of the United States of America*, 106: 9987-9994.

Alos, J. & Arlinghaus, R. (2013). Impacts of partial marine protected areas on coastal fish communities exploited by recreational angling. *Fisheries Research*, 137: 88-96.

Andrews, K. S., Williams, G. D. & Levin, P. S. (2010). Seasonal and Ontogenetic Changes in Movement Patterns of Sixgill Sharks. *Plos One*, 5 (9): 12.

Bekkevold, D., Hansen, M. M. & Mensberg, K. L. D. (2004). Genetic detection of sex-specific dispersal in historical and contemporary populations of anadromous brown trout Salmo trutta. *Molecular Ecology*, 13 (6): 1707-1712.

Bendall, B., Moore, A. & Quayle, V. (2005). The post-spawning movements of migratory brown trout Salmo trutta L. *Journal of Fish Biology*, 67 (3): 809-822.

Biro, P. A. & Stamps, J. A. (2008). Are animal personality traits linked to life-history productivity? *Trends in Ecology & Evolution*, 23 (7): 361-368.

Bøe, K. (2013). *You are what you get caught with: inter-individual variation in coastal Atlantic cod (Gadus morhua) behaviour.* Master thesis: Norwegian University og Life Science, Department of Ecology and Nature Resource Management. 49 pp.

Boel, M., Aarestrup, K., Baktoft, H., Larsen, T., Madsen, S. S., Malte, H., Skov, C., Svendsen, J. C. & Koed, A. (2014). The Physiological Basis of the Migration Continuum in Brown Trout (Salmo trutta). *Physiological and Biochemical Zoology*, 87 (2): 334-345.

Bohlin, T., Pettersson, J. & Degerman, E. (2001). Population density of migratory and resident brown trout (Salmo trutta) in relation to altitude: evidence for a migration cost. *Journal of Animal Ecology*, 70 (1): 112-121.

Borgstrøm, R. & Heggenes, J. (1988). Smoltification of sea trout(Salmo trutta) at short length as an adaptation to extremely low summer stream flow. *Polskie Archiwum Hydrobiologii/Polish Archives of Hydrobiology*, 35 (3): 375-384.

Bridger, C. J. & Booth, R. K. (2003). The effects of biotelemetry transmitter presence and attachment procedures on fish physiology and behavior. *Reviews in Fisheries Science*, 11 (1): 13-34.

Ciannelli, L., Knutsen, H., Olsen, E. M., Espeland, S. H., Asplin, L., Jelmert, A., Knutsen, J. A. & Stenseth, N. C. (2010). Small-scale genetic structure in a marine population in relation to water circulation and egg characteristics. *Ecology*, 91 (10): 2918-2930.

Claudet, J., Osenberg, C. W., Benedetti-Cecchi, L., Domenici, P., Garcia-Charton, J. A., Perez-Ruzafa, A., Badalamenti, F., Bayle-Sempere, J., Brito, A., Bulleri, F., et al. (2008). Marine reserves: size and age do matter. *Ecology Letters*, 11 (5): 481-489.

Conover, D. O. & Munch, S. B. (2002). Sustaining fisheries yields over evolutionary time scales. *Science*, 297 (5578): 94-96.

Cucherousset, J., Ombredane, D., Charles, K., Marchand, F. & Bagliniere, J. L. (2005). A continuum of life history tactics in a brown trout (Salmo trutta) population. *Canadian Journal of Fisheries and Aquatic Sciences*, 62 (7): 1600-1610.

Davidsen, J. G., Daverdin, M., Arnekleiv, J. V., Ronning, L., Sjursen, A. D. & Koksvik, J. I. (2014a). Riverine and near coastal migration performance of hatchery brown trout Salmo trutta. *Journal of Fish Biology*, 85 (3): 586-596.

Davidsen, J. G., Daverdin, M., Sjursen, A. D., Ronning, L., Arnekleiv, J. V. & Koksvik, J. I. (2014b). Does reduced feeding prior to release improve the marine migration of hatchery brown trout Salmo trutta smolts? *Journal of Fish Biology*, 85 (6): 1992-2002.

Davidsen, J. G., Eldøy, S. H., Sjursen, A. D., Rønning, L., Thorstad, E. B., Næsje, T. F., Aarestrup, K., Whoriskey, F., Rikardsen, A. H., Daverdin, M., et al. (2014c). Habitatbruk og vandringer til sjøørret i Hemnfjorden og Snillfjorden. *NTNU Vitenskapsmuseet naturhistorisk rapport*, 2014-6. 1-51 pp.

de Leeuw, J. J., ter Hofstede, R. & Winter, H. V. (2007). Sea growth of anadromous brown trout (Salmo trutta). *Journal of Sea Research*, 58 (2): 163-165.

del Villar-Guerra, D., Aarestrup, K., Skov, C. & Koed, A. (2014). Marine migrations in anadromous brown trout (Salmo trutta). Fjord residency as a possible alternative in the continuum of migration to the open sea. *Ecology of Freshwater Fish*, 23 (4): 594-603.

Dieperink, C., Pedersen, S. & Pedersen, M. I. (2001). Estuarine predation on radiotagged wild and domesticated sea trout (Salmo trutta L.) smolts. *Ecology of Freshwater Fish*, 10 (3): 177-183.

Dzadey, C. S. K. (2014). *Coastal habitat us in sea trout (Salmo trutta) from the inner parts of Oslo Fjord: a one-year acoustic temeletry study*. Master thesis. Ås: Norwegian University of Life Science, Departement of Ecology and Natural resource management 45 pp.

Elliott, J., M. (1994). *Quantitative Ecology and the Brown Trout*. UK: Oxford University Press. 286 pp.

Elliott, J. M. (1975). The Growth Rate of Brown Trout (Salmo trutta L.) Fed on Maximum Rations. *Journal of Animal Ecology*, 44 (3): 805-821.

Elliott, J. M. (1989). Wild brown trout salmo-trutta - An important national and international resource. *Freshwater Biology*, 21 (1): 1-5.

Fiske, P. & Aas, Ø. (2001). *Laksefiskeboka. Om sammenhenger mellom beskatning, fiske og verdiskaping ved elvefiske etter laks, sjøaure og sjørøye*, vol. 20: Trondheim, Stiftelsen for naturforskning og kulturminneforskning.

Forseth, T., Naesje, T. F., Jonsson, B. & Harsaker, K. (1999). Juvenile migration in brown trout: a consequence of energetic state. *Journal of Animal Ecology*, 68 (4): 783-793.

Forseth, T., Larsson, S., Jensen, A. J., Jonsson, B., Näslund, I. & Berglund, I. (2009). Thermal growth performance of juvenile brown trout Salmo trutta: no support for thermal adaptation hypotheses. *Journal of Fish Biology*, 74 (1): 133-149.

Francis, R. (1990). Back-calculation of fish length - a critical-review. *Journal of Fish Biology*, 36 (6): 883-902.

Friedlander, A. M. & Monaco, M. E. (2007). Acoustic tracking of reef fishes to elucidate habitat utilization patterns and residence times inside and outside marine protected areas around the island of St. John, USVI.

Frost, W., E. & Brown, M., E. (1967). *The Trout*. The New Naturalist. London: Collins. 286 pp.

Gjelland, K. O. & Hedger, R. D. (2013). Environmental influence on transmitter detection probability in biotelemetry: developing a general model of acoustic transmission. *Methods in Ecology and Evolution*, 4 (7): 665-674.

Gordon, M. S. (1959). Ionic regulation in the brown trout (Salmo trutta L.). *Journal of Experimental Biology*, 36 (2): 227-252.
Hansen, M. M., Ruzzante, D. E., Nielsen, E. E., Bekkevold, D. & Mensberg, K. L. D. (2002). Long-term effective population sizes, temporal stability of genetic composition and potential for local adaptation in anadromous brown trout (Salmo trutta) populations. *Molecular Ecology*, 11 (12): 2523-2535.
Harris, G. & Milner, N. (eds). (2006). *Sea Trout: Biology, Conservation and Management*: Blackwell Publishing Ltd. 520 pp.
Hedger, R. D., Martin, F., Dodson, J. J., Hatin, D., Caron, F. & Whoriskey, F. G. (2008). The optimized interpolation of fish positions and speeds in an array of fixed acoustic receivers. *Ices Journal of Marine Science*, 65 (7): 1248-1259.
Helland, A., Lindholm, O., Traaen, T., Uriansrud, F. & Rygg, B. (2003). Tiltaksplan for forurensede sedimenter i Aust-Agder. Fase 1- Miljøtilstand, kilder og prioriteringer, LNR 4744-2003: NIVA. 55 pp.
Heupel, M. R., Simpfendorfer, C. A. & Hueter, R. E. (2004). Estimation of shark home ranges using passive monitoring techniques. *Environmental Biology of Fishes*, 71 (2): 135-142.
Heupel, M. R. & Webber, D. M. (2012). Trends in Acoustic Tracking: Where are the Fish Going and How Will We Follow Them? In McKenzie, J. R., Parsons, B., Seitz, A. C., Kopf, R. K., Mesa, M. G. & Phelps, Q. (eds) American Fisheries Society Symposium, vol. 76 *Advances in Fish Tagging and Marking Technology*, pp. 219-231. Bethesda: Amer Fisheries Soc.
Hightower, J. E., Jackson, J. R. & Pollock, K. H. (2001). Use of telemetry methods to estimate natural and fishing mortality of striped bass in Lake Gaston, North Carolina. *Transactions of the American Fisheries Society*, 130 (4): 557-567.
Hyrenbach, K. D., Forney, K. A. & Dayton, P. K. (2000). Marine protected areas and ocean basin management. *Aquatic Conservation-Marine and Freshwater Ecosystems*, 10 (6): 437-458.
Ingebrigtsen, P. J. (1998). *Livshistorie hos ørret (Salmo trutta L.) i små kystvassdrag i Aust-Agder*. Ås: Norges Landbrukshøgskole, Insitutt for biologi og naturforvaltning. 43 pp.
Jensen, J. L. A. & Rikardsen, A. H. (2008). Do northern riverine anadromous Arctic charr Salvelinus alpinus and sea trout Salmo trutta overwinter in estuarine and marine waters? *Journal of Fish Biology*, 73 (7): 1810-1818.
Jensen, J. L. A., Rikardsen, A. H., Thorstad, E. B., Suhr, A. H., Davidsen, J. G. & Primicerio, R. (2014). Water temperatures influence the marine area use of Salvelinus alpinus and Salmo trutta. *Journal of Fish Biology*, 84 (6): 1640-1653.
Jensen, K., W. (1968). Seatrout (Salmo trutta, L.) of the River Istra, western Norway. *Report of the Institute of Freshwater reaserch, Drottningholm*, 48: 187-213.
Johnson, D., Ardron, J., Billett, D., Hooper, T., Mullier, T., Chaniotis, P., Ponge, B. & Corcoran, E. (2014). When is a marine protected area network ecologically coherent? A case study from the North-east Atlantic. *Aquatic Conservation-Marine and Freshwater Ecosystems*, 24: 44-58.
Jonsson, B. (1976). Comparison of scales and otoliths for age-determination in brown trout, salmo-trutta-L. *Norwegian Journal of Zoology*, 24 (4): 295-301.
Jonsson, B. (1985). Life History Patterns of Freshwater Resident and Sea-Run Migrant Brown Trout in Norway. *Transactions of the American Fisheries Society*, 114 (2): 182-194.
Jonsson, B. & Gravem, F. R. (1985). Use of space and food by resident and migrant brown trout, salmo-trutta. *Environmental Biology of Fishes*, 14 (4): 281-293.
Jonsson, B. & Jonsson, N. (1993). Partial migration - niche shift versus sexual-maturation in fishes. *Reviews in Fish Biology and Fisheries*, 3 (4): 348-365.

Jonsson, B. & L'Abèe-Lund, J. H. (1993). Latitudinal clines in life-history variables of anadromous brown trout in europe. *Journal of Fish Biology*, 43: 1-16.
Jonsson, B. (2000). Sjøaure. In Borgstrøm, R. & Hansen, L., P. (eds) *Fisk i ferskvann - Et samspill mellom bestander, miljø og forvaltning*, pp. 50-59: Landbruksforlaget.
Jonsson, B., Jonsson, N., Brodtkorb, E. & Ingebrigtsen, P. J. (2001). Life-history traits of Brown Trout vary with the size of small streams. *Functional Ecology*, 15 (3): 310-317.
Jonsson, B. & Jonsson, N. (2006). Life-history effects of migratory costs in anadromous brown trout. *Journal of Fish Biology*, 69 (3): 860-869.
Jonsson, B. & Jonsson, N. (2011). *Ecology of Atlantic Salmon and Brown Trout - Habitat as a template for life histories*. Fish & Fisheries Series, vol. 33: Springer. 708 pp.
Jonsson, N. & Jonsson, B. (1998). Body composition and energy allocation in life-history stages of brown trout. *Journal of Fish Biology*, 53 (6): 1306-1316.
Jonsson, N. & Jonsson, B. (1999). Trade-off between egg mass and egg number in brown trout. *Journal of Fish Biology*, 55 (4): 767-783.
Jonsson, N. & Jonsson, B. (2002). Migration of anadromous brown trout Salmo trutta in a Norwegian river. *Freshwater Biology*, 47 (8): 1391-1401.
Keeley, E. R. & Grant, J. W. (1995). Allometric and environmental correlates of territory size in juvenile Atlantic salmon (Salmo salar). *Canadian Journal of Fisheries and Aquatic Sciences*, 52 (1): 186-196.
Kellner, J. B., Tetreault, I., Gaines, S. D. & Nisbet, R. M. (2007). Fishing the line near marine reserves in single and multispecies fisheries. *Ecological Applications*, 17 (4): 1039-1054.
Kessel, S. T., Cooke, S. J., Heupel, M. R., Hussey, N. E., Simpfendorfer, C. A., Vagle, S. & Fisk, A. T. (2014). A review of detection range testing in aquatic passive acoustic telemetry studies. *Reviews in Fish Biology and Fisheries*, 24 (1): 199-218.
Klemetsen, A., Amundsen, P.-A., Dempson, J. B., Jonsson, B., Jonsson, N., O'Connell, M. F. & Mortensen, E. (2003). Atlantic salmon Salmo salar L., brown trout Salmo trutta L. and Arctic charr Salvelinus alpinus (L.) - a review of aspects of their life histories. *Ecology of freshwater fish*, 12: 1-59.
Knip, D. M., Heupel, M. R. & Simpfendorfer, C. A. (2012). Evaluating marine protected areas for the conservation of tropical coastal sharks. *Biological Conservation*, 148 (1): 200-209.
Knutsen, H., Knutsen, J. A. & Jorde, P. E. (2001a). Genetic evidence for mixed origin of recolonized sea trout populations. *Heredity*, 87: 207-214.
Knutsen, J. A., Knutsen, H., Gjosaeter, J. & Jonsson, B. (2001b). Food of anadromous brown trout at sea. *Journal of Fish Biology*, 59 (3): 533-543.
Knutsen, J. A., Knutsen, H., Olsen, E. M. & Jonsson, B. (2004). Marine feeding of anadromous Salmo trutta during winter. *Journal of Fish Biology*, 64 (1): 89-99.
Knutsen, J. A., Knutsen, H., Rinde, E., Christie, H., Bodvin, T. & Dahl, E. (2010). Mapping Biological Resources in the Coastal Zone: An Evaluation of Methods in a Pioneering Study from Norway. *Ambio*, 39 (2): 148-158.
Kramer, D. L., Rangeley, R. W. & Chapman, L. J. (1997). Habitat selection: patterns of spatial distribution from behavioural decisions. *Behavioural ecology of teleost fishes*: 37-80.
Kristoffersen, K., Halvorsen, M. & Jorgensen, L. (1994). Influence of parr growth, lake morphology, and fresh-water parasites on the degree of anadromy in different populations of arctic char (salvelinus-alpinus) in northern norway. *Canadian Journal of Fisheries and Aquatic Sciences*, 51 (6): 1229-1246.

L'Abèe-Lund, J. H., Jonsson, B., Jensen, A. J., Saettem, L. M., Heggberget, T. G., Johnsen, B. O. & Naesje, T. F. (1989). Latitudinal variation in life-history characteristics of sea-run migrant brown trout salmo-trutta. *Journal of Animal Ecology*, 58 (2): 525-542.

Lee, W. C. & Bergersen, E. P. (1996). Influence of thermal and oxygen stratification on lake trout hooking mortality. *North American Journal of Fisheries Management*, 16 (1): 175-181.

Lester, S. E., Halpern, B. S., Grorud-Colvert, K., Lubchenco, J., Ruttenberg, B. I., Gaines, S. D., Airame, S. & Warner, R. R. (2009). Biological effects within no-take marine reserves: a global synthesis. *Marine Ecology Progress Series*, 384: 33-46.

Lovdata. (2003). *Forskrift om åpning for fiske etter anadrome laksefisk (åpningsforskriften)*: Lovdata.

Lovdata. (2012). *Forskrift om bevaringssoner i Tvedestrand kommunes sjøområder, Aust-Agder*: Lovdata.

Lucas, M. C. & Baras, E. (2000). Methods for studying spatial behaviour of freshwater fishes in the natural environment. *Fish and Fisheries*, 1 (4): 283-316.

Lyse, A. A., Stefansson, S. O. & Ferno, A. (1998). Behaviour and diet of sea trout post-smolts in a Norwegian fjord system. *Journal of Fish Biology*, 52 (5): 923-936.

March, D., Palmer, M., Alos, J., Grau, A. & Cardona, F. (2010). Short-term residence, home range size and diel patterns of the painted comber Serranus scriba in a temperate marine reserve. *Marine Ecology Progress Series*, 400: 195-206.

March, D., Alos, J. & Palmer, M. (2014). Geospatial assessment of fishing quality considering environmental and angler-related factors. *Fisheries Research*, 154: 63-72.

Marshell, A., Mills, J. S., Rhodes, K. L. & McIlwain, J. (2011). Passive acoustic telemetry reveals highly variable home range and movement patterns among unicornfish within a marine reserve. *Coral Reefs*, 30 (3): 631-642.

Mathies, N. H., Ogburn, M. B., McFall, G. & Fangman, S. (2014). Environmental interference factors affecting detection range in acoustic telemetry studies using fixed receiver arrays. *Marine Ecology Progress Series*, 495: 27-38.

Miljødirektoratet. (2015). Faktaark: Naturtype - Furøya. Available at: http://faktaark.naturbase.no/naturtype?id=BN00043900 (accessed: 07.01.2015).

Mulcahy, D. M. (2003). Surgical implantation of transmitters into fish. *Ilar Journal*, 44 (4): 295-306.

Munday, P. L. & Wilson, S. K. (1997). Comparative efficacy of clove oil and other chemicals in anaesthetization of Pomacentrus amboinensis, a coral reef fish. *Journal of Fish Biology*, 51 (5): 931-938.

Nakagawa, S. & Schielzeth, H. (2010). Repeatability for Gaussian and non-Gaussian data: a practical guide for biologists. *Biological Reviews*, 85 (4): 935-956.

Nordeng, H. (1977). Pheromone hypothesis for homeward migration in anadromous salmonids. *Oikos*, 28 (2-3): 155-159.

Olsen, E. M., Knutsen, H., Simonsen, J. H., Jonsson, B. & Knutsen, J. A. (2006). Seasonal variation in marine growth of sea trout, Salmo trutta, in coastal Skagerrak. *Ecology of Freshwater Fish*, 15 (4): 446-452.

Olsen, E. M. & Moland, E. (2011). Fitness landscape of Atlantic cod shaped by harvest selection and natural selection. *Evolutionary Ecology*, 25 (3): 695-710.

Olsen, E. M., Heupel, M. R., Simpfendorfer, C. A. & Moland, E. (2012). Harvest selection on Atlantic cod behavioral traits: implications for spatial management. *Ecology and Evolution*, 2 (7): 1549-1562.

Pemberton, R. (1976a). Sea trout in north-argyll-sea lochs, population, distribution and movements. *Journal of Fish Biology*, 9 (2): 157-179.

Pemberton, R. (1976b). Sea trout in north argyll sea lochs .2. Diet. *Journal of Fish Biology*, 9 (3): 195-208.
Philipp, D. P., Cooke, S. J., Claussen, J. E., Koppelman, J. B., Suski, C. D. & Burkett, D. P. (2009). Selection for Vulnerability to Angling in Largemouth Bass. *Transactions of the American Fisheries Society*, 138 (1): 189-199.
Prunet, P., Boeuf, G., Bolton, J. P. & Young, G. (1989). Smoltification and seawater adaptation in Atlantic salmon (Salmo salar): Plasma prolactin, growth hormone, and thyroid hormones. *General and Comparative Endocrinology*, 74 (3): 355-364.
Pulido, F. (2011). Evolutionary genetics of partial migration - the threshold model of migration revis(it)ed. *Oikos*, 120 (12): 1776-1783.
R- Core Team. (2012). *R: a language and environment for statistical computing.* . R Development. Vienna, Austria.: R Foundation for Statistical Computing. Available at: http://www.R-project.org.
Rikardsen, A. H., Amundsen, P. A., Knudsen, R. & Sandring, S. (2006). Seasonal marine feeding and body condition of sea trout (Salmo trutta) at its northern distribution. *Ices Journal of Marine Science*, 63 (3): 466-475.
Rogers, K. B. & White, G. C. (2007). Analysis of movement and habitat use from telemetry data. *Analysis and interpretation of freshwater fisheries data. American Fisheries Society, Bethesda, Maryland*: 625-676.
Russ, G. R., Alcala, A. C., Maypa, A. P., Calumpong, H. P. & White, A. T. (2004). Marine reserve benefits local fisheries. *Ecological Applications*, 14 (2): 597-606.
Seytre, C. & Francour, P. (2008). Is the Cape Roux marine protected area (Saint-Raphael, Mediterranean Sea) an efficient tool to sustain artisanal fisheries? First indications from visual censuses and trammel net sampling. *Aquatic Living Resources*, 21 (3): 297-305.
Sheridan, M. A., Allen, W. V. & Kerstetter, T. H. (1983). Seasonal-variations in the lipid-composition of the steelhead trout, salmo-gairdneri richardson, associated with the parr-smolt transformation. *Journal of Fish Biology*, 23 (2): 125-134.
Sheridan, M. A. (1989). Alterations in lipid-metabolism accompanying smoltification and seawater adaptation of salmonid fish. *Aquaculture*, 82 (1-4): 191-203.
Simpfendorfer, C. A., Heupel, M. R. & Hueter, R. E. (2002). Estimation of short-term centers of activity from an array of omnidirectional hydrophones and its use in studying animal movements. *Canadian Journal of Fisheries and Aquatic Sciences*, 59 (1): 23-32.
Simpfendorfer, C. A., Olsen, E. M., Heupel, M. R. & Moland, E. (2012). Three-dimensional kernel utilization distributions improve estimates of space use in aquatic animals. *Canadian Journal of Fisheries and Aquatic Sciences*, 69 (3): 565-572.
Stobart, B., Warwick, R., Gonzalez, C., Mallol, S., Diaz, D., Renones, O. & Goni, R. (2009). Long-term and spillover effects of a marine protected area on an exploited fish community. *Marine Ecology Progress Series*, 384: 47-60.
Thorstad, E. B., Rikardsen, A. H., Alp, A. & Okland, F. (2013). The Use of Electronic Tags in Fish Research - An Overview of Fish Telemetry Methods. *Turkish Journal of Fisheries and Aquatic Sciences*, 13: 881-896.
Urke, H., Kristensen, T., Alfredsen, K. T., Daae, K. & Alfredsen, J. A. (2010). Utvandringstidspunkt og marin åtferd hjå smolt frå Lærdalselva, L.NR. 6033-2010: NIVA. 48 pp.
Voegeli, F. A., Smale, M. J., Webber, D. M., Andrade, Y. & O'Dor, R. K. (2001). Ultrasonic telemetry, tracking and automated monitoring technology for sharks. *Environmental Biology of Fishes*, 60 (1-3): 267-281.

White, J., Simpfendorfer, C. A., Tobin, A. J. & Heupel, M. R. (2014). Spatial ecology of shark-like batoids in a large coastal embayment. *Environmental Biology of Fishes*, 97 (7): 773-786.
Worton, B. J. (1987). A review of models of home range for animal movement. *Ecological Modelling*, 38 (3–4): 277-298.
Zeller, D. C. (1999). Ultrasonic telemetry: its application to coral reef fisheries research. *Fishery bulletin-national oceanic and atmospheric administration*, 97 (4): 1058-1065.
Zuur, A., Ieno, E. N., Walker, N., Saveliev, A. A. & Smith, G. M. (2009). *Mixed effects models and extensions in ecology with R*: Springer.

7. Appendix

Table A1: Fish Tagging and ID, tagging day, fish length and weight, fish peduncle height and width, and the fate of each fish.

Tagging	ID	Tagging day	Length (cm)	Weight (g)	Smolt length (mm)	Fate
8956	1158080	30.04.2013	360	490	192.3	Dead
8957	1158081	30.04.2013	364	535	127.2	Dead
8958	1158082	30.04.2013	478	1050	172.4	Caught
8959	1158083	02.05.2013	358	515	127.2	Caught
8960	1158084	02.05.2013	286	290	124.0	Alive
8962	1158086	03.05.2013	359	400	162.1	Caught
8963	1158087	06.05.2013	288	280	179.6	Dead
8964	1158088	06.05.2013	243	475	108.3	Alive
8965	1158089	07.05.2013	273	250	107.8	Emirgated
8966	1158090	07.05.2013	268	245	131.8	Emirgated
8968	1158092	07.05.2013	402	725	125.7	Emirgated
8969	1158093	07.05.2013	328	435	169.8	Dead
8970	1158094	07.05.2013	303	315	148.7	Emirgated
8971	1158095	07.05.2013	298	335	138.9	Emirgated
8972	1158096	09.05.2013	285	310	111.7	Dead
8973	1158097	09.05.2013	380	575	153.3	Caught
8974	1158098	09.05.2013	358	520	91.1	Dead
8975	1158099	09.05.2013	270	230	102.6	Caught
8976	1158100	09.05.2013	331	370	159.3	Dead
8977	1158101	09.05.2013	295	330	155.1	Emirgated
8978	1158102	09.05.2013	341	465	124.6	Alive
8979	1158103	09.05.2013	285	295	134.7	Caught
8980	1158104	09.05.2013	230	190	131.0	Dead
9006	1158130	15.05.2013	298	285	163.2	Emirgated
9007	1158131	15.05.2013	334	410	138.7	Emirgated
9008	1158132	16.05.2013	305	280	159.9	Emirgated
9009	1158133	16.05.2013	500	1330	131.0	Caught
9010	1158134	11.09.2013	319	430	119.5	Alive

9011	1158135	11.09.2013	235	235	97.7	Caught
9012	1158136	11.09.2013	384	700	144.2	Alive
9013	1158137	11.09.2013	386	650	114.8	Dead
9014	1158138	11.09.2013	635	2485	131.0	Emirgated
9015	1158139	11.09.2013	495	1200	153.9	Alive
9016	1158140	11.09.2013	461	1160	114.8	Emirgated
9018	1158142	11.09.2013	393	700	105.6	Dead
9019	1158143	13.09.2013	295	340	149.3	Emirgated
9020	1158144	13.09.2013	423	790	131.0	Caught
9021	1158145	13.09.2013	346	500	60.3	Dead
9022	1158146	13.09.2013	257	260	109.3	Emirgated
9023	1158147	18.09.2013	300	350	103.4	Dead
9024	1158148	18.09.2013	508	1385	104.0	Dead
9025	1158149	18.09.2013	345	460	130.2	Alive
9026	1158150	18.09.2013	259	290	118.6	Caught
9027	1158151	18.09.2013	238	215	91.1	Emirgated
9028	1158152	18.09.2013	253	255	122.3	Emirgated
9029	1158153	18.09.2013	265		151.4	Emirgated
9030	1158154	24.09.2013	302	350	102.3	Alive
9056	1158180	24.09.2013	347	500	134.2	Caught
9057	1158181	24.09.2013	257	300	150.3	Emirgated
9059	1158183	27.11.2013	310	315	153.8	Caught
9060	1158184	27.11.2013	363	475	137.3	Dead
9061	1158185	27.11.2013	473	900	128.0	Caught
9062	1158186	27.11.2013	380	920	131.0	Caught
9063	1158187	28.11.2013	335	405	104.6	Emirgated
9064	1158188	28.11.2013	335	445	204.0	Caught
9065	1158189	28.11.2013	282	290	113.2	Caught

Table A2: All LME-model structures with AIC values fitted to predict HR.50

Model	df	AIC	ΔAIC
Month + Smolt length	15	3937.92	
Month + Smolt length + Air pressure	16	3946.11	8.19
Month + Smolt length + Air pressure^2	17	3951.56	13.64
Month + Smolt length + Air temperature^2	17	3951.70	13.79
Month + Smolt length * Air temperature^2	19	3954.45	16.53
Month + Smolt length * Air pressure	17	3955.31	17.39
Month + Smolt length + Wind direction^2	17	3955.96	18.04
Month + Smolt length + Wind speed^2	17	3957.67	19.75
Month + Smolt length + Precipitation2	17	3959.00	21.08
Month * Smolt length	26	3964.39	26.47
Month + Smolt length + Air pressure^2 + Air temperature^2	19	3965.32	27.40
Month + Smolt length * Air pressure^2	19	3970.84	32.93
Month + Smolt length * Wind speed^2	19	3972.72	34.80
Month + Smolt length * Wind direction^2	19	3975.02	37.10
Month + Smolt length * Precipitation2	19	3980.77	42.85
Month + Smolt length + Air pressure^2 + Air temperature^2 + Wind speed^2	21	3984.67	46.76
Month + Smolt length + Air pressure^2 + Air temperature^2 + Wind speed^2 + Wind direction^2	23	4002.12	64.21
Month + Smolt length + Air pressure2+ Air temperature^2 + Wind speed^2 + Wind direction2+ Precipitation2	25	4020.92	83.00
Month + Smolt length * Air pressure^2 + Air temperature^2 + Wind speed^2 + Wind direction^2+ Precipitation^2	27	4040.22	102.30
Month * Smolt length * Air pressure	50	4058.77	120.85
Month * Smolt length * Air pressure^2	74	4184.06	246.15

Table A3: All LME-model structures with AIC values fitted to predict HR.95

Models	df	AIC	ΔAIC
Month + Smolt length	15	4628.26	
Month + Smolt length + Air pressure	16	4636.88	8.62
Month + Smolt length + Air temperature^2	17	4642.54	14.28
Month + Smolt length + Wind direction^2	17	4644.76	16.50
Month + Smolt length + Air pressure^2	17	4645.73	17.47
Month + Smolt length * Air pressure	17	4645.97	17.71
Month + Smolt length + Wind speed^2	17	4647.98	19.72
Month + Smolt length + Precipitation^2	17	4648.82	20.56
Month + Smolt length * Air temperature^2	19	4650.15	21.90
Month * Smolt length	26	4652.29	24.03
Month + Smolt length + Air pressure2+ Air temperature^2	19	4659.52	31.26
Month + Smolt length * Wind direction^2	19	4661.11	32.85
Month + Smolt length * Air pressure^2	19	4664.93	36.67
Month + Smolt length * Wind speed^2	19	4667.54	39.28
Month + Smolt length * Precipitation^2	19	4669.95	41.69
Month + Smolt length + Air pressure^2+ Air temperature^2 + Wind speed^2	21	4678.87	50.61
Month + Smolt length + Air pressure^2+ Air temperature^2 + Wind speed^2 + Wind direction^2	23	4694.43	66.17
Month + Smolt length + Air pressure^2+ Air temperature^2 + Wind speed^2 + Wind direction^2+ Precipitation^2	25	4712.52	84.26
Month * Smolt length * Air pressure	50	4753.62	125.37
Month * Smolt length * Air pressure^2	74	4877.15	248.89

Table A4: All LME-model structures with AIC values fitted to predict turboness in HR.95

Models	df	AIC	ΔAIC
Month + Smolt length + Air temperature^2	17	3534.89	
Month + Smolt length	15	3536.02	1.13
Month + Smolt length + Air pressure	16	3537.72	2.83
Month + Smolt length * Air pressure	17	3540.87	5.97
Month + Smolt length + Air pressure^2	17	3545.06	10.17
Month + Smolt length + Air pressure^2+ Air temperature^2	19	3545.87	10.98
Month + Smolt length * Air temperature^2	19	3553.14	18.25
Month + Smolt length + Wind speed^2	17	3553.49	18.59
Month + Smolt length + Wind direction^2	17	3555.49	20.60
Month + Smolt length * Air pressure^2	19	3556.09	21.20
Month + Smolt length + Precipitation^2	17	3557.69	22.80
Month + Smolt length + Air pressure2+ Air temperature^2 + Wind speed^2	21	3565.59	30.70
Month + Smolt length * Wind speed^2	19	3567.78	32.89
Month + Smolt length * Precipitation^2	19	3573.86	38.97
Month + Smolt length * Wind direction^2	19	3574.22	39.33
Month + Smolt length + Air pressure^2+ Air temperature^2 + Wind speed^2 + Wind direction^2	23	3583.89	49.00
Month* Smolt length	26	3601.55	66.66
Month + Smolt length + Air pressure^2+ Air temperature^2 + Wind speed^2 + Wind direction^2+ Precipitation^2	25	3604.94	70.05
Month* Smolt length * Air pressure	50	3723.05	188.15
Month* Smolt length * Air pressure^2	74	3849.97	315.08

Table A5: All LME-model structures with AIC values fitted to predict total distance

Models	df	AIC	ΔAIC
Month + Smolt length + Air pressure^2	17	2665.62	
Month + Smolt length * Air pressure	17	2666.14	0.52
Month + Smolt length * Air pressure^2	19	2670.05	4.43
Month + Smolt length + Air pressure	16	2671.20	5.58
Month + Smolt length + Air pressure^2+ Air temperature^2	19	2676.14	10.52
Month + Smolt length	15	2681.62	16.00
Month + Smolt length * Air temperature^2	19	2683.37	17.75
Month + Smolt length + Air temperature^2	17	2690.80	25.18
Month + Smolt length + Air pressure^2+ Air temperature^2 + Wind speed^2	21	2694.04	28.43
Month + Smolt length + Wind speed^2	17	2696.62	31.00
Month + Smolt length + Wind direction^2	17	2697.89	32.28
Month + Smolt length + Precipitation^2	17	2703.00	37.39
Month* Smolt length	26	2706.04	40.42
Month + Smolt length + Air pressure^2+ Air temperature^2 + Wind speed^2 + Wind direction^2	23	2711.68	46.07
Month + Smolt length * Wind direction^2	19	2712.71	47.09
Month + Smolt length * Wind speed^2	19	2714.00	48.39
Month + Smolt length * Precipitation^2	19	2720.07	54.45
Month + Smolt length + Air pressure^2+ Air temperature^2 + Wind speed^2 + Wind direction^2+ Precipitation^2	25	2725.42	59.80
Month* Smolt length * Air pressure	50	2762.81	97.20
Month* Smolt length * Air pressure^2	74	2885.60	219.98

Table A6: All log-transformed LME-model structures with AIC values fitted to predict mean depth use

Models	**df**	**AIC**	**ΔAIC**
Month * Smolt length * Air pressure^2	74	837902.304	
Month * Smolt length * Air pressure	50	841782.151	3879.84735
Month + Smolt length * Air pressure^2 + Air temperature^2 + Wind speed^2 + Wind direction^2 + Precipitation^2	27	841899.627	3997.32313
Month + Smolt length + Air pressure^2 + Air temperature^2 + Wind speed^2 + Wind direction^2	23	842260.503	4358.1994
Month + Smolt length + Air pressure^2 + Air temperature^2 + Wind speed^2 + Wind direction^2 + Precipitation^2	25	842267.162	4364.85881
Month + Smolt length + Air pressure^2+ Air temperature^2 + Wind speed^2	21	842472.041	4569.73702
Month + Smolt length + Air pressure^2+ Air temperature^2	19	842634.07	4731.76623
Month + Smolt length * Air temperatures^2	19	844370.748	6468.44446
Month + Smolt length + Air temperature^2	17	844384.224	6481.92091
Month * Smolt length + Air pressure^2	28	846287.129	8384.82582
Month * Smolt length	26	847959.819	10057.5151
Month + Smolt length * Air pressure^2	19	848275.886	10373.5821
Month + Smolt length + Air pressure^2	17	848616.663	10714.3592
Month + Smolt length * Air pressure	17	849331.11	11428.8063
Month + Smolt length + Air pressure	16	849440.117	11537.8138
Month + Smolt length * Wind speed^2	19	849706.413	11804.109
Month + Smolt length + Wind speed^2	17	849708.691	11806.3873
Month + Smolt length * Wind direction^2	19	849727.542	11825.2381
Month + Smolt length + Wind direction^2	17	849735.887	11833.5836
Month + Smolt length * Precipitation^2	19	850198.848	12296.5446
Month + Smolt length + Precipitation^2	17	850262.17	12359.8668
Month + Smolt length	15	850299.338	12397.0348

Table A7: Fixed effects parameter estimates for the most supported LME-model fitted to predict mean depth use. The random structure, ID, yielded variance = 0.51± 0.72 (SD).

Terms	Estimate	SE	t	p
Intercept	1.1209132	0.096982	11.56	0.00236427
month2	0.0661765	0.008512	7.77	0.00518649
month3	0.0262262	0.007644	3.43	0.02493634
month4	0.008821	0.007089	1.24	0.12543738
month5	-0.4530253	0.006389	-70.91	6.3292E-05
month6	-0.3794581	0.006658	-56.99	9.7976E-05
month7	-0.2086476	0.006841	-30.5	0.00034181
month8	-0.3173412	0.006726	-47.18	0.00014294
month9	-0.6228046	0.007045	-88.4	4.0728E-05
month10	-0.3919735	0.007242	-54.13	0.0001086
month11	-0.286426	0.007176	-39.91	0.00019972
month12	-0.3488982	0.006606	-52.82	0.00011405
Smolt.length	0.1504245	0.084657	1.78	0.07636261
poly(PO)1	0.1729157	0.004261	40.58	0.00019318
poly(PO)2	-0.0129718	0.004704	-2.76	0.03693719
month2:Smolt.length	-0.0328285	0.008455	-3.88	0.01982696
month3:Smolt.length	-0.0438395	0.007439	-5.89	0.00891822
month4:Smolt.length	0.0134357	0.0072	1.87	0.07078429
month5:Smolt.length	-0.0161283	0.006396	-2.52	0.04330511
month6:Smolt.length	-0.0652203	0.006994	-9.32	0.00362282
month7:Smolt.length	0.0095905	0.007065	1.36	0.11170336
month8:Smolt.length	0.0344288	0.006861	5.02	0.01214905
month9:Smolt.length	-0.1198074	0.007246	-16.53	0.00116069
month10:Smolt.length	0.0899623	0.008169	11.01	0.0026044
month11:Smolt.length	-0.029751	0.007332	-4.06	0.0182062
month12:Smolt.length	-0.0392282	0.006477	-6.06	0.00843795
month2:poly(PO)1	-0.2162046	0.012344	-17.51	0.00103482
month3:poly(PO)1	-0.1432713	0.004986	-28.74	0.0003849
month4:poly(PO)1	-0.1418929	0.007383	-19.22	0.00085935
month5:poly(PO)1	-0.0803264	0.005212	-15.41	0.00133481
month6:poly(PO)1	-0.1269746	0.007028	-18.07	0.00097186
month7:poly(PO)1	-0.0404167	0.00954	-4.24	0.01677293
month8:poly(PO)1	-0.0987718	0.005765	-17.13	0.00108108
month9:poly(PO)1	-0.1329584	0.005953	-22.34	0.00063652
month10:poly(PO)1	-0.2114046	0.005174	-40.86	0.00019054

month11:poly(PO)1	-0.1799468	0.006032	-29.83	0.00035732
month12:poly(PO)1	-0.1702453	0.005482	-31.05	0.00032982
month2:poly(PO)2	0.020082	0.006313	3.18	0.02864457
month3:poly(PO)2	0.004064	0.005379	0.76	0.20176844
month4:poly(PO)2	-0.0056361	0.007002	-0.8	0.19409139
month5:poly(PO)2	0.17726	0.005593	31.69	0.00031665
month6:poly(PO)2	-0.0404354	0.008573	-4.72	0.01367404
month7:poly(PO)2	-0.0666068	0.007781	-8.56	0.00428564
month8:poly(PO)2	-0.0861036	0.006192	-13.9	0.001639
month9:poly(PO)2	0.0173908	0.005664	3.07	0.03053362
month10:poly(PO)2	0.0205238	0.005046	4.07	0.01812193
month11:poly(PO)2	0.0156326	0.005152	3.03	0.0312654
month12:poly(PO)2	0.0237171	0.004967	4.77	0.01340089
Smolt.length:poly(PO)1	0.0341202	0.004132	8.26	0.00459802
Smolt.length:poly(PO)2	-0.0128184	0.004627	-2.77	0.03670167
month2:Smolt.length:poly(PO)1	-0.0736928	0.013618	-5.41	0.01051635
month3:Smolt.length:poly(PO)1	-0.02496	0.004804	-5.2	0.01135199
month4:Smolt.length:poly(PO)1	0.001446	0.007924	0.18	0.30832031
month5:Smolt.length:poly(PO)1	-0.0466913	0.00501	-9.32	0.00362282
month6:Smolt.length:poly(PO)1	-0.047511	0.007161	-6.63	0.00708033
month7:Smolt.length:poly(PO)1	-0.0045468	0.009345	-0.49	0.25668082
month8:Smolt.length:poly(PO)1	0.043073	0.005496	7.84	0.00509576
month9:Smolt.length:poly(PO)1	-0.0364047	0.005869	-6.2	0.00807074
month10:Smolt.length:poly(PO)1	-0.0328839	0.005525	-5.95	0.00874418
month11:Smolt.length:poly(PO)1	-0.0533255	0.006224	-8.57	0.00427578
month12:Smolt.length:poly(PO)1	-0.0285092	0.005229	-5.45	0.01036756
month2:Smolt.length:poly(PO)2	0.0149611	0.006745	2.22	0.05369238
month3:Smolt.length:poly(PO)2	0.0173735	0.005253	3.31	0.02662322
month4:Smolt.length:poly(PO)2	0.0008421	0.007265	0.12	0.31379129
month5:Smolt.length:poly(PO)2	0.0241636	0.005452	4.43	0.01543328
month6:Smolt.length:poly(PO)2	0.0732634	0.008676	8.44	0.00440667
month7:Smolt.length:poly(PO)2	0.0011982	0.007584	0.16	0.31036455
month8:Smolt.length:poly(PO)2	-0.0063207	0.005975	-1.06	0.14989164
month9:Smolt.length:poly(PO)2	0.0427288	0.005616	7.61	0.00540313
month10:Smolt.length:poly(PO)2	0.0084824	0.005181	1.64	0.08627219
month11:Smolt.length:poly(PO)2	0.0180154	0.005168	3.49	0.02415079
month12:Smolt.length:poly(PO)2	0.01818	0.004859	3.74	0.02123822

Table A8: All LME-model structures with AIC values fitted to predict UVol.50

Models	df	AIC	ΔAIC
Month + Smolt length + Air temperature^2 + month:Smolt.length + month:Air temperature^2	50	16973.7269	
Month + Smolt length + Air temperature^2 + month:Smolt.length + month:Air temperature^2 + Smolt.length:Air temperature^2	52	16984.5119	10.7849669
Month * Smolt length* Air temperature^2	74	16993.7988	20.0718808
Month * Smolt length	26	17000.6108	26.8839072
Month * Smolt length + Air pressure	27	17004.9495	31.2225236
Month * Smolt length + Air temperature^2	28	17007.3895	33.6625141
Month * Smolt length + Wind direction^2	28	17007.6511	33.9241933
Month * Smolt length + Air pressure^2	28	17012.0502	38.3232855
Month + Smolt length	15	17013.3084	39.5815097
Month * Smolt length * Air pressure^2 * Air temperature^2	218	17014.175	40.4480499
Month * Smolt length + Wind direction^2	28	17015.0001	41.2731744
Month * Smolt length + Precipitation^2	28	17015.1245	41.397525
Month + Smolt length + Air pressure	16	17018.0095	44.2825538
Month + Smolt length * Air pressure	17	17023.4183	49.6914114
Month + Smolt length * Air pressure^2	19	17038.1999	64.4729811
Month * Smolt length + Air pressure^2 * Air temperature^2	34	17040.6408	66.9138834
Month * Smolt length + Air pressure^2 * Air temperature^2 + Wind speed^2	36	17047.6757	73.9487403
Month * Smolt length + Air pressure^2 * Air temperature^2 + Wind speed^2 + Wind direction^2	38	17061.7678	88.0408751
Month * Smolt length + Air pressure^2 * Air temperature^2 + Wind speed^2 + Wind direction^2 + Precipitation^2	40	17073.6061	99.8791771
Month * Smolt length * Air pressure^2	74	17104.1877	130.460729
Month * Smolt length * Wind direction^2	74	17121.3765	147.649532
Month * Smolt length * Precipitation^2	74	17129.394	155.667023
Month * Smolt length * Wind speed^2	74	17146.5198	172.792905

Table A9: Fixed effects parameter estimates for the most supported LME-model fitted to predict UVol.50. The random structure, ID, yielded variance = 1.67±1.30 (SD).

Terms	Estimate	SE	t	p
Intercept	8.15559	1.25494	6.49900	0.00736
month2	2.84861	4.07313	0.69900	0.21383
month3	-1.63782	2.17005	-0.75500	0.20274
month4	2.37798	1.25060	1.90100	0.06899
month5	2.69933	1.24692	2.16500	0.05597
month6	0.43309	1.31839	0.32800	0.28739
month7	0.71176	1.55130	0.45900	0.26292
month8	3.37726	1.87943	1.79700	0.07526
month9	1.26421	1.24965	1.01200	0.15726
month10	1.36796	1.24828	1.09600	0.14461
month11	1.31737	1.28204	1.02800	0.15476
month12	0.88223	1.35640	0.65000	0.22377
Smolt length	-0.08986	0.23254	-0.38600	0.27703
Air temperature	-1.40332	2.06174	-0.68100	0.21746
Air temperature^2	-0.48036	0.77969	-0.61600	0.23075
month2:Smolt.length	0.46750	0.24854	1.88100	0.07014
month3:Smolt.length	0.52249	0.18475	2.82800	0.03538
month4:Smolt.length	0.19884	0.18664	1.06500	0.14915
month5:Smolt.length	0.31601	0.17630	1.79200	0.07559
month6:Smolt.length	0.08115	0.19872	0.40800	0.27288
month7:Smolt.length	-0.25564	0.20146	-1.26900	0.12194
month8:Smolt.length	-0.42128	0.19229	-2.19100	0.05488
month9:Smolt.length	-0.25189	0.19477	-1.29300	0.11913
month10:Smolt.length	0.23525	0.21778	1.08000	0.14693
month11:Smolt.length	0.08518	0.20303	0.42000	0.27058
month12:Smolt.length	0.32485	0.17864	1.81800	0.07394
month2:poly(TA.all)	4.96563	5.81542	0.85400	0.18407
month3:poly(TA.all)	-4.39393	4.20750	-1.04400	0.15231
month4:poly(TA.all)	1.54004	2.13488	0.72100	0.20944
month5:poly(TA.all)	1.18301	2.06598	0.57300	0.23963

month6:poly(TA.all)	3.89882	2.42551	1.60700	0.08885
month7:poly(TA.all)	2.03518	2.50560	0.81200	0.19183
month8:poly(TA.all)	-1.68143	3.17252	-0.53000	0.24850
month9:poly(TA.all)	1.60397	2.12388	0.75500	0.20274
month10:poly(TA.all)	1.72518	2.08231	0.82800	0.18884
month11:poly(TA.all)	1.10561	2.22609	0.49700	0.25526
month12:poly(TA.all)	2.21594	2.36843	0.93600	0.16967
month2:poly(TA.all)2	1.74851	2.02418	0.86400	0.18226
month3:poly(TA.all)2	-2.53018	1.99688	-1.26700	0.12218
month4:poly(TA.all)2	-0.02945	0.93654	-0.03100	0.31800
month5:poly(TA.all)2	-0.13527	0.81548	-0.16600	0.30977
month6:poly(TA.all)2	-1.11483	1.17919	-0.94500	0.16815
month7:poly(TA.all)2	0.48084	0.94569	0.50800	0.25302
month8:poly(TA.all)2	2.02250	1.26854	1.59400	0.08990
month9:poly(TA.all)2	0.88079	0.90945	0.96800	0.16433
month10:poly(TA.all)2	-0.21868	0.85735	-0.25500	0.29888
month11:poly(TA.all)2	0.19566	0.90390	0.21600	0.30412
month12:poly(TA.all)2	1.07834	0.94439	1.14200	0.13815

Table A10: All LME-model structures with AIC values fitted to predict UVol.95

Models	df	AIC	ΔAIC
Month *Smolt length	26	16633.00	
Month * Smolt length + Air temperature^2	28	16635.79	2.79
Month * Smolt length * Air temperature^2	74	16638.04	5.03
Month * Smolt length + Air pressure	27	16638.31	5.31
Month + Smolt length	15	16639.11	6.10
Month * Smolt length + Wind speed^2	28	16641.72	8.72
Month + Smolt length + Air pressure	16	16644.59	11.58
Month * Smolt length + Precipitation2	28	16646.15	13.14
Month * Smolt length + Air pressure^2	28	16646.24	13.23
Month * Smolt length + Wind direction^2	28	16647.39	14.38
Month + Smolt length * Air pressure	17	16651.07	18.07
Month + Smolt length * Air pressure^2	19	16666.81	33.80
Month * Smolt length + Air pressure^2 * Air temperature^2	34	16672.24	39.24
Month * Smolt length + Air pressure^2 * Air temperature^2 + Wind speed^2	36	16680.15	47.15
Month * Smolt length * Air pressure^2 * Air temperature2	218	16686.78	53.77
Month * Smolt length + Air pressure^2 * Air temperature^2 + Wind speed^2 + Wind direction^2	38	16694.03	61.03
Month * Smolt length + Air pressure^2 * Air temperature^2 + Wind speed^2 + Wind direction^2 + Precipitation^2	40	16703.74	70.74
Month * Smolt length * Air pressure^2	74	16753.28	120.27
Month * Smolt length * Precipitation^2	74	16766.01	133.01
Month * Smolt length * Wind direction^2	74	16771.03	138.02
Month * Smolt length * Wind speed^2	74	16786.81	153.81

Table A11: All LME-model structures with AIC values fitted to predict probability of No-take zone use.

Model	df	AIC	ΔAIC
Month * Length * Smolt length	49	220817.7	
Month * Smolt length * Air pressure^2	73	225122.4	4304.722289
Month * Smolt length * Air temperature^2	73	226311.6	5493.973514
Month * Smolt length * Air pressure	49	226508.6	5690.982044
Month * Smolt length * Precipitation^2	73	228223.6	7405.955556
Month * Smolt length * Wind direction^2	73	228251.7	7434.068645
Month * Smolt length * Wind speed^2	73	229856.4	9038.7251
Month * Smolt length + Wind direction^2	27	231254.6	10436.92182
Month * Smolt length + Air temperature^2	27	231507.7	10690.05087
Month * Smolt length + Air pressure	26	231543.2	10725.49518
Month * Smolt length + Wind speed^2	27	231565.9	10748.22436
Month * Smolt length	25	231695.7	10877.99612
Month * Length	25	242270.9	21453.26348
Month * Length + Smolt length	26	242272.7	21455.07579
Month + Smolt length * Air temperature^2	18	242994.7	22177.0033
Month + Smolt length * Wind direction^2	18	244709.7	23892.00503
Month + Smolt length + Air pressure^2 + Air temperature^2 + Wind speed^2 + Wind direction^2 + Precipitation^2	24	244716.1	23898.41561
Month + Smolt length * Air pressure^2	18	244757.8	23940.18078
Month + Smolt length + Air pressure^2 + Air temperature^2 + Wind speed^2 + Wind direction^2	22	244921	24103.30912
Month + Smolt length * Wind speed^2	18	244994.8	24177.10704
Month + Smolt length * Precipitation^2	18	245053.2	24235.53393
Month + Smolt length + Air pressure^2 + + Air temperature^2 + Wind speed^2	20	245192.3	24374.64744
Month + Smolt length * Air pressure	16	245315.5	24497.78915
Month + Smolt length + Wind direction^2	16	245358.6	24540.91566
Month + Smolt length + Air pressure^2 + + Air temperature^2	18	245426.1	24608.47155
Month + Smolt length + Precipitation^2	16	245541.9	24724.25043
Month + Smolt length + Air temperature^2	16	245600.3	24782.60913
Month + Smolt length + Air pressure^2	16	245612.3	24794.68808
Month + Smolt length + Wind speed^2	16	245618.3	24800.61487
Month + Smolt length + Air pressure	15	245696.2	24878.51459
Month + Length	14	245791.5	24973.8535
Month + Smolt length	14	245791.6	24973.92841
Month + Length + Smolt length	15	245793.3	24975.67375
Month + Length * Smolt length	16	245795.3	24977.62523

Table A12: Logit parameter estimates for the most supported GLM-model fitted to No-take probability use. The random structure, ID, yielded variance = 17.35± 4.16 (SD).

Terms	Estimate	SE	z-value	Pr(>|z|)
Intercept	-1.23864	0.146533	-8.45	< 2e-16
month2	-1.396707	0.042181	-33.11	< 2e-16
month3	-0.092345	0.045235	-2.04	0.041208
month4	-0.173439	0.035596	-4.87	1.10E-06
month5	0.719968	0.033281	21.63	< 2e-16
month6	-0.366643	0.03499	-10.48	< 2e-16
month7	0.040586	0.037865	1.07	0.283778
month8	-0.090202	0.037373	-2.41	0.015797
month9	-0.563181	0.035251	-15.98	< 2e-16
month10	0.133458	0.037582	3.55	0.000384
month11	0.777987	0.037365	20.82	< 2e-16
month12	1.101125	0.036126	30.48	< 2e-16
Length	0.171334	0.216643	0.79	0.429027
Smolt.length	1.885238	0.140324	13.43	< 2e-16
month2:Length	-0.948249	0.063038	-15.04	< 2e-16
month3:Length	-0.487053	0.044357	-10.98	< 2e-16
month4:Length	-1.1648	0.042646	-27.31	< 2e-16
month5:Length	-0.80722	0.039182	-20.6	< 2e-16
month6:Length	-1.331027	0.040637	-32.75	< 2e-16
month7:Length	-0.626786	0.041633	-15.05	< 2e-16
month8:Length	-0.183469	0.041349	-4.44	9.12E-06
month9:Length	-0.107854	0.040167	-2.69	0.007249
month10:Length	-0.222837	0.045285	-4.92	8.62E-07
month11:Length	-0.044617	0.048351	-0.92	0.356129
month12:Length	-0.948919	0.045247	-20.97	< 2e-16
month2:Smolt.length	0.797043	0.046233	17.24	< 2e-16
month3:Smolt.length	0.575673	0.038816	14.83	< 2e-16
month4:Smolt.length	-1.370377	0.04766	-28.75	< 2e-16

month5:Smolt.length	-2.330026	0.037414	-62.28	< 2e-16
month6:Smolt.length	-1.482194	0.03847	-38.53	< 2e-16
month7:Smolt.length	-1.059711	0.039257	-26.99	< 2e-16
month8:Smolt.length	-1.872553	0.038234	-48.98	< 2e-16
month9:Smolt.length	-2.289705	0.03735	-61.3	< 2e-16
month10:Smolt.length	-1.449755	0.043629	-33.23	< 2e-16
month11:Smolt.length	-1.831848	0.040473	-45.26	< 2e-16
month12:Smolt.length	-0.502832	0.038458	-13.07	< 2e-16
Length:Smolt.length	0.048314	0.133476	0.36	0.717376
month2:Length:Smolt.length	0.643083	0.08225	7.82	5.34E-15
month3:Length:Smolt.length	0.191458	0.067171	2.85	0.004368
month4:Length:Smolt.length	1.116663	0.058544	19.07	< 2e-16
month5:Length:Smolt.length	-0.199992	0.046334	-4.32	1.59E-05
month6:Length:Smolt.length	0.0682	0.047014	1.45	0.146886
month7:Length:Smolt.length	-0.285905	0.047691	-5.99	2.04E-09
month8:Length:Smolt.length	-1.060308	0.046691	-22.71	< 2e-16
month9:Length:Smolt.length	-0.35545	0.045891	-7.75	9.52E-15
month10:Length:Smolt.length	1.989101	0.05845	34.03	< 2e-16
month11:Length:Smolt.length	-0.442878	0.055062	-8.04	8.75E-16
month12:Length:Smolt.length	0.008697	0.059464	0.15	0.883719

Table A13: Station info over the used VR2Ws **Error! Reference source not found.** (Vemco Dicision, Amirix Systems Inc.) in the study. Four stations have received new serial after data downloading

Serial	Latitude	Longitude	Name
110979	58.62201	8.95298	VR2 1
110973	58.61931	8.93800	VR2 2
102667	58.61816	8.94716	VR2 3
110972	58.61539	8.93794	VR2 4
110975	58.61545	8.94621	VR2 5
103843	58.61299	8.93847	VR2 6
110980	58.61097	8.94550	VR2 7
110978	58.61076	8.93773	VR2 8
110961	58.60726	8.94184	VR2 9
110990	58.60811	8.94749	VR2 10
110971	58.60790	8.95204	VR2 11
103842	58.60499	8.94828	VR2 12
103849	58.60484	8.94310	VR2 13
102670	58.60226	8.94251	VR2 14
110995	58.60343	8.95347	VR2 15
110989	58.60239	8.95854	VR2 16
102820	58.60042	8.94771	VR2 17
102650	58.59946	8.95081	VR2 18
102651	58.59732	8.94553	VR2 19
102668	58.59592	8.94885	VR2 20
111604	58.59350	8.94532	VR2 21
111607	58.59386	8.95263	VR2 22
103847	58.59582	8.95447	VR2 23
111606	58.59813	8.95996	VR2 24
111589	58.59703	8.96488	VR2 25
111588	58.60046	8.96463	VR2 26
111590	58.60413	8.96470	VR2 27
111593	58.60292	8.96967	VR2 28
102663	58.59862	8.97147	VR2 29
111598	58.59431	8.96673	VR2 30
111605	58.59300	8.97464	VR2 31
111594	58.59081	8.96863	VR2 32
102664	58.58966	8.97537	VR2 33

102665	58.61308	8.94477	VR2 34
110977	58.60886	8.94079	VR2 35
110988	58.60964	8.94542	VR2 36
102819	58.60924	8.95018	VR2 37
103841	58.60649	8.95419	VR2 38
103845	58.60607	8.95062	VR2 39
103840	58.60457	8.95597	VR2 40
110982	58.60304	8.94974	VR2 41
102818	58.60309	8.94623	VR2 42
110992	58.60001	8.94433	VR2 43
103844	58.59870	8.94803	VR2 44
110968	58.59700	8.94963	VR2 45
110976	58.59539	8.94443	VR2 46
110958	58.59340	8.94284	VR2 47
110994	58.60471	8.95236	VR2 48
102657	58.62500	8.95481	VR2 49
110967	58.58480	8.93935	VR2 50
110962	58.60005	8.95888	VR2 51
102837	58.61076	8.93773	VR2 8
111591	58.59862	8.97147	VR2 29
111600	58.58966	8.97537	VR2 33
111609	58.59582	8.95447	VR2 23

Table A14: An overview of every position of the 56 individuals during a year. Color palette change with the months

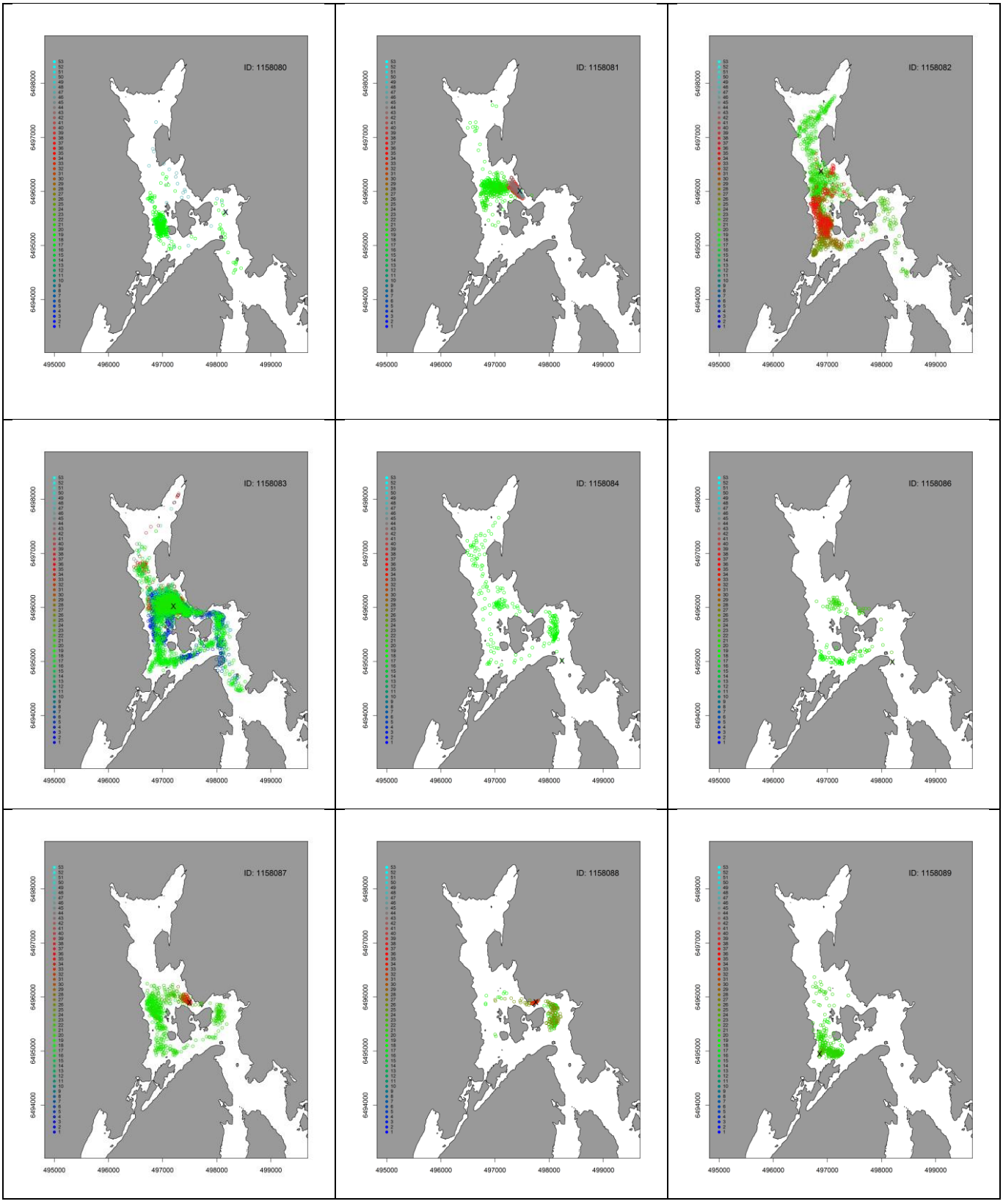

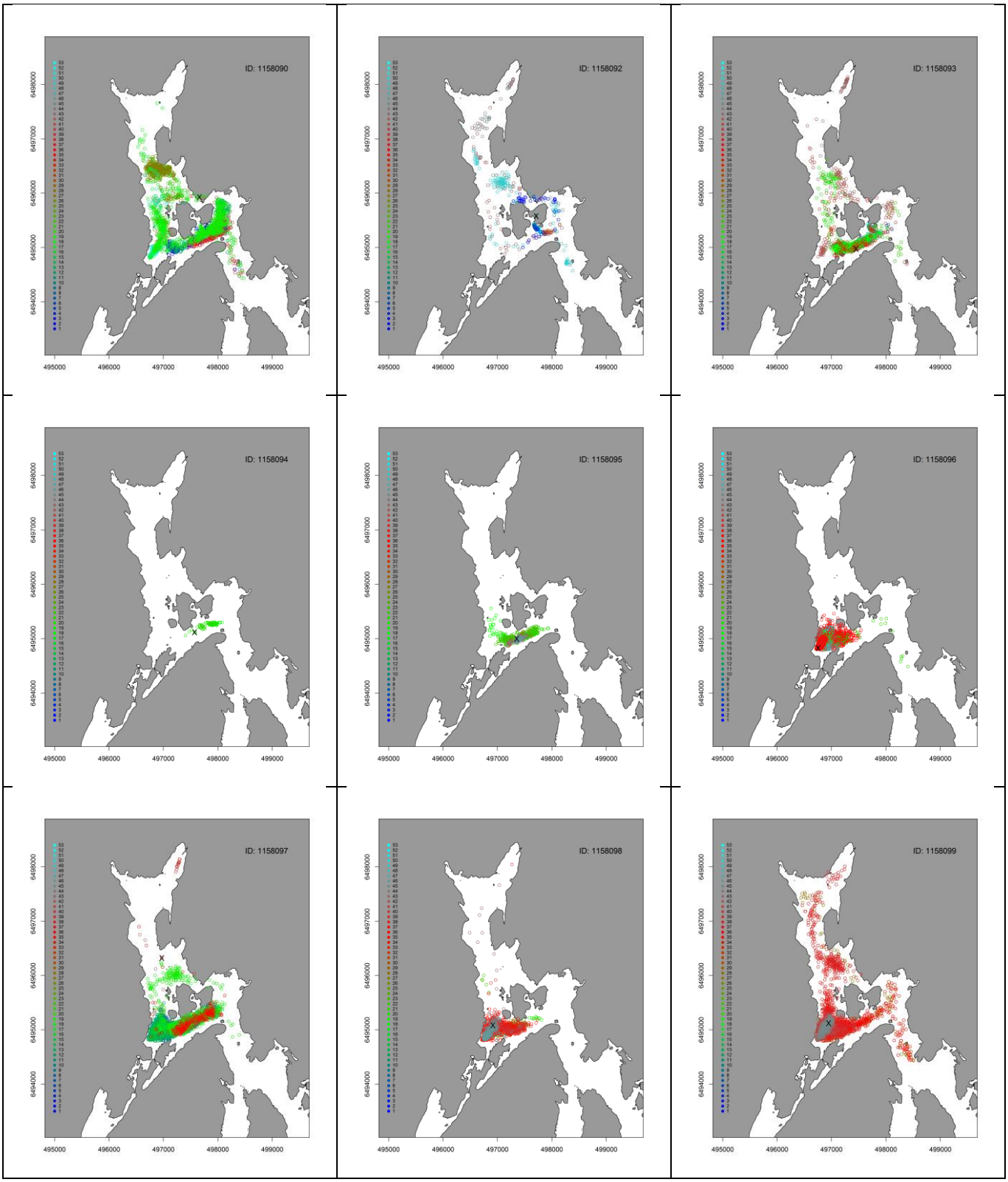
ID: 1158090
ID: 1158092
ID: 1158093
ID: 1158094
ID: 1158095
ID: 1158096
ID: 1158097
ID: 1158098
ID: 1158099
6498000
6497000
6496000
6495000
6494000
495000
496000
497000
498000
499000

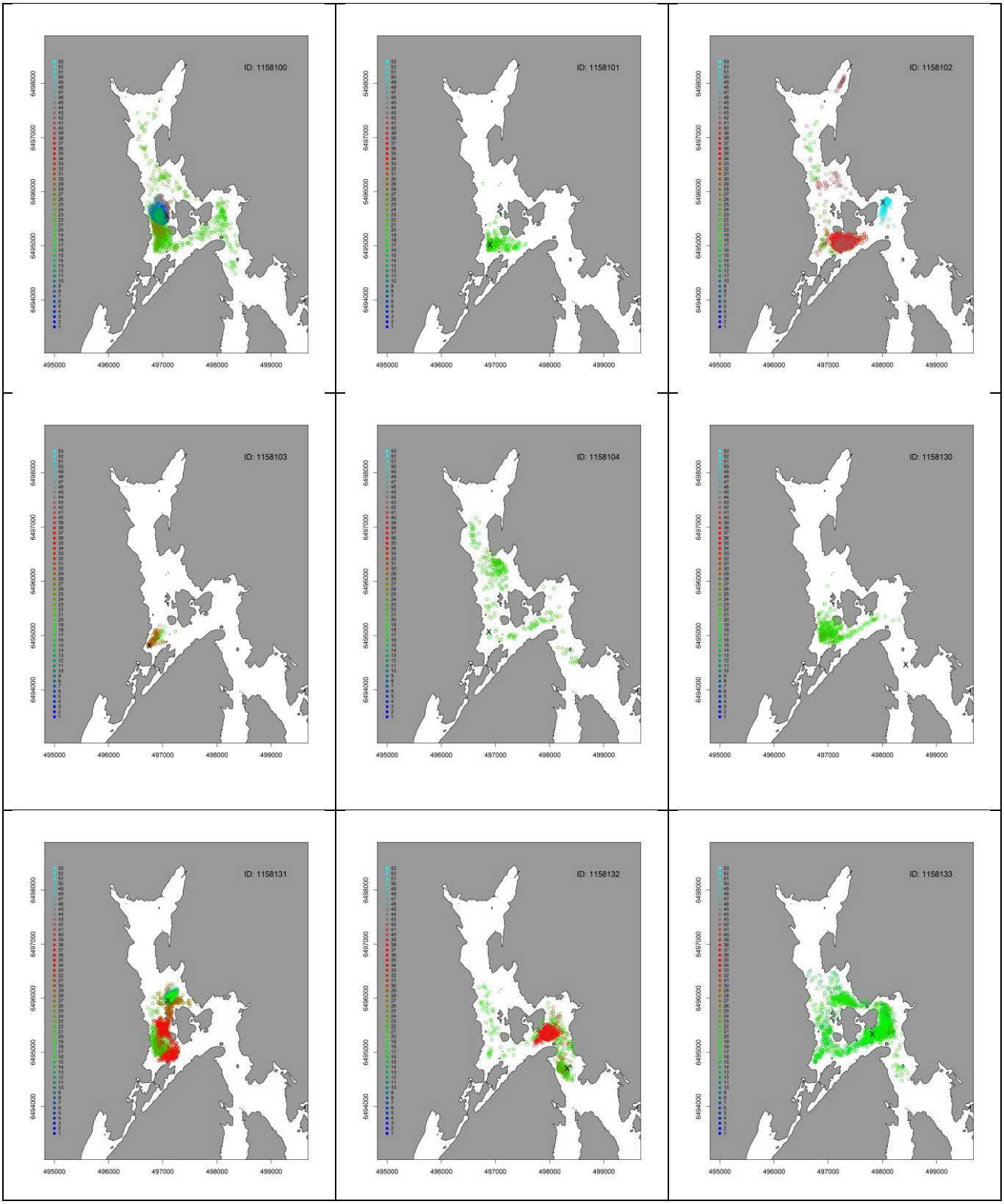
ID: 1158100
ID: 1158101
ID: 1158102
ID: 1158103
ID: 1158104
ID: 1158130
ID: 1158131
ID: 1158132
ID: 1158133
495000
496000
497000
498000
499000
6494000
6495000
6496000
6497000
6498000

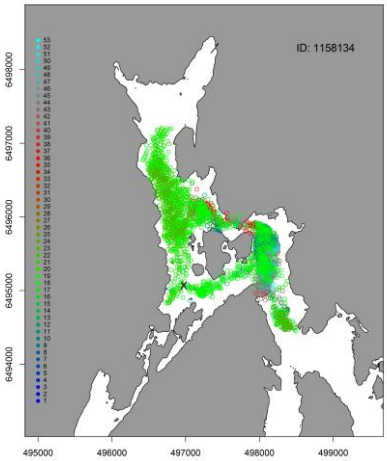
ID: 1158134
6498000
6497000
6496000
6495000
6494000
495000
496000
497000
498000
499000

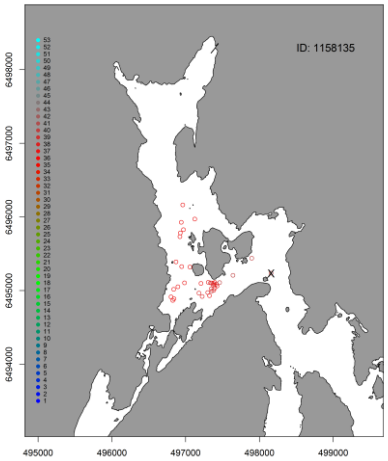
ID: 1158135
6498000
6497000
6496000
6495000
6494000
495000
496000
497000
498000
499000

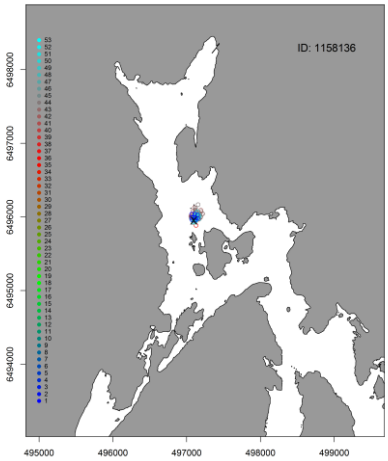
ID: 1158136
6498000
6497000
6496000
6495000
6494000
495000
496000
497000
498000
499000

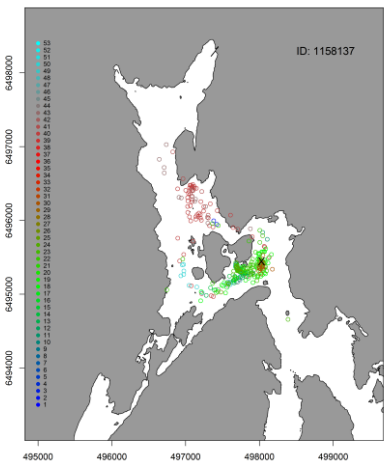
ID: 1158137
6498000
6497000
6496000
6495000
6494000
495000
496000
497000
498000
499000

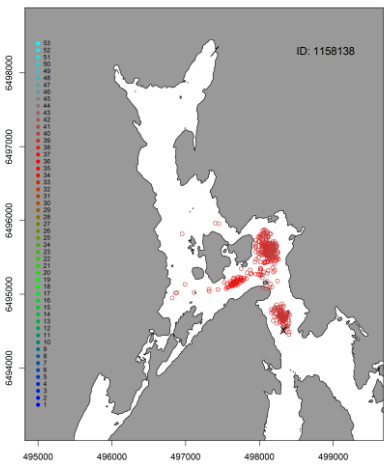
ID: 1158138
6498000
6497000
6496000
6495000
6494000
495000
496000
497000
498000
499000

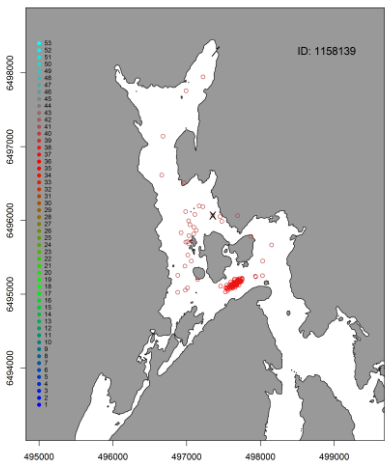
ID: 1158139
6498000
6497000
6496000
6495000
6494000
495000
496000
497000
498000
499000

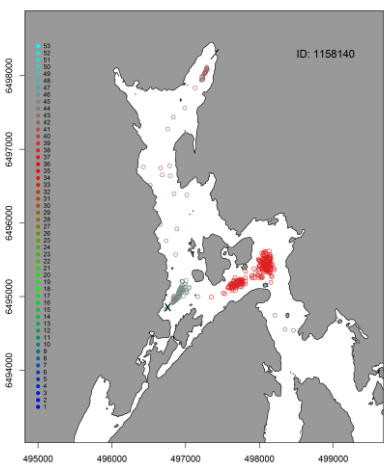
ID: 1158140
6498000
6497000
6496000
6495000
6494000
495000
496000
497000
498000
499000

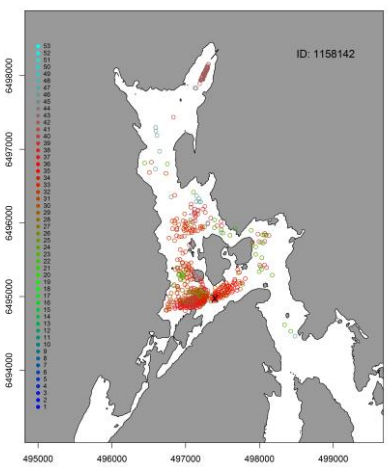
ID: 1158142
6498000
6497000
6496000
6495000
6494000
495000
496000
497000
498000
499000

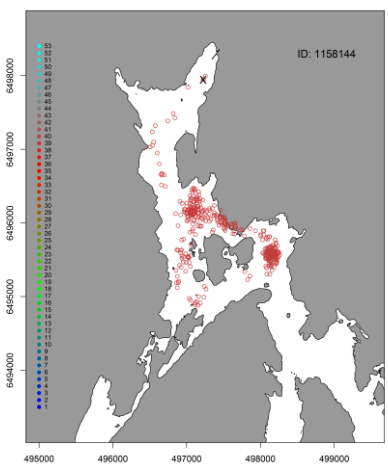
ID: 1158144
6498000
6497000
6496000
6495000
6494000
495000
496000
497000
498000
499000

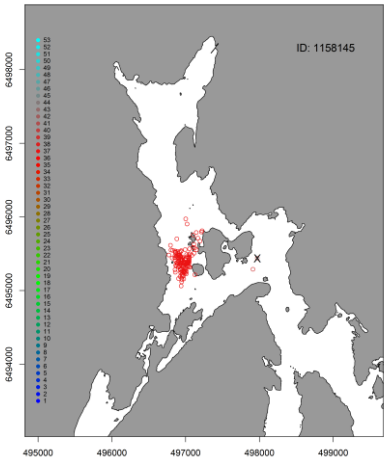
ID: 1158145
6498000
6497000
6496000
6495000
6494000
495000
496000
497000
498000
499000

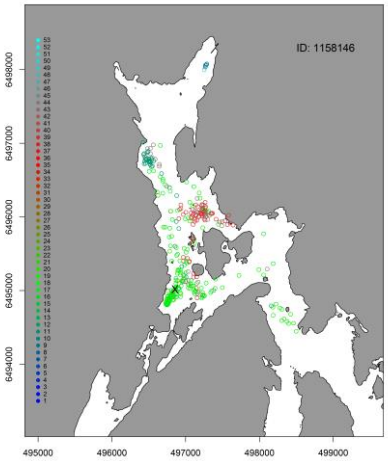
ID: 1158146
6498000
6497000
6496000
6495000
6494000
495000
496000
497000
498000
499000

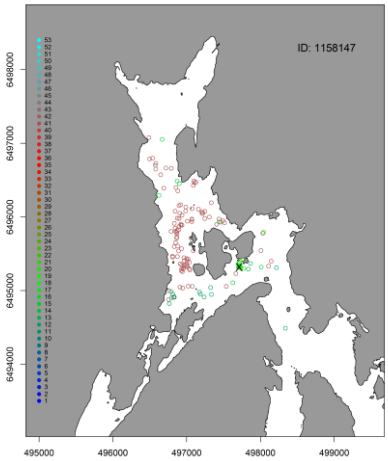
ID: 1158147
6498000
6497000
6496000
6495000
6494000
495000
496000
497000
498000
499000

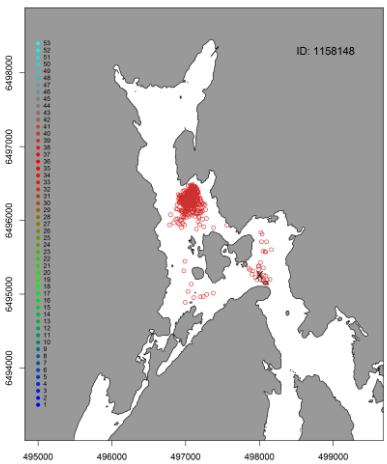
ID: 1158148
6498000
6497000
6496000
6495000
6494000
495000
496000
497000
498000
499000

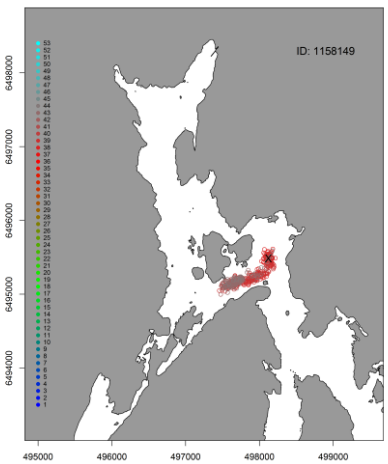
ID: 1158149
6498000
6497000
6496000
6495000
6494000
495000
496000
497000
498000
499000

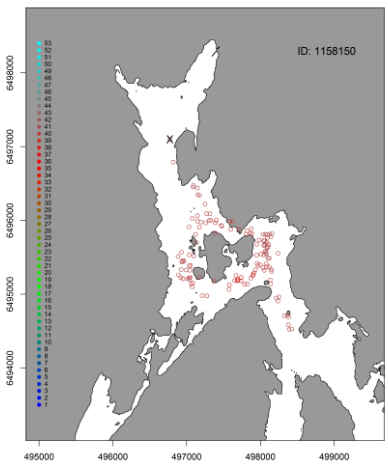
ID: 1158150
6498000
6497000
6496000
6495000
6494000
495000
496000
497000
498000
499000

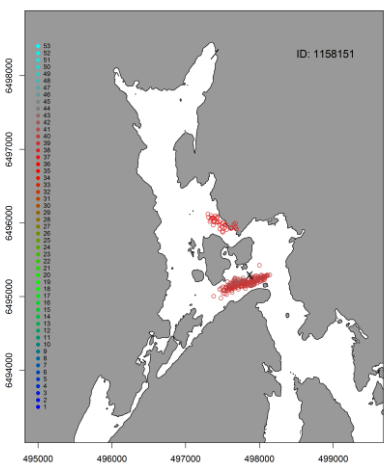
ID: 1158151
6498000
6497000
6496000
6495000
6494000
495000
496000
497000
498000
499000

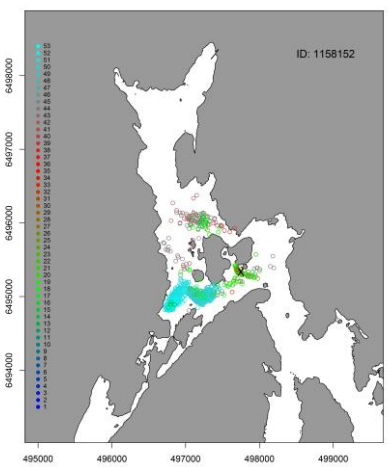
ID: 1158152
6498000
6497000
6496000
6495000
6494000
495000
496000
497000
498000
499000

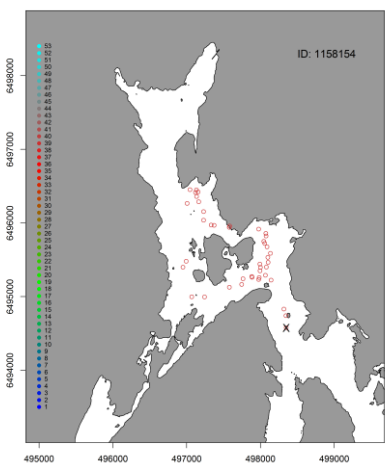
ID: 1158154
6498000
6497000
6496000
6495000
6494000
495000
496000
497000
498000
499000

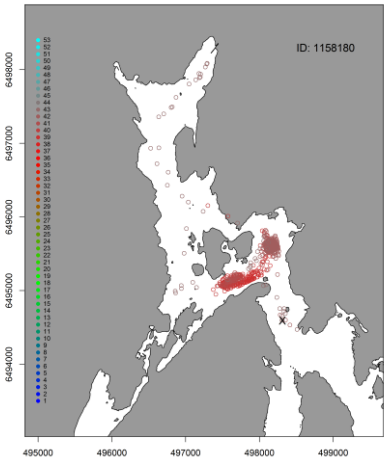
ID: 1158180
6498000
6497000
6496000
6495000
6494000
495000
496000
497000
498000
499000

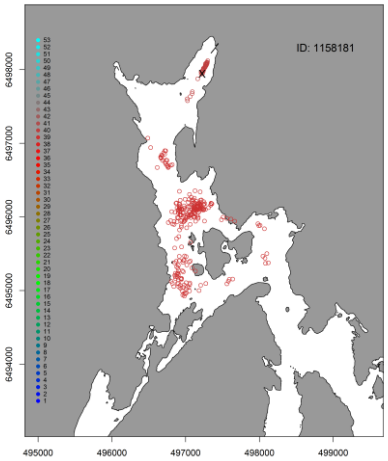
ID: 1158181
6498000
6497000
6496000
6495000
6494000
495000
496000
497000
498000
499000

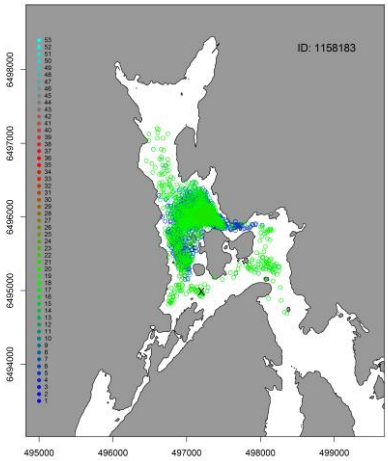
ID: 1158183
6498000
6497000
6496000
6495000
6494000
495000
496000
497000
498000
499000

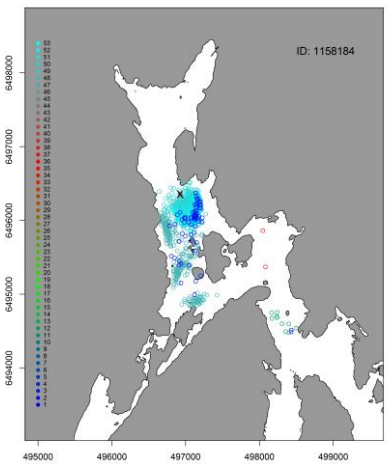
ID: 1158184
6498000
6497000
6496000
6495000
6494000
495000
496000
497000
498000
499000

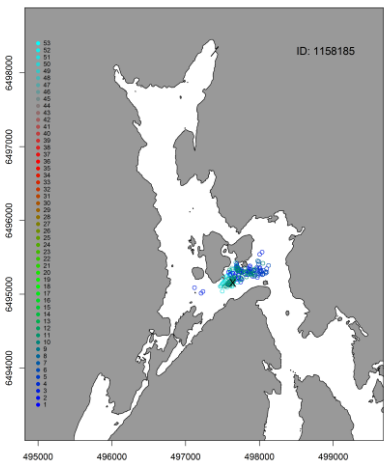
ID: 1158185
6498000
6497000
6496000
6495000
6494000
495000
496000
497000
498000
499000

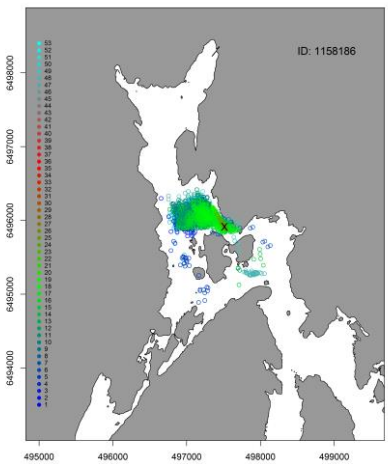
ID: 1158186
6498000
6497000
6496000
6495000
6494000
495000
496000
497000
498000
499000

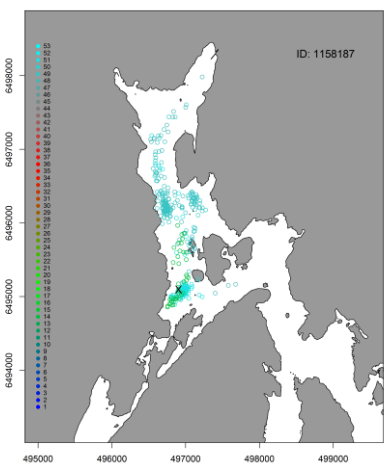
ID: 1158187
6498000
6497000
6496000
6495000
6494000
495000
496000
497000
498000
499000

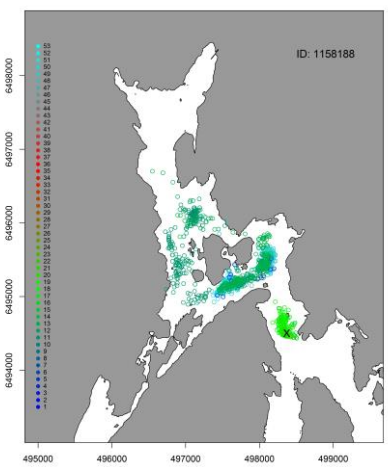
ID: 1158188
6498000
6497000
6496000
6495000
6494000
495000
496000
497000
498000
499000

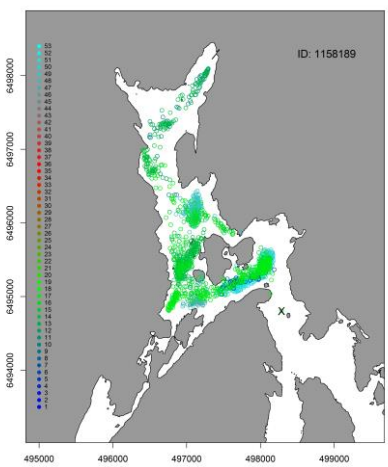
ID: 1158189
6498000
6497000
6496000
6495000
6494000
495000
496000
497000
498000
499000

Norwegian University
of Life Sciences

Postboks 5003
NO-1432 Ås, Norway
+47 67 23 00 00
www.nmbu.no